January 2014

Mitochondrial Dynamics: Exploring A Novel Target Against Myocardial Ischemia-Reperfusion Injury

Yi Dong
Wayne State University, ydong@med.wayne.edu

MITOCHONDRIAL DYNAMICS: EXPLORING A NOVEL TARGET AGAINST MYOCARDIAL ISCHEMIA-REPERFUSION INJURY

by

YI DONG

DISSERTATION

Submitted to the Graduate School

of Wayne State University,

Detroit, Michigan

in partial fulfillment of the requirements

for the degree of

DOCTOR OF PHILOSOPHY

2014

MAJOR: PHYSIOLOGY

Approved by:

_____

Advisor Date

_____

_____

_____

_____

DEDICATION

I dedicate this to my wife, Dr. Zheyu (Jessie) Lu, who suspended her residency training, came to this country and accompanied me to complete this critical time in my Ph.D. program. She used her tenderness and understanding to comfort me whenever my experiments did not work or I encountered difficult moments in life and my studies. Sometimes, a family dinner and a heart-warming conversation at the dinner table are more soothing than any intelligent advice. I really cherish those sleep-deprived nights when we studied together for USMLE and practiced for the Clinical Skills exam after my long day in the lab.

I dedicate this to my son, Daniel Dong, who is going to be born in late June. You do not know how excited we were when your mom and I knew that we would have you; it is like a miracle to witness your growth in your mom's body. You have changed our whole family. I wish you will have a healthy, happy life.

I dedicate this to my parents and sister, who live in China. Without your support and encouragement, I cannot make this journey to excellence that started in 2000. Thanks mom, dad and sister; I owe you too much.

ACKNOWLEDGEMENTS

To begin with, I would like to express my special appreciation and gratitude to my mentor, Dr. Karin Przyklenk for her patience and, support from the first day I joined her lab. She is involved in every step of my growth and academic development: every idea in formulating the research project, every piece of data that are the building blocks of the whole project, every sentence I wrote, every presentation that I made in the lab, committee meeting and national and international conferences. She is the best mentor in the world. Her recommendation and help is the also key factor helping me to achieve my residency position.

I would also like to thank my committee members, Drs. Roy McCauley, Steven Cala, Rita Kumar and Robert Mentzer, for their support and input over the years. After each committee meeting and data presentation, I always gained new inspiration, which brought my research project closer to completeness.

I would like to extend a special thanks to Mr. Vishnu Undyala, who trained me in several key techniques that were used in this project. The beneficial communication between us helped to find a better way to solve technical problems.

I cannot forget the help from our CVRI family members: Dr. Thomas Sanderson gave me hands-on training to use the Leica microscope and the software that turns the imaging into data; Dr. Rita Kumar taught me how to secure cells on coverslip when hypoxia made them vulnerable; Dr. Peter Whittaker used his British- style humor and instruction to make hard-to-understand ideas more understandable. His training also helped me to prepare for the resident selection interviews and finally win the position. Mr. Joe Wider shared a lot of fun moments with me when we both were struggling for good data.

I could not have made it to this point without the help and assistance from the fellow students, staff and faculty from the Physiology Department, particularly our faculty who opened the world of Physiology to us graduate students. A special thanks is given to Ms. Christine Cupps, who tolerates our naivetés and annoying questions in junior years and always give us the correct information and smartest path to follow.

TABLE OF CONTENTS

LISTS OF TABLES

LISTS OF FIGURES

LIST OF ABBRVIATIONS

ADP	Adenosine diphosphate
AKAP121	A-kinase anchor protein 121
Akt	also called Protein kinase B, also named as Akt
ANOVA	Analysis of variance
ANT	Adenine nucleotide translocase
ATP	Adenosine triphosphate
ATPB	ATP synthase β subunit
BAK	Bcl-2 homologous antagonist/killer
BAX	Bcl-2-associated X protein
Bcl-2	B-cell lymphoma 2
BH	Bcl-2 homology
Bnip3	BCL2/adenovirus E1B 19kDa interacting protein 3
BSA	Bovine serum albumin
CABG	Coronary artery bypass grafting
CO_2	Carbon dioxide dixodie
CsA	Cyclosporine A
CVD	Cardiovascular diseases
CYPD	Cyclophilin D
DAPI	4',6-diamidino-2-phenylindole
DD	Death domain
DED	Death effector domain
DIABLO	Direct inhibitor of apoptosis (IAP)-binding protein with low pI
DNA	Deoxyribonucleic acid

DRP1	Dynamin-related protein 1
$DRP1^{K38A}$	DRP1 mutant, of which Lysine residue 38 replaced by Alanine
$DRP1^{K38E}$	DRP1 mutant, of which Lysine residue 38 replaced by Glutamic acid
ER	Endoplasmic reticulum
$FADH_2$	Flavin adenine dinucleotide
FBS	Fetal bovine serum
FIS1	Fission protein 1
FL-	Full-length
GAPDH	Glyceraldehyde 3-phosphate dehydrogenase
GDP	Guanosine diphosphate
GPCR	G-protein coupled receptor
GTP	Guanosine Triphosphate
H_2O_2	Hydrogen peroxide
HM-Mito	Mitochondria-enriched heavy membrane
$HO^{\cdot}$	Hydroxyl radical
HOCl	Hypochlorous acid
HR	Hypoxia-reoxygenation
HRP	Horseradish peroxidase
IF	Immunofluorescence
IMM	Inner mitochondrial membrane
IR	Ischemia-reperfusion
Mdivi-1	Mitochondrial division inhibitor 1
MFN1/2	Mitofusin1/2

MiD49	Mitochondrial dynamics proteins of 49 kDa
MiD51	mitochondrial dynamics proteins of 51 kDa
mK_{ATP}	mitochondrial ATP-sensitive potassium channel
mPTP	Mitochondrial permeability transition pore
mRNA	Messenger RNA
NAD^+/NADH	Nicotinamide adenine dinucleotide/reduced form of NAD^+
NCX	Na^+/Ca^{++} exchanger
NHE	Na^+/H^+ exchanger
NO	Nitric oxide
NS	Not significant (*P*> 0.05)
$O2^{\cdot -}$	Superoxide anion
OMM	Outer mitochondrial membrane
$ONOO^-$	Peroxynitrite
OPA1	Optic atrophy 1
P110 peptide	A short peptide inhibitor of mitochondrial fission, mimicking homologous sequence between DRP1 and FIS1 and blocking their interaction: $DRP1_{49-55}$ (Asp-Leu-Leu-Pro-Arg-Gly-Thr)
PBS	Phosphate buffered saline
PCI	Percutaneous coronary intervention
PGAM5	Phosphoglycerate mutase family member 5
Pim-1	Proviral integration site for Moloney murine leukemia virus kinase-1
PKA	Protein kinase A
post-R	Post-reoxygenation
PUMA	p53 upregulated modulator of apoptosis

RIP1	Receptor interaction protein 1
RIP3	Receptor interaction protein 3
RIPA	Radioimmunoprecipitation assay buffer
RISK	Reperfusion injury survival kinase
RNA	Ribonucleic acid
RNS	Reactive nitrogen species
ROS	Reactive oxygen species
RyR	Ryanodine receptor
SAFE	Survival activating factor enhancement
SDS-PAGE	Sodium dodecyl sulfate-polyacrylamide gel electrophoresis
SEM	Standard error of mean
SERCA	Sarcoplasmic reticulum Ca^{++} ATPase
SFCC	Serum-free Claycomb medium
Siah1a/2	Seven in absentia homolog 1a/2
siRNA	Small interfering RNA
SMAC	Second mitochondria-derived activator of caspases
SR	Sarcoplasmic reticulum
SUMO	Small ubiquitin-like modifier
SUMOylation	The process of generating SUMOylated proteins by covalently binding to small ubiquitin-like modifier proteins
TAT-carrier	TAT peptide, derived from the transactivator of transcription (TAT) of human immunodeficiency virus
TBS	Tris-buffered saline
TBST	Tris-buffered saline containing 0.1% Tween 20

TCA cycle	Tricarboxylic acid cycle
TNFR-1	TNF-α receptor-1
TNF-α	Tumor necrosis factor-α
UPR	Unfolded protein responses
VDAC	Voltage-dependent anion channel
Δψm	Mitochondrial transmembrane potential

CHAPTER 1

PERSPECTIVE: MYOCARDIAL ISCHEMIA-REPERFUSION INJURY

1. Clinical Significance: Coronary Heart Disease and Myocardial Ischemia-reperfusion Injury

Cardiovascular disease (CVD) is the leading cause of mortality in the industrialized world; in 2009, CVD accounted for nearly one in every three deaths in the United States. Half of these deaths are due to acute myocardial infarction or 'heart attack', caused by obstruction of a coronary artery; each year, ~ 635,000 Americans have a new heart attack, and ~ 280,000 suffered from recurrent attacks, in addition to ~150,000 patients with silent presentation (1).

Since infarct size (that is, amount of irreparable damage caused to the heart by prolonged obstruction of a coronary artery) is the most important independent predictor of post-infarct mortality and long-term prognosis, shortening of ischemic duration by reperfusion (reintroduction of blood flow as soon as possible to the ischemic myocardium) is the therapeutic target (2-4). Therefore, the current clinical strategy for managing acute myocardial infarction is restoration of blood flow by either primary percutaneous coronary intervention (PCI), coronary thrombolysis or coronary artery bypass grafting (CABG). Reintroduction of blood supply to ischemic regions, however, paradoxically exacerbates lethal cardiomyocyte death and significantly attenuates the benefits of reperfusion, a phenomenon termed as lethal myocardial ischemia-reperfusion (IR) injury (5). With decades of efforts by clinicians and scientists, there is still lack of approved treatment, beyond early reperfusion, to reduce damage caused by heart attack. Novel strategies are therefore urgently needed to address myocardial ischemia-reperfusion injury. To achieve this goal, a thorough understanding of the

pathophysiology of ischemia-reperfusion injury is required.

2. Current Knowledge

2.1 Key mediators of ischemia-reperfusion injury

2.1.1 pH and calcium overload

Early effects of ischemia (i.e., inadequate delivery of oxygen to myocardium after coronary occlusion) lead to a rapid conversion from aerobic to anaerobic glycolysis and accumulation of lactate, insufficient removal of carbon dioxide (CO_2), and impaired production of adenosine triphosphate (ATP) (6-9). The decrease in intracellular pH can be observed 15 seconds after ischemia and, within 15 minutes, pH dropped to ~6.2 from the normal value of ~7.05 (8). Sarcolemmal acidosis drives the Na^+/H^+ exchanger (NHE) to transport hydrogen ions out of cells at the expense of sodium entry. The low ATP levels make Na^+/K^+ ATPase unable to work efficiently to pump sodium out of the cell, which results in sodium accumulation and activation of Na^+/Ca^{++} exchanger (NCX) (10). Additionally, low ATP levels disrupt the activity of the sarcolemmal Ca^{++} pump and sarcoplasmic reticulum Ca^{++} ATPase (SERCA) required to maintain low cytoplasmic Ca^{++} concentration; both significantly contribute to calcium overload during ischemia (10-12). Among the multiple deleterious consequences of calcium overload, the mitochondrion is the major target due to its capacity as an intracellular Ca^{++} reservoir and expression of multiple calcium-handling enzymes (13). Deposition of Ca^{++} into mitochondria further aggravates impaired oxidative phosphorylation and ATP generation and facilitates mitochondrial swelling. However, the mitochondrial permeability transition pore (mPTP) – the large, nonspecific conductance channel discussed in more detail in Section 2.1.4 – remains closed due to low intracellular pH (14).

Following reperfusion, there is a rapid wash-out of extracellular hydrogen ions;

the intracellular acidosis is also quickly rectified resulting in an increase in pH. In addition, with repletion of oxygen and metabolic substrates to the previously ischemic area, the generation of ATP is resumed. Reperfusion and the fast correction of intracellular acidosis are, however, also accompanied by adverse events. More specifically, normalization of pH reactivates many direct and indirect calcium-handling proteins that are functionally inhibited in ischemic phase, including NHE, NCX, SERCA and Ryanodine receptors (RyRs) (15-18). Firstly, there is a substantial increase in Ca^{++} influx due to reversed mode of NCX and prolonged low Na^{+}/K^{+} ATPase and Ca^{++} ATPase activity. Secondly, resumption of ATP synthesis may activate rapid sarcoplasmic reticulum (SR) Ca^{++} cycling and cytosolic Ca^{++} oscillation through RyR, when SR storage capacity is exceeded. As a result, Ca^{++} activates calcium-dependent protease and kinases system such as calpains, phospholipases and Ca^{++}/calmodulin-dependent kinase and these activated signaling pathways favor cardiomyocyte death. Thirdly, further increased sarcoplasmic Ca^{++} and neutralizing pH accelerates Ca^{++} binding to the contractile apparatus and causes hypercontracture and dysfunction or 'stunning' of injured myocardium. Finally, restoration of pH, in the presence of calcium overload and reactive oxygen species (ROS: discussed in Section 2.1.3) triggers a potentially lethal event – the opening of mPTP (19, 20) (Figures 1-1 and 1-2).

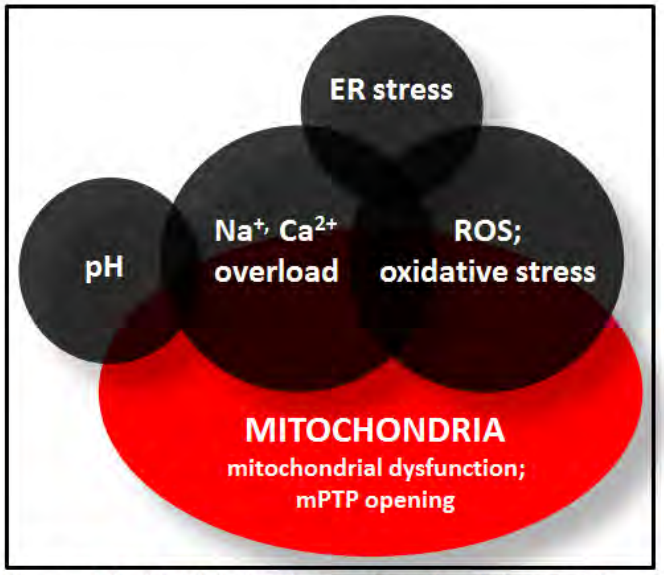

Figure 1-1. Simplified scheme of major determinants of ischemia-reperfusion injury and their interactions in mediating IR injury. ER, endoplasmic reticulum; ROS, reactive oxygen species; mPTP, mitochondrial permeability transition pore.

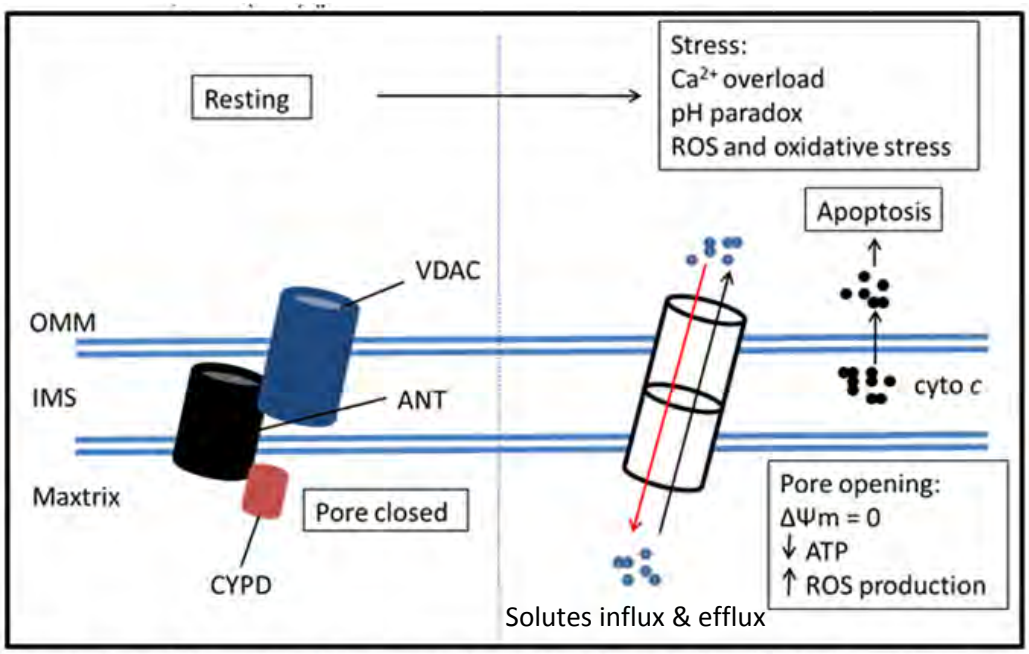

Figure 1-2. Diagraph of the opening of mPTP and cell death. OMM, outer mitochondrial membrane; IMS, intermembrane space; cyto *c*, cytochrome *c*; Δψm, mitochondrial transmembrane potential. Adapted from Abou-Sleiman *et al*, Nat Rev Neuroscience, 2006 (183).

2.1.2 Endoplasmic reticulum (ER) stress

ER [or, in muscle, the sarcoplasmic reticulum (SR)] is the tubular endosome network system of eukaryotic cells. ER performs the housekeeping functions that maintain cell survival, including protein synthesis, lipid biosynthesis, folding and posttranslational modification of proteins, membrane synthesis and trafficking, calcium storage and release, and unfolded protein responses in physiological and pathological conditions (21-24). Additionally, SR in cardiac muscles carries out more cell-specific functions such as control of calcium release that is essential to excitation-contraction coupling (22). The characteristic unfolded protein responses (UPR) of ER stress is mediated through three key pathways: i) arrest of translation through phosphorylation of eukaryotic initiation factor 2-α decreases loading burden to ER; ii) activation of activating transcription factor 6 upregulates expression of ER stress-sensing genes such as chaperon proteins and ER-associated degradation proteins; and iii) expression

of cleaved mRNA of X-box binding protein 1 transcription factor increases the expression of proteins that participate in protein folding, transporting and degradation (21, 22, 25). Importantly, any insults that result in loss of energy balance and/or nutrient homeostasis causes ER stress (21). For example, in myocardial ischemia-reperfusion injury, the depletion of oxygenation and glucose, drastic increase in ROS production and perturbation in ATP supply and calcium homeostasis lead to accumulation of misfolded proteins in ER, which is buffered by the initiation of UPR (21, 26, 27).

2.1.3 Reactive oxygen species (ROS) and oxidative stress

The major contributors of oxidative stress in ischemia-reperfusion injury are the family of reactive oxygen species including the superoxide anion ($O_2^{\cdot -}$), hydroxyl radical ($HO^{\cdot}$), lipid radicals, and nitric oxide (NO), as well as non-radical species including hydrogen peroxide (H_2O_2), peroxynitrite ($ONOO^-$), and hypochlorous acid (HOCl). In addition, $O_2^{\cdot -}$ is unstable and can react with NO to form reactive nitrogen species (RNS); the cytotoxicity induced by RNS is known as nitrosative stress (28, 29). Under normal physiological conditions, excess ROS is efficiently removed by the antioxidant system, e.g., superoxide dismutase quickly catalyzes $O_2^{\cdot -}$ to H_2O_2, which is further converted to H_2O by catalase (30). However, under pathophysiological conditions such as IR injury, ROS production is increased (as described below) and the endogenous antioxidant defenses are overwhelmed.

The most important source of ROS in cardiomyocytes, particularly in IR injury, is from mitochondria. During ischemia, the interruption in blood flow and oxygen supply depletes metabolic substances, shuts down the tricarboxylic acid (TCA) cycle, and increases the ratio of NAD^+/NADH. These alterations are associated with the generation of moderate amounts of $O_2^{\cdot -}$ from complexes I (NADH dehydrogenase) and

III of mitochondrial electron transfer chain (31), although complex II (succinate dehydrogenase) may also play a role (32). In contrast, the pathologic component of oxidant stress occurs at reperfusion. Reintroduction of oxygen to ischemic tissue triggers a burst in ROS production, occurring via different sources and mechanisms than in the ischemic episode (33). The proposed model is that calcium overload, normalization of intracellular pH, opening of mPTP, the reactivation of TCA cycle, the availability of reducing electrons from NADH and reduced form of $FADH_2$ and restoration of molecular oxygen work simultaneously to promote ROS spikes (19, 29, 31, 33-35). Of note, the reperfusion-associated burst in ROS production amplifies mPTP formation and, in turn, exacerbates ROS generation, resulting in a vicious cycle of ROS-induced ROS release (19, 36) (Figures 1-1 and 1-2). Excess ROS produced in this manner can cause direct damage to multiple cellular macromolecules, including proteins, lipids, and DNA, and can be cytotoxic (37, 38).

2.1.4 Mitochondrial dysfunction and the mPTP: the epicenter of ischemia-reperfusion injury

There is growing evidence suggesting that the network of mediators contributing to myocardial ischemia-reperfusion injury converges on mitochondria (39). The mitochondrion can be considered both the 'victim' or target and the 'executor' of myocardial IR injury. The deleterious molecular events that are relevant to mitochondrial dysfunction and occur in the context of IR injury include, but are not limited to, i) inhibition of electron transfer chain function and oxidative phosphorylation; ii) loss of mitochondrial membrane potential; iii) calcium overload within mitochondria; iv) ROS production and ROS-induced ROS release; and v) prolonged opening of mPTP and its consequences, such as loss of proton gradient, matrix swelling, release of

proapoptotic proteins, (i.e., cytochrome *c*) mitochondrial rupture and irreversible cardiomyocyte death (40-42).

The mPTP is postulated to act as a conductance pore that connects the matrix, inner and outer mitochondrial membranes (IMM and OMM), as well as the inter-membrane space (Figure 1-2). Although there is functional evidence for the existence of the mPTP, morphologic evidence has not been well-established (43-45). Previous studies propose that three vital proteins form the channel of the transition pore: voltage-dependent anion channel (VDAC, outer membrane protein), adenine nucleotide translocase (ANT, inner membrane protein), and cyclophilin D (CYPD, residing in matrix as important regulator of pore opening: Figure 1-2) (43). Recent data imply that none of the above-mentioned proteins are indispensable for mPTP-dependent cell death as knockout experiments revealed no effects on cell responsiveness to B-cell leukemia/lymphoma-2 (Bcl-2) family member-driven apoptosis or other multiple apoptotic inducers (44, 46, 47). mPTP opening is characterized by dissipation of mitochondrial transmembrane potential ($\Delta\psi m$), mitochondrial swelling and rupture of the OMM, and massive leakage of intermembrane proteins into cytosol (48).

2.2 How do cardiomyocytes die?

Loss of viable cardiomyocytes contributes to pathogenesis of acute myocardial infarction and post-ischemic cardiac dysfunction. There are three major types of cell death that play causal roles in myocardial ischemia-reperfusion injury: apoptosis, necrosis and macroautophagy (referred as autophagy in this thesis).

2.2.1 Apoptosis

Apoptosis or ‘programmed cell death’ is the first defined, controllable form of cell death. It is an energy-dependent and precisely regulated process that is mediated by

two pathways: the intrinsic and extrinsic apoptotic pathways.

The intrinsic pathway (49) starts from mitochondrial release apoptogenic proteins in response to apoptotic stimuli. The well-defined proteins include cytochrome *c*, second mitochondria-derived activator of caspases (SMAC)/direct inhibitor of apoptosis-binding protein with low pI (DIABLO), apoptosis-inducing factor, etc. For example, once a large quantity of cytochrome *c* is released into the cytoplasm, it binds with apoptotic-protease-activating factor-1 along with 2-deoxy-ATP. This is followed by recruitment of procaspase 9 to form the apoptosome (50). Similar to procaspase 8 activation (discussed below), procaspase 9 is activated within the apoptosome and, subsequently, cleaves and activates effector procaspases into their functional formats that perform suicidal functions. The classic stimuli that activate the intrinsic pathway include depletion of grow factors, nutrient deprivation, hypoxia, oxidative stress, DNA damage and chemical and biological toxins. Release of apoptogenic proteins from mitochondria is dependent on the relative activities of two classes of proapoptotic Bcl-2 family proteins [BAX (Bcl-2-associated X protein) and BAK (Bcl-2 homologous antagonist/killer)] *versus* the antiapoptotic Bcl-2 proteins (51, 52). Under conditions of stress (including IR), the proapoptotic Bcl-2 proteins predominate; hence, BAX is released and translocates to OMM, and, in combination with BAK, forms pore structures and triggers cytochrome *c* release, a process termed as OMM permeabilization (49, 53).

The extrinsic pathway (49) is initiated by the binding of death ligands to death receptors, e.g., Tumor necrosis factor-α (TNF-α) to TNF-α receptor-1 (TNFR-1) and Fas ligand to Fas) and subsequent recruitment of cytosolic factors such as procaspase 8. Once activated, caspase 8 further cleaves and activates the so-called ‘effector’ caspases, 3 and 7, ultimately responsible for cell suicide. Importantly, the intrinsic and

extrinsic pathways are not independent, with crosstalk between the two apoptotic pathways mediated by active caspase 8 (49, 54-57).

Myocardial ischemia-reperfusion is a classical model of apoptotic activation. Multiple mechanisms and signaling pathways contribute to cardiomyocyte apoptosis. For example, impaired calcium homeostasis in the setting of IR injury, as discussed above, leads to activation and translocation of cysteine proteases including calpains (58, 59). Activated calpain reportedly interacts with apoptotic proteins contributing to formation of the apoptosome and, as a result, promoting cytochrome *c* leakage and apoptotic cardiomyocyte death (60, 61). It is also proposed that excessive intracellular calcium concentration may directly activate the apoptotic machinery (62, 63). Finally, a large body of data, obtained largely from genetic mouse models, suggests that both intrinsic and extrinsic apoptotic pathways play a role myocardial IR injury (51-53, 64, 65).

2.2.2 Autophagy

Macroautophagy (herein referred as autophagy) is an evolutionally reserved house-keeping process that isolates and, ultimately, degrades damaged and dysfunctional organelles and protein aggregates. This process plays a pivotal role in maintaining homeostasis for cell survival under many physiologic and pathophysiologic conditions (66, 67). Growing evidence indicates that autophagic machinery is activated in myocardial IR injury. The triggering factors, in the context of IR, include i) nutrient deprivation and ATP depletion, ii) induction of Bnip3 (the so-called BH-3 only subfamily of Bcl-2 family proteins) via hypoxia and acidosis, iii) calcium overload, iv) massive ROS production, v) opening of mPTP, and vi) ER stress. The hydrolyzed products produced by autophagy, such as amino acids, free fatty acids, and substrates, can be used for ATP generation during metabolic crisis as occurs in IR injury (68, 69). However, the

precise relationship between autophagy and cell fate (whether it is a mechanism of cell death, or whether upregulation of autophagy may be a protective mechanism) is controversial and poorly understood (68, 70, 71).

2.2.3 Necrosis and necroptosis

Necrosis is the dominant contributor to the loss of viable myocardium under conditions of IR. In the setting of IR injury, long-term opening of the mPTP (Figure 1-2) results in dissipation of inner membrane potential, exacerbation of impaired ATP generation, and inward diffusion of solutes along electro-chemical gradients. This subsequently draws free water into the matrix, and causes mitochondrial swelling. If swelling is severe and mitochondrial membranes burst, necrosis ensues. The activated calpains (discussed above) degrade important membrane and cellular structural proteins, e.g., leading to dysfunction of Na^+-K^+-ATPase. If there is no effective intervention to recover sodium pump activity, the consequence of severe inhibition of Na^+-K^+-ATPase function is intracellular sodium overload, cell swelling and cardiomyocyte necrosis (72, 73). In addition, reducing calpain activity significantly reduced its destruction of sarcolemmal integrity and attenuated myocardial necrosis in the isolated perfused heart model of IR

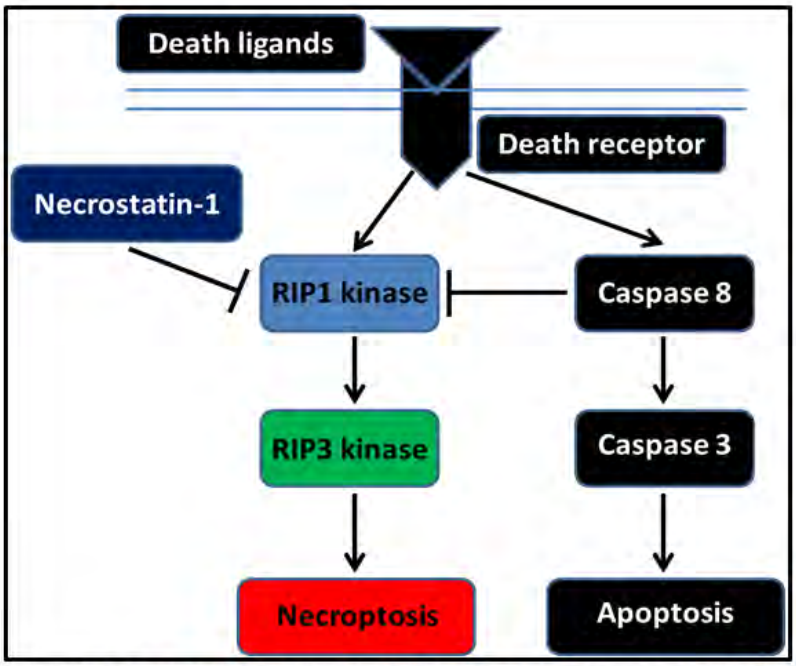

Figure 1-3. Simplified scheme of the crosstalk between apoptotic and necroptotic pathways. RIP1, receptor interaction protein 1; RIP3, receptor interaction protein 3.

injury (74).

Necrosis has been traditionally viewed as a passive, unregulated cell death. Emerging evidence, however, indicates that a subdivision of necrosis, when death receptor activation occurs simultaneously with caspase inhibition, is an active, orchestrated process and depends on a signaling cascade still awaiting clarification. This regulated form of necrosis is termed as necroptosis (75, 76) (Figure 1-3).

When death ligand binds to death receptor (77-79), e.g., TNF-α to TNFR-1, it can induce both death and survival signaling depending on the participating protein factors and the formed complexes. In the absence of survival signals, the binding of TNF-α to TNFR-1 initiates the formation of death complex I that comprises TNFR-1, TNFR1-associated death domain protein, receptor interaction protein 1 (RIP1), TNF receptor-associated factor 2, and cellular inhibitor of apoptosis protein1/2 via the interaction between respective death domains (DDs) (80). The cytosolic component of death complex I is converted to complex II following the deubiquitination of RIP1, including recruited Fas-associated death domain protein via DD-DD interactions, and procaspase-8 (via DED (death effector domains)-DED interactions) (54, 75, 76). Normally, activated caspase 8 degrades RIP1, while simultaneously activating effector caspases 3 and 7 mediating apoptosis. However, when procaspase 8 activation is inhibited, either by genetic maneuvers or pharmacologic antagonists, the preserved RIP1 is able to interact with RIP3, and, by as-yet unknown mechanisms, initiates the necroptotic pathway (81). Administration of Necrostatin-1 (82), a pharmacologic antagonist of RIP1 blocking its kinase activity, provides cardioprotection against IR injury and decreases myocardial necrosis (83, 84) (Figure 1-3).

Necrosis/necroptosis and apoptosis are not two parallel lines. Rather, there is

cross-talk between the two processes, as shown by the fact that many signaling cascades can cause both necrotic and apoptotic cardiomyocyte death. For example, excessive ROS production in IR injury leads to prolonged opening of mPTP, resulting in loss mitochondrial potential, arrested ATP generation, matrix swelling and mitochondrial structural rupture and, finally, cardiomyocyte necrosis. Meanwhile, apoptogenic proteins from ruptured mitochondria will activate the apoptotic pathway. A sequential model of cell death has been proposed (54, 55): no matter which type of cell death comes first, either necrosis or apoptosis, will finally leads to the activation of the other type of cell death, e.g., activated BAX and BAK in the apoptotic pathway forms pores in the OMM and causes OMM permeabilization. The released mitochondrial proteins, such as cytochrome *c,* initiate the formation of apoptosome and ultimately activate effector caspases, such as caspase 3. The activated caspase 3 in turn degrades important IMM proteins, leading to disruption of mitochondrial potential, matrix swelling, and mitochondrial structural rupture; as a result, cardiomyocytes also display the necrotic phenotype (35, 54, 55).

3. Application of Current Mechanistic Insights for Development of Cardioprotective Strategies

3.1 Historical strategies based on key players

Over the past decades, all of the proposed mediators of myocardial ischemia-reperfusion injury discussed previously, including dysregulation of pH, sodium-hydrogen exchanger and calcium overload, ER stress and ROS generation, have been targeted as therapeutic strategies to counteract the detrimental effects of IR and maximize the benefits of reperfusion (15, 27, 85-101). All of these interventions showed benefit (i.e., attenuated IR injury and reduced infarct size) in at least some preclinical models and

studies. For example: In 1970's, Jennings's lab reported that IR caused significant increase of calcium accumulation in mitochondria (88). Based on the findings, calcium channel blockade with agents such as verapamil were investigated and reported to attenuate IR injury (89). Many of these strategies (including NHE inhibitors and ROS scavenger and antioxidants) were developed to the point of being tested in clinical trials (102-107). However, none of the above described strategies have been progressed to clinical application and bring benefits to patients suffering from acute or prolonged ischemia-reperfusion injury.

3.2 Conditioning-mediated cardioprotection

3.2.1 Ischemic conditioning and clinical application

In 1986, Murry and colleagues opened a new era in the field of cardioprotection. Using the canine model, they reported that four cycles of 5 min ischemia each separated by 5 min reperfusion applied prior to ischemia significantly reduced the infarct size after forty mins of ischemia and four days of reperfusion. They named this phenomenon as "ischemic preconditioning" (108). In the >20 years since its discovery, infarct size reduction with ischemic preconditioning has been demonstrated in every model and species tested (109-112). In addition, many small-scale clinical trials in multiple institutions confirmed the protective effects of preconditioning on the human heart, most notably in patients undergoing coronary artery bypass graft surgery (113, 114). However, despite the effectiveness of preconditioning in reducing IR injury, the feasibility for clinical application is limited: i.e., myocardial ischemic events are unpredictable and ischemic preconditioning is by definition a pretreatment, making this strategy impractical in any clinical context except scheduled cardiac surgeries.

More recently, the concept of conditioning has been expanded to include the

concepts of postconditioning and remote conditioning. Postconditioning was discovered by Zhao *et al*., who observed that stuttered recovery of blood flow to previous ischemic myocardium, instead of abrupt reperfusion, protects against lethal myocardial IR injury (115). The advantage of postconditioning is that the intervention is applied at the time of reperfusion (rather than as a pretreatment), and has been reported to be as effective as preconditioning in reducing myocardial infarct size (115, 116). Remote conditioning, first described in 1993, is the phenomenon whereby *brief ischemia applied in a remote tissue or organ* protects the heart against subsequent sustained ischemia (117). Interest in the concept of remote conditioning was increased by two subsequent observations. First, brief periods of skeletal muscle ischemia-reperfusion, implemented by the simple technique of inflation-deflation of a blood pressure cuff on an arm or leg, was demonstrated to be an effective trigger for cardioprotection (118). In addition, pretreatment is not a requirement; infarct size reduction with remote *preconditioning* (that is, implementation of the remote stimulus during myocardial ischemia), has also been demonstrated (119). Both postconditioning and remote conditioning are attractive candidates for clinical application; both strategies have been shown to limit clinical markers of IR injury in many (but not all) small Phase II clinical trials (114), and larger Phase III trials are currently in progress to evaluate the acute effects and longer-term outcomes of patients receiving remote ischemic conditioning protocols prior to PCI ((120); ClinicalTrials.gov: NCT01665365)). Results of this latter, ongoing trial are expected to be released by December 2014 (ClinicalTrials.gov: NCT01665365).

3.2.2 Governing mechanisms of conditioning-mediated cardioprotection

The cellular mechanisms responsible for conditioning-mediated cardioprotection remain incompletely understood, and a comprehensive review is beyond the scope of

the thesis. However, in brief, the general, current paradigm (121) for the *cardiac component* of all forms of ischemic conditioning (including pre-, post- and remote conditioning) can be summarized as:

i. conditioning protocols generate autocoid signaling triggers (e.g., bradykinin (122, 123), adenosine (123-126), opioids (127-129)), which bind to specific G-protein coupled receptors (GPCRs) (130-135);

ii. on binding with respective GPCR, the intracellular signaling mediators are recruited and activated (121, 131, 136-144). Activated signaling cascades further phosphorylate downstream targets including, most notably, components of the so-called RISK (reperfusion injury survival kinase) (136, 145, 146) and SAFE (survival activating factor enhancement) pathways) (121, 147-149), (i.e., phosphoinositide 3-kinase/Akt, extracellular signal-regulated kinase 1/2, janus kinase/signal transducers and activators of transcription 3, endothelial nitric oxide synthase, glycogen synthase kinase 3β, mammalian target of rapamycin, p70S6 kinase, etc (135, 137-143, 150-154);

iii. ultimately, the protective effects were realized by one or more end-effectors, with emphasis on two mitochondrial targets: the mitochondrial ATP-sensitive potassium channel (mK_{ATP}) (121, 155-159) and the mPTP (160-162).

3.3 Mitochondria as therapeutic targets

As discussed above, insights from ischemic conditioning reinforce the hypothesis that mitochondria may be the epicenter of ischemia-reperfusion injury and, thus, may be the most logical target for potential treatments.

3.3.1 Mitochondrial ATP-sensitive Potassium channel

The mK_{ATP} channel is a low-conductance inner membrane channel that allows K^+

to move into matrix when it is opened. It is named “ATP-sensitive” because ATP or ADP inhibits its opening with a cofactor of Mg^{++} and GTP or GDP activates it, although the structural identity and regulatory mechanisms remain elusive (163). The pathophysiologic significance of mK_{ATP} opening in myocardial IR injury and ischemic conditioning can be summarized as: i) volume expansion in the matrix and decrease in intermembrane space help preserve the low permeability of OMM and prevent ATP hydrolysis (163-167); ii) depolarization and reduced $\Delta\psi_m$ reduced Ca^{++} accumulation, thus increasing resistance to mPTP openers (168, 169); and iii) ROS generation by mK_{ATP} opening is beneficial, which significantly reduces ROS burst during reperfusion, a major mechanism for IR injury (170-174). In the procedures of PCI or CABG, the results of two small-scale clinical trials suggested that selective mK_{ATP} and non-selective K_{ATP} inhibitors significantly reduced cardiac enzymes release and facilitated cardiac functional recovery (175, 176).

3.3.2 Mitochondrial permeability transition pore (mPTP)

As discussed in section 2.1.4, unregulated, prolonged opening of mitochondrial permeability transition pore, in the context of ischemia-reperfusion injury, causes loss of proton gradient, dissipation of mitochondrial membrane potential, matrix swelling, release of proapoptotic proteins, mitochondrial structural collapse and irreversible cardiomyocyte death (40-42). Therefore, inhibition of persistent mPTP opening has been investigated as a strategy to protect the heart from IR injury. In 2001, Di Lisa *et al*., reported that cyclosporine A (CsA), a well-known immunosuppressant and mPTP opening inhibitor, significantly reduced IR-induced NAD^+ depletion and lactate dehydrogenase release in rat hearts (177). Subsequent studies in cell models, isolated hearts and *in vivo* models have documented the beneficial potentials of inhibiting mPTP

opening in the setting of IR (161, 178, 179), although negative results were obtained in the *in vivo* rat model when treatment with CsA was begun at 5 min before reperfusion (180).

In two small, pilot clinical trials, administration of CsA has had mixed results. When administered prior to thrombolysis, CsA had no effect on peak circulating levels of cardiac enzymes (creatine kinase, troponin I: considered surrogate markers of infarct size) measured following reperfusion (181). In contrast, when given immediately before PCI, treatment with CsA was associated with a significant reduction in creatine kinase release, but a non-significant trend toward lower circulating levels of troponin I, over the first 72 hours post-reperfusion (182). A large, Phase III clinical trial – CIRCUS: Cyclosporine and Prognosis in Acute Myocardial Infarction Patients – is currently in progress and the results, anticipated in September 2015, are expected to provide clear evidence on the role of mPTP inhibition as therapy for IR injury in patients (ClinicalTrials.gov: NCT01502774).

CHAPTER 2

BACKGROUND: MITOCHONDRIAL DYNAMICS

1. Mitochondrial Integrity and Cardioprotection: Expanding the Concepts

As reviewed in Chapter 1, maintenance of mitochondrial integrity is well-recognized as a critical determinant of cardiomyocyte viability; as a result, mitochondria have emerged as a cellular target in efforts to mitigate IR injury (184-186). In the past decade, the major emphasis has been on the mPTP and modulation of its opening. However, there is growing evidence that other aspects related to the preservation of the function and structure of mitochondria (186, 187), (in addition to, in combination with, or instead of the status of the mPTP) may play a role in cardioprotection. Recent specific attention has focused on mitochondrial dynamics, particularly, mitochondrial fission, as a mediator of cell fate in the setting of ischemia-reperfusion injury (188).

2. Definitions and Key Molecular Mediators

An important feature of mitochondria is their dynamic nature, where a mitochondrion changes its shape to meet the physiological and pathological status of the cell (189). Mitochondrial dynamics is also an important mechanism for mixing of mitochondrial DNA and maintenance of a healthy population of mitochondria (190).

The most commonly observed morphologies are fusion and fission. During fusion, adjacent mitochondria join to form an elongated mitochondrial network by membrane fusion and content exchange (191-193). Two groups of GTPases, mitofusins (MFN1/2) and optic atrophy 1 (OPA1), reportedly regulate this process by mediating the fusion of mitochondrial outer and inner membrane, respectively (192). In contrast, fission is the division of a mitochondrion, resulting in fragmented mitochondria (191). The ‘master regulator’ of mitochondrial fragmentation is Dynamin-related protein 1 (DRP1): this large

GTPase typically resides in the cytosol but, during fission, translocates to mitochondria and serves as the mechanoenzyme that constricts and cleaves the mitochondrion (194-196). Posttranslational modification, most notably phosphorylation/dephosphorylation of DRP1, reportedly determines its intracellular distribution and its GTPase activity, although recent data suggests that SUMOylation may also play a role (197). Dephosphorylation at serine-637 (S637) by the phosphatase calcineurin promotes its trafficking to mitochondria, and phosphorylation at the same residue by protein kinase A (PKA) retains DRP1 within cytosol (198-200). Interestingly, activation of a mitochondrial phosphatase identified to play a role in necroptosis - phosphoglycerate mutase family member 5 (PGAM5) – has been implicated to participate in fission by contributing to dephosphorylation DRP1 at S637, resulting in DRP1 accumulation to mitochondria and mitochondrial fragmentation (201, 202). Finally, Fission protein 1 (FIS1) is considered to be the primary adaptor of DRP1 at the OMM (191). However, very recent studies suggest that other proteins, specifically mitochondrial fission factor, and mitochondrial dynamics proteins of 49 and 51 kDa (MiD49 and MiD51), may work independently of FIS1 in recruiting DRP1 and mediating mitochondrial fission in mammalian cells (203-205).

3. Current Consensus: Fusion, Fission and Cell Viability

The current, general consensus, derived largely from experiments conducted in non-cardiac cells, is that mitochondrial fusion and the formation of mitochondrial networks favors cell survival, while mitochondrial fission and fragmentation is associated with cell death (206) (Figure 2-1). In support of this concept, multiple studies have described DRP1 translocation and mitochondrial fragmentation during apoptosis (194, 207-210). Moreover, manipulating mitochondrial dynamics by overexpressing a

dominant-negative DRP1 (DRP1^{K38A} or DRP1^{K38E}) or dominant-active MFN2 mutant both impaired mitochondrial fission under apoptotic stimuli and inhibited cytochrome *c* release and apoptotic cell death (208, 211-213). The role of mitochondrial dynamics in cardiac models (and, specifically, in IR injury) is, however, largely unexplored. The limited evidence obtained to date suggests that: i) the pathophysiologic stress of myocardial ischemia-reperfusion favors an up-regulation in mitochondrial fission, triggered by the well-described increase in intracellular [Ca^{2+}] and Ca^{2+}–dependent activation of calcineurin (196, 214, 215); ii) IR injury was accompanied by mitochondrial fragmentation; and iii) pre-ischemic inhibition of DRP1 was reported to be cardioprotective in both *in vivo* and *ex vivo* models (185, 216, 217).

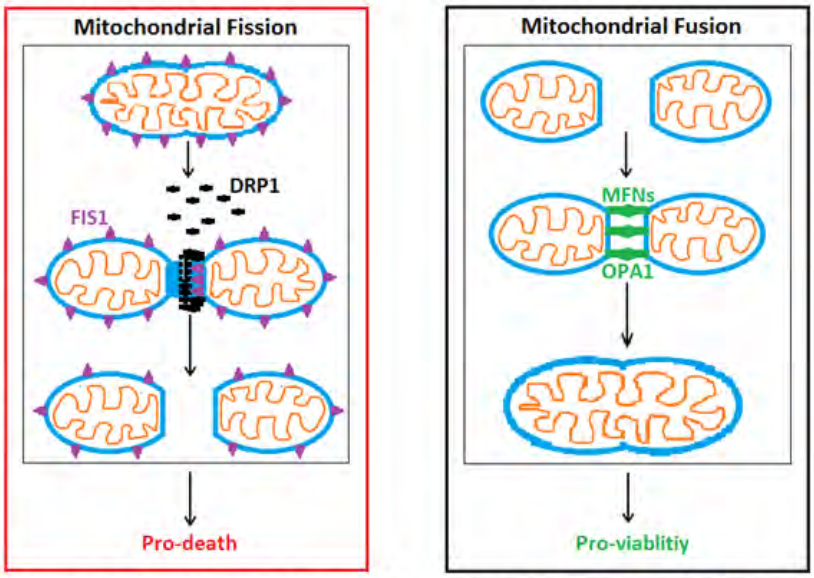

Figure 2-1. Simplified Scheme of mitochondrial fission and fusion. DRP1, dyanmin-related protein 1; FIS1, fission 1 protein; MFN, mitofusin; OPA1, optical atrophy 1.

4. Summary and Hypotheses

The role of mitochondrial dynamics in regulating cell fate is an enigma that, to date remains unresolved. Little work has been done to unequivocally establish whether mitochondrial fission simply coincides with, or actively controls, cytochrome *c* release and apoptosis. In addition, it is not clear whether DRP1 translocation onto mitochondrial outer membrane participates in proapoptotic protein release, e.g., cytochrome *c*. Previous studies aimed at defining the pathophysiologic role of

mitochondrial fission have, with only a few exceptions, been done in non-cardiac cells and non-ischemia-reperfusion models; the role of mitochondrial dynamics in the pathogenesis of myocardial ischemia-reperfusion injury is largely unexplored.

Accordingly, in this project, I have used an established *in vitro*, immortal cultured cardiomyocyte model of hypoxia-reoxygenation (mimicking IR injury) to investigate three primary hypotheses:

i. subcellular redistribution of DRP1 is i) triggered by hypoxia-reoxygenation, and ii) plays a mechanistic role in hypoxia-reoxygenation-induced cytochrome *c* release and cell apoptosis;

ii. inhibition of DRP1 translocation prior to hypoxia is cardioprotective;

iii. inhibition of DRP1 in a time-frame that is relevant as a therapeutic strategy (i.e., begun at reoxygenation) will also attenuate cardiomyocyte death, although possibly less robust than pretreatment.

CHAPTER 3

HYPOTHESIS I: HYPOXIA-REOXYGENATION TRIGGERS SUBCELLULAR REDISTRIBUTION OF DRP1

1. Rationale

Previous studies have reported that, during apoptosis: (i) DRP1 translocates to mitochondria, and (ii) mitochondria become fragmented. In addition, (iii) antagonizing DRP1 via overexpressing dominant-negative DRP1 has been shown to mitigate both cytochrome *c* release from mitochondria and apoptotic cell death in many pathological conditions. However, the vast majority of this research has been conducted in non-cardiac tissues. No studies to date have investigated whether myocardial IR injury, a classic model of apoptotic activation, will trigger DRP1 accumulation onto mitochondria, or whether DRP1 translocation contributes to cytochrome *c* release and apoptotic cardiomyocyte death in the setting of IR injury.

Accordingly, we hypothesized that hypoxia-reoxygenation (HR, simulating IR injury) will trigger DRP1 translocation to mitochondria, and that this translocation is associated with cytochrome *c* release into cytosol, apoptotic activation and cardiomyocyte death. To test this concept, we used an established model of hypoxia-reoxygenation in cultured HL-1 cardiomyocytes. In this first hypothesis, we focused on the *acute* responses to HR injury (i.e., assessed within the first 2 hours post-reoxygenation: Figure 3-1), by immunoblotting for the cellular redistribution of DRP1, cytochrome *c* leakage into cytosol, and apoptotic activation indicated by cleavage of caspase 3.

2. Materials

HL-1 mouse cardiomyocytes were kindly provided by Dr. William Claycomb

(Louisiana State University Health Science Center, New Orleans, LA). Claycomb culture medium, fetal bovine serum (FBS), L-glutamine, ascorbic acid, norepinephrine, penicillin/streptomycin, gelatin, fibronectin, 0.05% trypsin/EDTA, HEPES, sodium bicarbonate, 2-deoxy-D-glucose, mannitol, KCl, sucrose $CaCl_2$, Na-lactate, Krebs-Henseleit (KH) buffer, KCl, mannitol, and sucrose were all purchased from Sigma-Aldrich, Inc. (St Louis, MO). EGTA and EDTA solutions were ordered Boston BioProducts, Inc. (Ashland, MA). Sodium dodecyl sulfate (SDS), 30% polyacrylamide, ammonium persulfate, tetramethylethylenediamine, Tris base, nitrocellulose membranes, Triton X-100 and Tween 20 were from Bio-Rad Laboratories (Hercules, CA). Protease inhibitor cocktail tablets were ordered from Roche Diagnostics Corporation (Indianapolis, IN). Phosphatase inhibitor cocktail, Coomassie Blue Protein Assay Kit and bovine serum albumin (BSA) were purchased from Thermo Fisher Scientific Inc. (Rockford, IL).

3. Methods

3.1 HL-1 cardiomyocyte culture

HL-1 cell is an immortal mouse atrial cardiomyocyte cell line capable of maintaining a stable, contractile phenotype throughout multiple (~20) passages (218). HL-1 cells were fed every day with Claycomb medium supplemented with 10% of FBS, L-glutamine (2 mM), norepinephrine (0.1 mM) and penicillin/streptomycin (100 U/ml: 100 µg/ml). The cells were grown at 37°C in an atmosphere of 5% CO_2 and 95% air at a relative humidity of approximately 95%. Cells were grown in gelatin/fibronectin precoated culture flasks and passaged only after reaching 100% of confluence.

3.2 Hypoxia-reoxygenation

HL-1 cells, grown to ≥ 90% confluence, were subjected to 2 hours of hypoxia

achieved by a buffer exchange to ischemia-mimetic solution and placement in a sealed hypoxic chamber along with GasPak EZ Gas Generating Sachets (GasPakTM EZ, BD Biosciences, San Jose, CA) (219). Ingredients of ischemic buffer are mM, pH 6.6): 125 NaCl, 8 KCl, 1.2 KH_2PO_4 1.25 $MgSO_4$, 1.2 $CaCl_2$, 6.25 $NaHCO_3$, 20 HEPES, 5.5 glucose, 20 2-deoxy-D-glucose, 5 Na-lactate (219). Reoxygenation was achieved by a buffer exchange to serum-free Claycomb medium (SFCC) and incubation with 95% room air, 5% CO_2, 95% relative humidity at 37°C. SFCC is the same as supplemented Claycomb medium except that no FBS is added so the effects of FBS on cell signaling and cell growth are excluded. Time-matched normoxic controls were incubated for 2 hours with SFCC followed by exchange to new SFCC medium.

3.3 Cell lysis and lysate fractionation

At 5, 30 and 120 min post-reoxygenation (post-R), HL-1 cells were scraped down with the cell fractionation buffer (described below), and further lysed by multiple passes through a 26G×1/2" needle. Ingredients of sucrose-based cell fractionation buffer are (mM): 10 HEPES (pH 7.5), 1 EDTA, 1 EGTA, 10 KCl, 210 mannitol, 70 sucrose, 1.5× protease inhibitor, 1.5× phosphatase inhibitor. Cell lysates were first centrifuged at 1,000g × 5 min to discard large debris and unbroken cells. A further centrifugation at 14,000g × 15 min was used to separate the mitochondria-enriched heavy membrane (HM-Mito) from cytosol (220) . After collection of the supernatant (cytosolic proteins), the HM-Mito proteins were dissolved in fractionation buffer containing 1% Triton X-100.

3.4 Gel electrophoresis and immunoblotting

Protein concentration was determined by the Bradford assay (Bradford, *942051*). For each endpoint, proteins (10-60 µg per lane) were resolved by SDS-PAGE and transferred onto a nitrocellulose membrane. The membrane blots were blocked with 5%

nonfat dry milk in Tris-buffered saline (TBS) solution containing 0.1% Tween 20 (TBST) for 1 hr at room temperature. Blots were subsequently incubated with primary antibodies diluted in 5% BSA in TBST for overnight at 4°C, and immunoreactive bands were visualized by incubation with horseradish peroxidase (HRP)-conjugated secondary antibody diluted in 5% nonfat dry milk/TBST solution for 1 hr at room temperature. After development, images were scanned. The relative expression level of proteins was quantified by using NIH ImageJ software and normalized to corresponding loading controls (beta-actin and VDAC for cytosolic and mitochondrial proteins, respectively).

Proteins of interest were probed with the following primary antibodies: anti- DRP1 (BD Biosciences, San Jose, CA), cytochrome *c* (BD Biosciences, San Jose, CA) full-length (FL) and cleaved caspase 3 (Cell Signaling Technology, Boston, MA), and VDAC and beta-actin (Cell Signaling Technology, Boston, MA). HRP-conjugated anti- rabbit and mouse secondary antibodies were purchased from Sigma-Aldrich, Inc. (St Louis, MO). For detailed information of antibody dilution, please refer to Table 3-1.

Table 3-1. Immunoblotting protocol

Proteins / Items	HM-Mito			Cytosol/ Whole cell lysate				
	DRP1	**cytochrome *c***	**VDAC**	**DRP1**	**cytochrome *c***	**FL-caspase 3**	**cleaved-caspase 3**	**β-actin**
Loading (µg)	35	5	5	10	10	10	50 - 60	10
Gel concentration (%)	8	12	12	8	12	12	15	8 - 12
PAGE	100 volts/120 mins at RT							
Transfer	100 volts/90 mins at 4°C							
1st Ab dilution (5% BSA in TBST)	1:1000	1: 8000	1:4000	1:8000	1: 1000	1: 4000	1:500	1:1000
Time of 1st Ab	> = 15 hrs at 4°C							
Vendors of 1st Abs	BD	BD	CST	BD	BD	CST	CST	CST
2nd Ab dilution (5% NFDM in TBST)	1:10K	1: 20K	1:10K	1:20K	1:10K	1:10K	1:5K	1:5K
Time of 2nd Ab	1 hr at RT							
Exposure & development	Seconds to minutes: dependent on protein and quality of blotting.							

PAGE, polyacrylamide gel electrophoresis; BSA, bovine serum albumin; TBST, tris-base buffered saline containing 0.1% Tween 20; Ab, antibody; NFDM, nonfat dry milk; RT, room temperature; BD, BD Biosciences, San Jose, CA; CST, Cell Signaling Technology, Boston, MA.

3.5 Data and statistical analysis

Data are presented as means ± SEM and analyzed with GraphPad Prism software, (GraphPad Software, Inc, La Jolla, CA). Endpoints were compared among groups by one-way Analysis of Variance (ANOVA) and, if significant F-values were obtained, pairwise *post-hoc* comparisons were made using the Newman–Keuls method. *P* values < 0.05 were considered statistically significant.

4. Results

4.1 HR triggers DRP1 translocation to mitochondria

As shown in Figure 3-1 (right), hypoxia-reoxygenation triggered a rapid and significant increase in DRP1 in the mitochondria-enriched heavy membrane (HM-mito) fraction. The increase was seen at 5 min post-R (*****P < 0.05 *versus* normoxic controls), and was maintained for at least 2.0 hrs post-R (******P < 0.01 at 30 and 120 min post-R *versus* normoxic controls. As expected, mitochondrial recruitment of DRP1 to mitochondria was accompanied by significant reductions in DRP1 expression within cytosol *versus* normoxic controls (Figure 3-2, left).

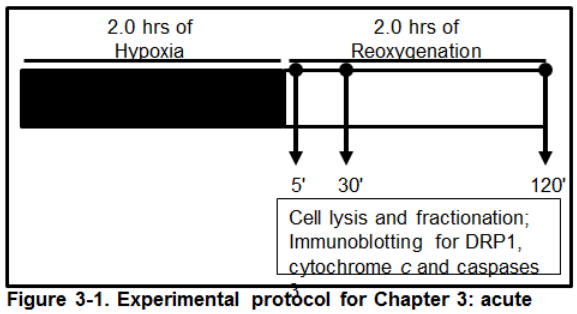

Figure 3-1. Experimental protocol for Chapter 3: acute responses in HR injury.

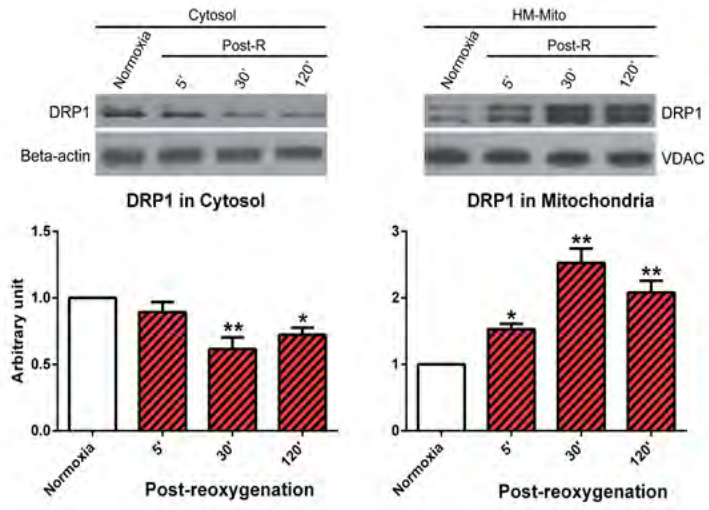

Figure 3-2. Hypoxia-reoxygenation triggers DRP1 translocation to mitochondria. Original immunoblots of DRP1 (top panels), and mean values of DRP1 expression (±SEM: bottom panels) in HL-1 cells subjected to 2 hrs hypoxia followed by 5 min, 30 min or 2 hrs reoxygenation and normoxic controls. Results obtained in the cytosolic and mitochondria-enriched heavy membrane (HM-mito) fractions are shown in the left and right panels, respectively. N-values = 4 replicates per group. **P*<0.05; ***P*<0.01 *versus* normoxic controls.

4.2 DRP1 movement to mitochondria is associated with cytochrome *c* release into cytosol

Redistribution of DRP1 accumulation to mitochondria was associated with release of cytochrome *c* from mitochondria into cytosol. As shown in Figure 3-3 (left), HR caused significant cytochrome *c* leakage into cytosol that was seen as early as 5 min post-R and continued at 30 min and 2 hr post-R (*****P* < 0.05 *versus* normoxic controls). This was accompanied by a decrease in expression of cytochrome *c* in the HM-Mito fraction (******P* < 0.01 *versus* normoxic controls (Figure 3-2, right)).

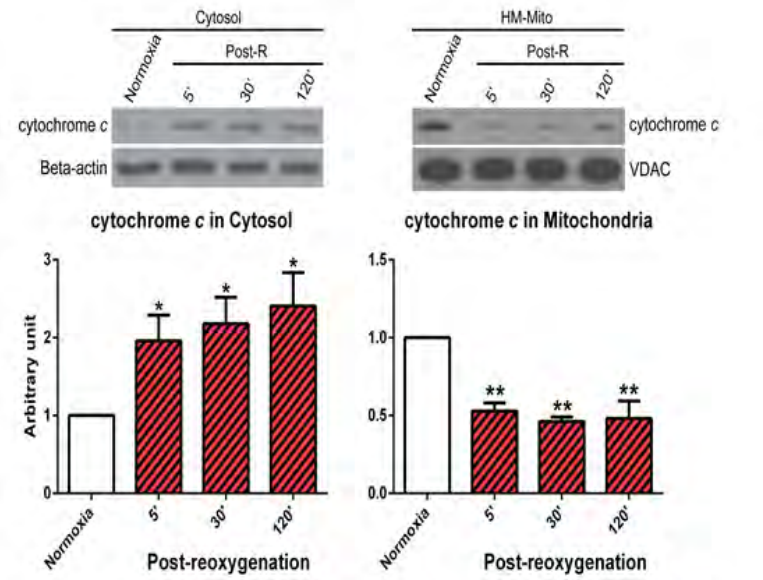

Figure 3-3. HR causes cytochrome *c* release into cytosol from mitochondria. Original immunoblots of cytochrome *c* (top panels), and mean values of cytochrome *c* expression (±SEM: bottom panels) in HL-1 cells subjected to 2 hrs hypoxia followed by 5 min, 30 min or 2 hrs reoxygenation and normoxic controls. Results obtained in the cytosolic and mitochondria-enriched heavy membrane (HM-mito) fractions are shown in the left and right panels, respectively. N-values = 7 and 5 replicates per group in cytosolic and HM-Mito fractions, respectively. **P*< 0.05; ***P*< 0.01 *versus* normoxic controls.

4.3 DRP1 translocation and cytochrome *c* release leads to apoptotic activation

Caspase 3 is the effector caspase, located in the cytosol, that performs the suicidal function during apoptosis. Accordingly, we focused on assessment of the expression of FL- and cleaved caspase 3 in our model. We found that DRP1 translocation to mitochondria and cytochrome *c* release into cytosol was accompanied by: (i) a significant reduction in the expression of FL-caspase 3 (*****P* < 0.05 at 5 and 30 min; ******P* < 0.01 at 120 min post-R *versus* normoxic controls) and (ii) a corresponding increase in cleaved caspase 3 that achieved significance at 2 hrs post-R (Figure 3-4).

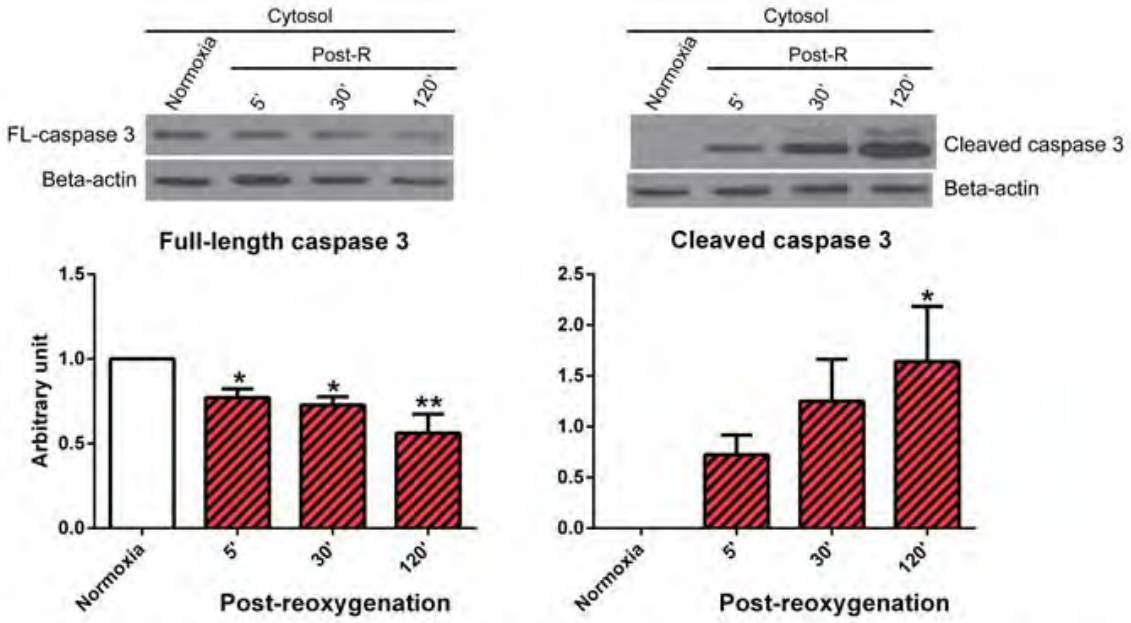

Figure 3-4. DRP1 translocation and cytochrome *c* release leads to apoptotic activation, indicated by increased production of cleaved caspase 3 and decreased expression FL-caspase. Original immunoblots of FL-caspase 3 and cleaved caspase 3 (top panels), and mean values of FL-caspase 3 and cleaved caspase 3 expression (±SEM: bottom panels) in HL-1 cells subjected to 2 hrs hypoxia followed by 5 min, 30 min or 2 hrs reoxygenation and normoxic controls. Results obtained in the cytosolic and mitochondria-enriched heavy membrane (HM-mito) fractions are shown in the left and right panels, respectively. N-values = 5 and 4 replicates per group for immunoblots of FL-caspase 3 and cleaved caspase 3, respectively. *P< 0.05; **P< 0.01 *versus* normoxic controls.

5. Summary

In summary, HR triggered DRP1 translocation to mitochondria. This translocation was associated with cytochrome *c* release into cytosol and the resultant activation of apoptosis, indicated by the reduced expression of FL-caspase 3 and increased production of cleaved caspase 3.

CHAPTER 4

HYPOTHESIS II: PREISCHEMIC INHIBITION OF DRP1 IS CARDIOPROTECTIVE– PHARMACOLOGIC APPROACH: MDIVI-1

1. Rationale

Our studies summarized in Chapter 3 demonstrate that hypoxia-reoxygenation promotes DRP1 translocation to mitochondria, which is associated with cytochrome *c* release and apoptotic activation, indicated by increased production of cleaved caspase 3 in HL-1 cardiomyocytes. However, these data do not establish a cause-effect relationship between DRP1 redistribution to mitochondria and cardiomyocyte injury.

There is a small molecule antagonist, mitochondrial division inhibitor 1 (Mdivi-1), that specifically inhibits DRP1 self-assembly and its mitochondrial accumulation and mitochondrial fission during apoptosis, reportedly without off-target effects on other GTPase family members (210, 221). Mdivi-1 has also been shown to significantly reduce cytochrome *c* release and attenuate the effects of apoptotic stimuli (221). Moreover, one previous study (185), conducted using heart and cardiomyocyte models, has reported that inhibition of DRP1 by Mdivi-1 prior to ischemia mitigates mitochondrial fission and attenuates IR injury. However, the detailed molecular machinery of DRP1-inhibition mediated cardioprotection is still largely unknown.

We hypothesize that inhibition of DRP1 with Mdivi-1 prior to hypoxia will: i) attenuate DRP1 translocation, reduce cytochrome *c* release and blunt apoptosis activation; and ii) provide cardioprotection against HR injury. To test our hypothesis, we used the same model-cultured HL-1 cardiomyocytes subjected to hypoxia-reoxygenation – described in Chapter 3. We focus on both the acute responses (up to 2 hours of reoxygenation) and late responses (24 hours post-R). The main endpoints

assessed acutely are the subcellular expression of DRP1, cytochrome *c* and caspase 3 by immunoblotting (Figure 4-1, top panel). The main focus of the late response includes viability assessment by trypan blue staining, immunoblotting for DRP1 in the HM-Mito fraction, and evaluation of apoptosis, mitochondrial morphology and co-localization of DRP1 with mitochondria by immunofluorescence (IF) microscopy (Figure 4-1, bottom panel).

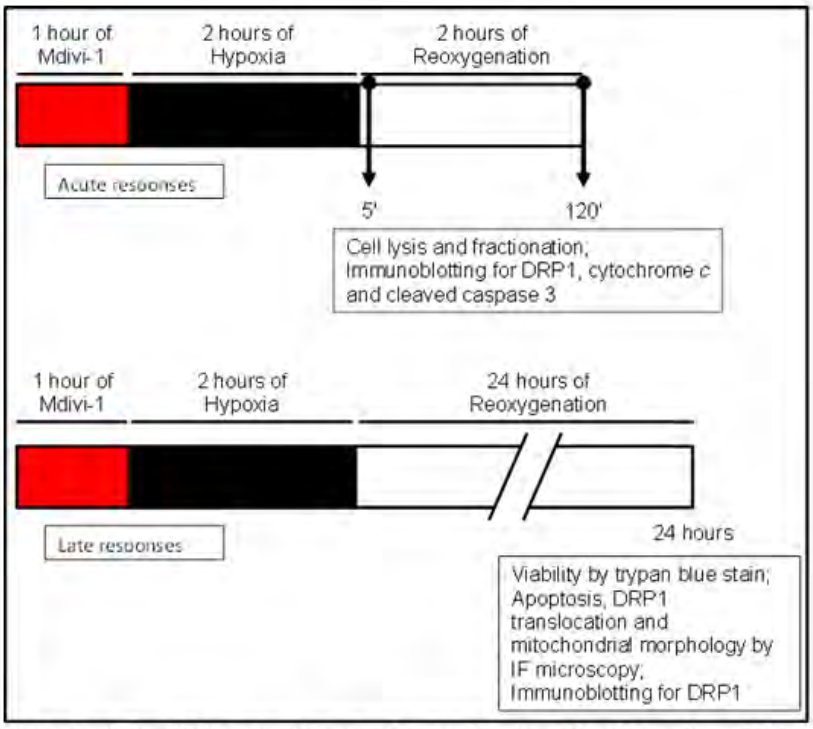

Figure 4-1. Scheme of experiments in Chapter 4. Major endpoints of acute responses (top panel) and late responses (bottom panel) to Mdivi-1 treatment. Treatment groups: Mdivi-1 (50 μM) or vehicle-control.

2. Materials

Cultured HL-1 cardiomyocyte and all chemicals and reagents were the same as those used in Chapter 3 unless annotated below. Mdivi-1 was ordered from Sigma-Aldrich, Inc. (St Louis, MO) and dissolved in DMSO in a stock concentration of 50 mM. Trypan blue dye (0.4%) was ordered from Fisher Scientific (Pittsburg, PA).

3. Methods

3.1 HL-1 cardiomyocyte culture

Refer to Chapter 3, Section 3.1.

3.2 Cytotoxicity of Mdivi-1

One previous study (185), conducted using HL-1 cardiomyocyte model, has

reported that inhibition of DRP1 by 50 μM Mdivi-1 prior to ischemia attenuated mitochondrial fission and reduced IR injury, while a lower concentration of Mdivi-1 (10 μM) had no effect on either endpoint. Additionally, in non-cardiac system, 50 μM Mdivi-1 was reported to cause net-like mitochondrial morphology, nullify GTPase activity of DRP1 and attenuate cell apoptosis caused by apoptotic stimuli (221). Therefore, based on these previous studies, we started our protocols focusing on DRP1 inhibition with a dose of 50 μM Mdivi-1.

For assessment of toxicity, HL-1 cardiomyocytes were incubated with 50 μM Mdivi-1 (diluted in the media from a stock concentration of 50 mM prepared in DMSO), vehicle (DMSO), or media alone for 5 hours under normoxic conditions to match the time courses of our later, acute hypoxia-reoxygenation experiments (see Figure 4-1). After that, cells were lysed. To assess whether Mdivi-1 treatment alters the expression of DRP1 or causes cytotoxicity, the whole cell lysates were probed (by immunoblotting) for the expression of DRP1, and FL- and cleaved caspase 3.

3.3 Hypoxia-reoxygenation

Refer to Chapter 3, Section 3.2. Cells were incubated for 1 hour under normoxic conditions with 50 μM Mdivi-1 or vehicle, and then subjected to 2 hours of hypoxia. For assessment of acute responses, cells were reoxygenated for up to 2 hours, and, for late responses, cells were reoxygenated for 24 hours.

3.4 Cell lysis and lysate fractionation

Refer to Chapter 3, Section 3.3.

3.5 Cell viability assay using trypan blue staining

At 24 hours post-R, HL-1 cells were trypsinized and resuspended in media to reach a final cell density of 2,000,000 to 3,000,000 per mL. Each volume of cells was

mixed with equal volume of 0.4% trypan blue dye. Trypan blue dye penetrates dead cells, in which the sarcolemmal membrane is compromised, but it fails to enter (is excluded from) viable myocytes with an intact cell membrane. Thus, dead cells appear blue while viable cells are unstained. By this mean, viable *versus* dead cells were quantified from phase contrast illumination for 20x objective on an inverted phase-contrast light microscope (Fisher Scientific, Pittsburg, PA); a total of 250 cells counted in every group per independent experiment.

3.6 Gel electrophoresis and immunoblotting

Refer to Chapter 3, Section 3.4.

3.7 Immunofluorescence (IF) microscopy

3.7.1 Protocol

HL-1 cells were grown on gelatin/fibronectin precoated coverslips for 24 hours to reach 40 – 50% confluence, pretreated with 50 μM Mdivi-1 or vehicle for 1 hour, and subjected to 2 hours of hypoxia and 24 hours of reoxygenation. Cells were then fixed in 4% paraformaldehyde (PFA), permeabilized and blocked in 5% goat serum/ 0.3% Triton X-100/ 1× PBS, and incubated overnight at 4°C in primary antibodies against:

i. ATP synthase β subunit (ATPB; Abcam, Cambridge, MA: to identify mitochondria) + cleaved caspase 3 (Cell Signaling Technology, Boston, MA), or
ii. ATPB + DRP1 (Cell Signaling Technology, Boston, MA).

This was followed by 90 min of incubation with goat anti- rabbit (Alexa Fluor 488-conjugated) or mouse (Alexa Fluor 555-conjugated) secondary antibodies (targeting rabbit derived anti- DRP1 or cleaved caspase 3 IgGs and mouse derived anti-ATPB IgG , respectively: Life Technologies, Carlsbad, CA) at room temperature. After the addition of one drop of antifade reagent with DAPI (Life Technologies, Carlsbad, CA) to

stain nuclei, the coverslips were mounted on glass slides and sealed with nail polisher. For a detailed summary of the staining protocol and antibody dilutions, please refer to Table 4-1.

Table 4-1. Immunofluorescence staining protocol

Proteins / Items	DRP1	ATPB	cleaved caspase 3
Fixation	4% PFA × 15 mins		
Permeabilization & block	5% Goat serum/ 0.3% Triton X-100/ 1×PBS		
1st Ab dilution (5% Goat serum/ 0.3% Triton X-100/1×PBS)	1:50 (Rb)	1:2000 (Ms)	1:200 (Rb)
1st Ab incubation time	4°C overnight		
Vendors of 1st Abs	CST	Abcam	CST
2nd Ab dilution (5% Goat serum/ 0.3% Triton X-100/ 1×PBS)	1:200	1:2000	1:200
2nd Ab incubation time	90 mins at RT		
Vendor of 2nd Abs	Alexa Fluor 488/anti-Rb, Life Technologies	Alexa Fluor 555/anti-Ms, Life Technologies	Alexa Fluor 488/anti-Rb, Life Technologies

ATPB, ATP synthase β subunit; PFA, polyformaldehyde; PBS, phosphate buffered saline; Ab, antibody; Rb, rabbit; Ms: mouse; RT, room temperature; CST, Cell Signaling Technology, Boston, MA; Abcam, Cambridge, MA; Life Technologies, Carlsbad, CA

Cells were imaged with a Leica TCS SP5 confocal system (Leica Microsystems, Heidelberg, Germany), using a 63× immersion oil objective and CCD camera. In short, 405 nm diode laser, 488 nm Argon laser and 543 nm HeNe laser were used to excite the fluorescence dyes. The image format was set as 1,024 × 1,024 pixels with a scan speed of 400 Hz. To further optimize the image quality, the Line Average was set as 6. The emitted fluorescence passing through an emission filter was detected by CCD camera. For identification of proteins or structures of interest, mitochondria were marked red by an antibody bound to Alexa Fluor 555, DRP1 or cleaved caspase 3 were labeled green by antibodies bound to Alexa Fluor 488, and nuclei were stained blue with DAPI. To resolve multi-focal profiles of mitochondrial morphology and co-localization of mitochondrial and DRP1 signals, the acquisition model was selected as XYZ and Z-Stack. The step size was set as 0.4-0.5 µM and, usually, the complete mitochondrial

morphology required 3-5 sequential Z-scans. The sequential images were subsequently exported as TIFF files in either merged or separate channels, with each file representing an individual image of a Z-slice (every 0.4-0.5 µM in step size). The individual Z-slices were then reconstructed into a single Z-stack image composed of merged Z-slices using NIH ImageJ software Z-projection function (222). Confocal images were processed for contrast and brightness adjustment and cropped to have uniform size for publication using Photoshop software (Adobe Systems Inc.). Representative images were obtained from four replicates of three independent experiments. For each replicate, at least 3-4 images were taken for vehicle and Mdivi-1 groups, respectively.

3.7.2 Detection of apoptotic cells

During the activation of apoptosis, full-length caspase 3 is cleaved into smaller fragments, e.g., P17 and P12 subunits (223-225). Samples were probed with fluorescent (green) labeled anti-cleaved caspase 3 antibody that only recognizes fragments resulting from cleavage adjacent to Asp175 rather than the FL-caspase 3 (226, 227), thereby allowing us to differentiate apoptotic (green) *versus* non-apoptotic cells.

Cells were imaged with a Leica TCS SP5 confocal system (Leica Microsystems, Heidelberg, Germany) using the same parameters described in Section 3.7.1 with one exception: no Z-scan was required for the detection of apoptotic activation. For each image, we counted the number of cleaved caspase 3 positive cells (green), normalized to the total number of cells (marked by staining of DAPI (blue)-labeled nuclei). Results were obtained from four replicates of three independent experiments. For each replicate, 3-4 images were taken for vehicle and Mdivi-1 groups, respectively, and at

least 100 cells were counted.

3.7.3 Co-localization and hue analysis

To assess the spatial association of DRP1 (green) with mitochondria (ATPB: red), two techniques were applied:

i. Standard co-localization analysis (228, 229): confocal images were analyzed with NIH ImageJ software using Just Another Colocalization Plugin (JACOP) (230) and Pearson's coefficient was calculated. Co-localization analysis provides an index of the spatial overlap between the red channel (labeling mitochondria) and green channel (labeling DRP1), or in other words, assesses whether DRP1 and mitochondria are located at the same sites within the cell. Pearson's coefficient is an indicator of overlap and co-localization, and ranges from a maximum of 1 (denoting complete spatial overlap between the red and green channels) to a minimum of -1 (denoting no overlap at all).

ii. Hue analysis (231-233): using merged images, in which both mitochondria (red) and DRP1 (green) were visualized, the numbers of red, green and yellow pixels were quantified using SigmaScan 5.0 (Systat Software Inc., San Jose, CA). Red + yellow pixels represent the total mitochondrial signal, and green + yellow pixels represent the total DRP1 signal, while yellow pixels (overlap of red and green) reflect the proportion of the DRP1 signal spatially associated with the mitochondrial signal. For a detailed description of hue analysis, please refer to the Appendix.

3.8 Data and statistical analysis

Data are presented as means ± SEM and analyzed with GraphPad Prism software, GraphPad Software, Inc (La Jolla, CA). For comparison between two groups,

unpaired student *t*-test was performed. For comparisons among three or more groups, one or two-way ANOVAs were performed as appropriate and pairwise *post-hoc* comparisons were made using the Newman–Keuls method if F-values reached significance. *P*- values < 0.05 were considered statistically significant.

4. Results

4.1 Mdivi-1 is not toxic

There were no differences in expression of DRP1 or FL-caspase 3 among groups of normoxic cells incubated for 5 hours with 50 µM Mdivi-1, DMSO vehicle or blank control (media only) (Figure 4-2). In addition, there was no evidence of caspase 3cleavage in any of the three groups, including cells treated with Mdivi-1 (data not shown as there was no detection of cleaved caspase 3 by immunoblotting). Thus, prolonged incubation with Mdivi-1 is not toxic.

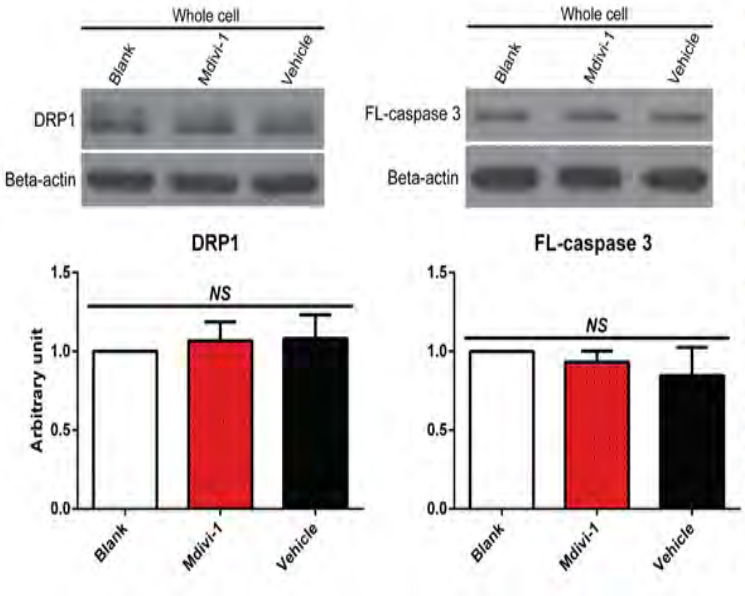

Figure 4-2. Incubation with Mdivi-1 is not toxic. Five hours of incubation with 50µM Mdivi-1 did not change the expression of either DRP1 or full-length caspase 3. Original immunoblots of DRP1 and FL-caspase 3 (top panels, – left and – right, respectively), and mean values of DRP1 and FL-caspase 3 expression (±SEM: bottom panels, – left and – right , respectively) in HL-1 cells incubated for five hours with 50 µM Mdivi-1, DMSO vehicle or blank control (media only) under normoxic conditions. There were no differences in expression of DRP1 or caspase 3 among groups. In addition, there was no evidence of caspase 3 cleavage in any of the three groups, including cells treated with Mdivi-1 (data not shown). N-values = 3 replicates per group. ***NS***, not significantly differ among groups.

4.2 Acute responses

4.2.1 Mdivi-1, given prior to hypoxia, attenuated DRP1 translocation to mitochondria

As expected from the results obtained in Chapter 3, hypoxia-reoxygenation was associated with translocation of DRP1 to mitochondria (Figure 4-3). Preincubation with Mdivi-1 for 1 hour before hypoxia attenuated this subcellular redistribution of DRP1 to mitochondria (***P*< 0.05 *versus* vehicle control at 120 min post-R; Figure 4-3).

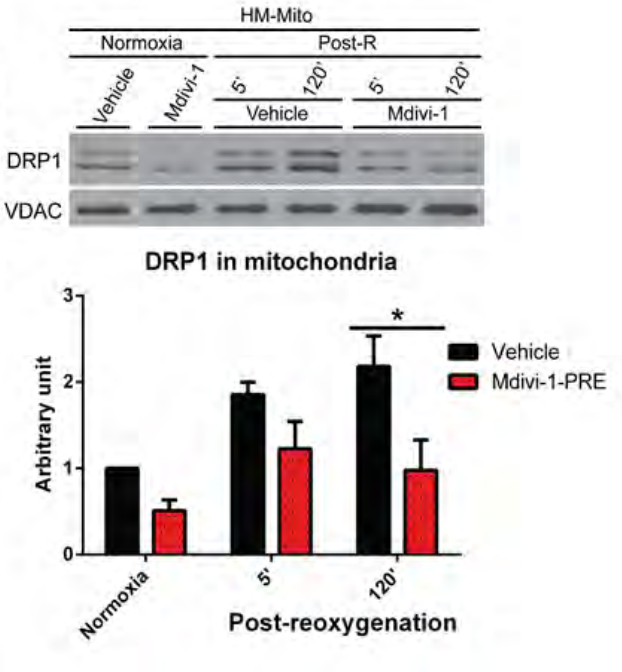

Figure 4-3. Prehypoxic administration of Mdivi-1 significantly attenuated DRP1 accumulation onto mitochondria. Original immunoblots of DRP1 (top panels), and mean values of DRP1 expression (±SEM: bottom panels) in HL-1 cells subjected to i) normoxia, and ii) 2 hours hypoxia followed by 5 min or 2 hours reoxygenation. Results obtained in the mitochondria-enriched heavy membrane (HM-mito) fraction are shown. N-values = 5 replicates per group. **P*< 0.05 *versus* vehicle controls at 2 hours post-R.

4.2.2 Pretreatment with Mdivi-1 reduced cytochrome c release and cleaved caspase 3 production

In the vehicle-control group, DRP1 translocation was, as expected, accompanied by release of cytochrome *c* into cytosol (left panel, Figure 4-4) and activation of apoptotic machinery as indicated by production of cleaved caspase 3 (right panel, Figure 4-4). In contrast, in cells pretreated with Mdivi-1, release of cytochrome *c* into cytosol and production of cleaved caspase 3 were both attenuated when compared with

vehicle control: ***P*< 0.01 at 120 min post-R *versus* vehicle control; Figure 4-4).

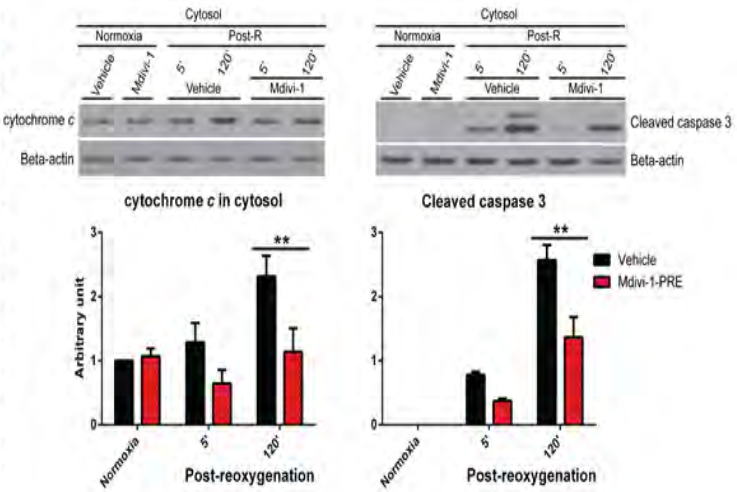

Figure 4-4. Attenuated DRP1 translocation to mitochondrial was associated with significant reductions in cytochrome *c* release into cytosol and caspase 3 cleavage (marker of apoptotic activation). Original immunoblots of cytochrome *c* and cleaved caspase 3 (top panels, – left and –right, respectively), and mean values of cytochrome *c* expression and cleaved caspase 3 (±SEM: bottom panels, – left and – right, respectively) in HL-1 cells subjected to i) normoxia, or ii) 2 hours hypoxia followed by 5 min or 2 hours reoxygenation. Results obtained in the cytosolic fraction are shown. N-values = 5 and 6 replicates per group for the results of cytochrome *c* and cleaved caspase 3 immunoblots, respectively. ***P*< 0.01; ***P*< 0.01 *versus* vehicle controls at 2 hours post-R.

4.3 Late responses

4.3.1 Mdivi-1, given prior to hypoxia, increased HL-1 cardiomyocyte viability

Two hours of hypoxia + 24 hours of reoxygenation reduced the proportion of viable cells (assessed by trypan blue staining) in the vehicle control group to 65±3% (Figure 4-5). Administration of Mdivi-1 before hypoxia significantly increased HL-1 cardiomyocyte viability to 79±3% (**: *P*< 0.01*versus* vehicle control; Figure 4-5).

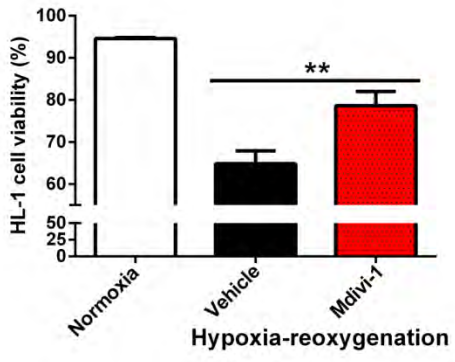

Figure 4-5. Addition of Mdivi-1 (50 μM) prior to hypoxia is cytoprotective. Mean values of viability (%, ± SEM) in HL-1 cells subjected to 2 hours hypoxia followed by 24 hours reoxygenation or a time-matched normoxic period. Treatment with Mdivi-1 prior to hypoxia was protective: % cell viability was 79±3% *vs*. 65±3% in vehicle controls (**: *P*< 0.01). N-values ≥ 5 replicates per group; for each replicate, at least 250 cells were counted for every group.

4.3.2 Prehypoxic administration of Mdivi-1 attenuated the proportion of apoptotic cells

At 24 hours post-reoxygenation, the proportion of cleaved caspase 3-positive

cells (as detected by green immunofluorescence) in vehicle-control cells was 17±2% (Figure 4-6). In contrast, in cells pretreated with Mdivi-1, the % of apoptosis-positive cells was reduced to 5±1% (**: *P*< 0.01 *versus* vehicle-control; Figure 4-6).

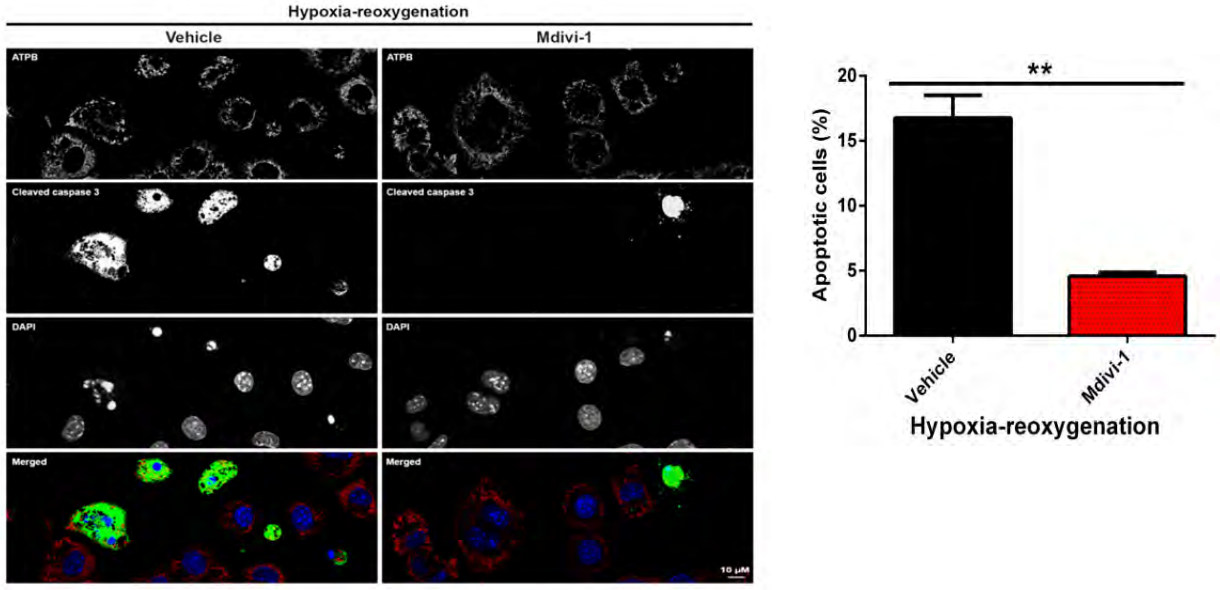

Figure 4-6. Addition of Mdivi-1 prior to hypoxia reduced the percentage of cleaved caspase 3-positive cells. Left panel: Original confocal IF images of HL-1 cells subjected to 2 hours hypoxia followed by 24 hrs reoxygenation. Cleaved caspase 3 was detected using a green fluorescent-labeled antibody, the mitochondrial network was labeled using an antibody targeting ATPB antibody (red) and nuclei were counter-stained with DAPI (blue). Representative images were taken from four replicates (N-values = 4 replicates per group). Right panel: quantitative analysis of cleaved caspase 3 positive HL-1 cells, expressed as a % of the total number of cells (marked by DAPI-labeled nuclei). Treatment with Mdivi-1 (50 µM) prior to hypoxia was protective: % cleaved caspase 3 positive cells was significantly reduced from 17±2% in vehicle controls to 5±1% in Mdivi-1 treated cells (**P< 0.01). N-values = 4 replicates per group; for each replicate, 3 – 4 images were taken for vehicle and Mdivi-1 groups, respectively; at least 100 cells were counted.

4.3.3 Prehypoxic administration of Mdivi-1 decreased mitochondrial fragmentation and preserved normal mitochondrial morphology

Qualitative inspection of cells stained with the mitochondrial marker ATPB showed that normoxic cells were, as expected, characterized by a fiber-like network of mitochondria (Figure 4-7: normoxia panel – left). Hypoxia-reoxygenation caused fragmentation (fission) of mitochondria, as indicated by the punctate pattern of ATPB staining that persisted at 24 hours post-R (Figure 4-7, hypoxia-reoxygenation panel – left). However, 1 hour of prehypoxic treatment with Mdivi-1 attenuated fission and in

part preserved the fiber-like normoxic mitochondrial phenotype (Figure 4-7, hypoxia-reoxygenation panel – right).

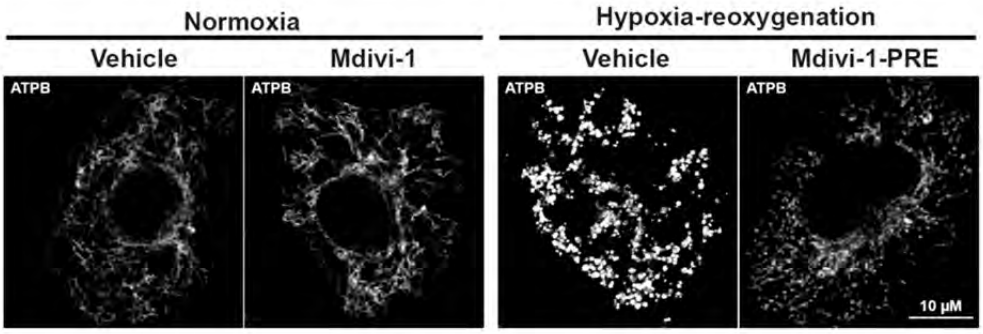

Figure 4-7. Prehypoxic administration of Mdivi-1 preserved mitochondrial morphology. Original gray-scale confocal IF images of HL-1 cells subjected to 2 hours hypoxia followed by 24 hours reoxygenation using ATPB (mouse-derived) antibody to label the mitochondrial network. Representative images were taken from four replicates (N-values = 4 replicates per group). Hypoxia-reoxygenation caused mitochondrial fission; i.e., the mitochondrial phenotype was changed from the fiber-like network seen under normoxic conditions (left) into punctate dots (HR panel, – left). Mdivi-1 (50 µM) given prior to hypoxia-reoxygenation preserved the fiber-like normoxic mitochondrial morphology (HR panel, – right).

4.3.4 Effect of pretreatment with Mdivi-1 on the subcellular distribution of DRP1 was not maintained at 24 hours post-reoxygenation.

4.3.4.1 Immunoblot evidence

In our acute-phase experiments, we found that Mdivi-1 given prior to hypoxia significantly reduced DRP1 translocation to mitochondria during the first 2 hours post-R as assessed by immunoblotting (Figure 4-3). However, at 24 hours post-R, DRP1 expression in the HM-Mito fraction in cells pretreated with Mdivi-1 did not differ significantly *versus* vehicle-controls (Figure 4-8: all *P* values≥ 0.2).

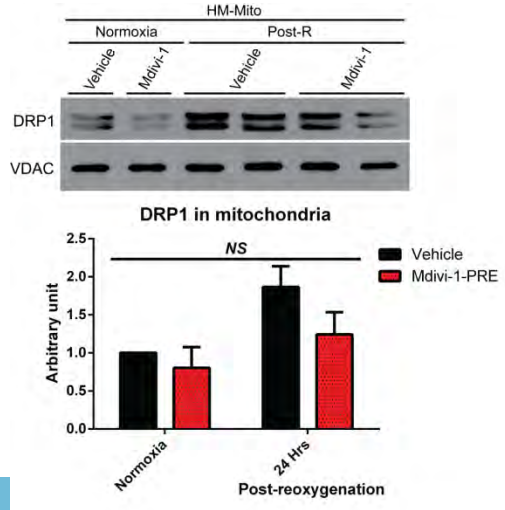

Figure 4-8. Prehypoxic administration of Mdivi-1 had no significant effect on the association of DRP1 with mitochondria assessed at 24 hours post-R: immunoblot evidence. Original immunoblots of DRP1 (top panels), and mean values of DRP1 expression (±SEM: bottom panels) in HL-1 cells subjected to i) normoxia, or ii) 2 hours hypoxia followed by 24 hours reoxygenation. Results obtained in the mitochondria-enriched heavy membrane (HM-Mito) fraction are shown. N-values = 3 and 6 replicates for normoxic and hypoxia-reoxygenation groups, respectively. ***NS***, no difference in DRP1 expression in the HM-Mito fraction in Mdivi-1 treated groups *versus* vehicle controls at 24 hrs post-R (all *P* values≥ 0.2).

4.3.4.2 Co-localizaion analysis via ImageJ

Results obtained by immunoblotting were supported by co-localization analysis of immunofluorescence images. There were no differences in the co-localization of the red channel (labeling mitochondria) and green channel (labeling DRP1) at 24 hours post-R, as determined by comparison of the Pearson's coefficients among cells subjected to HR or maintained under normoxic conditions and treated with Mdivi-1 or vehicle (Figure 4-9).

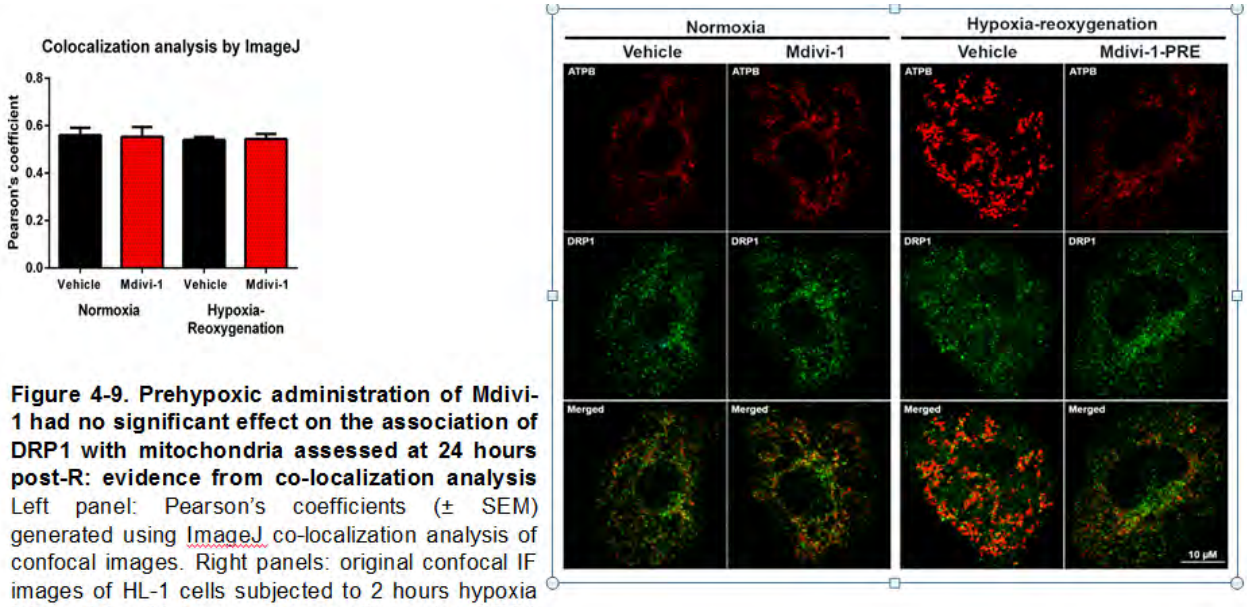

Figure 4-9. Prehypoxic administration of Mdivi-1 had no significant effect on the association of DRP1 with mitochondria assessed at 24 hours post-R: evidence from co-localization analysis Left panel: Pearson's coefficients (± SEM) generated using ImageJ co-localization analysis of confocal images. Right panels: original confocal IF images of HL-1 cells subjected to 2 hours hypoxia followed by 24 hours reoxygenation using DRP1 (rabbit-derived) antibody (green) labeling the cellular distribution of DRP1 and ATPB (mouse-derived) antibody (red) visualizing the mitochondrial network. There were no differences among groups in the co-localization of the red channel (labeling mitochondria) and green channel (labeling DRP1) at 24 hours post-R: correlation coefficients averaged 0.54-0.56 in all groups. N-values ≥ 20 cells per group.

4.3.4.3 Hue analysis

Similar results were obtained by hue analysis: there was no difference in the association of the DRP1 signal with the mitochondrial signal among groups at 24 hours post-reoxygenation (Figure 4-10).

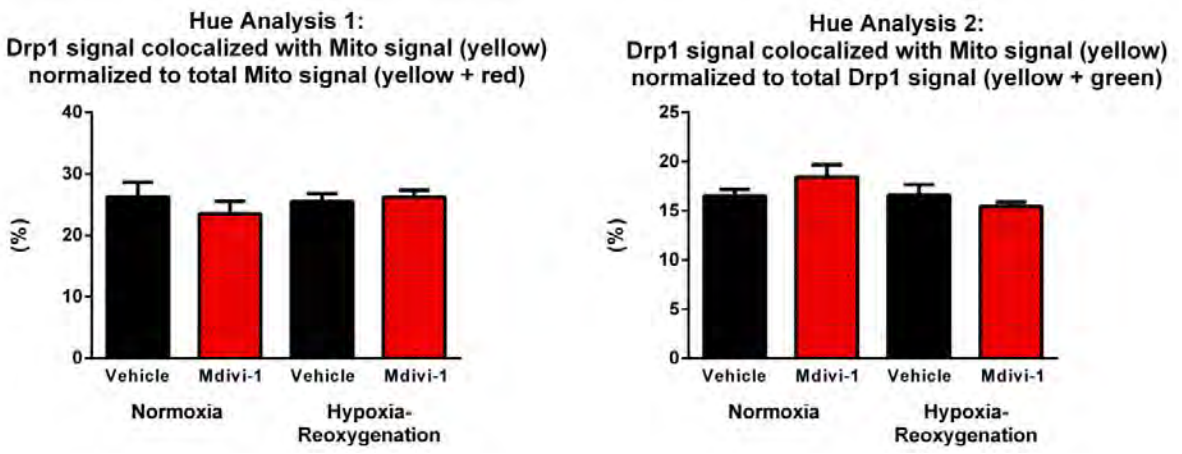

Figure 4-10. Prehypoxic administration of Mdivi-1 had no significant effect on the association of DRP1 with mitochondria assessed at 24 hours post-R: evidence from hue analysis. Quantitative results of hue analysis: % yellow pixels (overlap of green and red fluorescent signals) at 24 hours post-reoxygenation with or without Mdivi-1 pretreatment. There were no differences among groups in the association of the DRP1 signal with the mitochondrial signal at 24 hours post-reoxygenation, as determined either by: i) % DRP1 signal co-localized with mitochondrial signal (yellow) when normalized to total mitochondrial signal (yellow + red) (left panel), or ii) % DRP1 signal co-localized with mitochondrial signal (yellow) when normalized to total DRP1 signal (yellow + green) (right panel). N-values ≥ 20 cells per group.

5. Summary

In summary, and consistent with our hypothesis, we found that pretreatment with Mdivi-1 was protective. This is supported by our evidence that prehypoxic administration of Mdivi-1: i) significantly reduced DRP1 translocation to mitochondria, attenuated cytochrome c release and blunted apoptotic activation (indicated by a decrease in caspase 3 cleavage) at 2 hours post-R; and ii) significantly increased cell viability (assessed by trypan blue staining) and reduced the proportion of apoptotic cells (detected by IF) at 24 hours post-reoxygenation.

We also confirmed by IF microscopy that, as expected, HR triggered mitochondrial fission and that prehypoxic administration of Mdivi-1 attenuated the fragmentation of the mitochondrial network. These qualitative observations are consistent with the immunoblot data obtained acutely (within 2 hours post-R), and suggest that the effects of HR and Mdivi-1 pretreatment on mitochondrial morphology

persist at 24 hours post-reoxygenation. In contrast, results obtained by both immunoblotting and IF microscopy showed that HR-induced subcellular redistribution of DRP1 to the mitochondria appears to be an early and acute effect. That is: using three analyses, we found no difference in the co-localization of DRP1 with mitochondria at 24 hours post-R among normoxic or hypoxia-reoxygenated cells, treated with Mdivi-1 or vehicle.

CHAPTER 5

GENETIC APPROACH: siRNA

1. Rationale

Our studies presented in Chapter 4 support the hypothesis of a cause-effect relationship between DRP1 translocation to mitochondrial and cardiomyocyte injury in the setting of HR: i.e., inhibition of DRP1 translocation by treatment with Mdivi-1 prior to hypoxia significantly reduced DRP1 accumulation to mitochondria, cytochrome *c* release and apoptotic activation, thus better preserving mitochondrial morphology and significantly increasing cardiomyocyte viability. If this is true, then genetic down-regulation of DRP1 expression before HR should achieve similar cardioprotective effects as inhibition of DRP1 translocation with Mdivi-1. The results of genetic approach, that is to silence DRP1 expression before hypoxia will further confirm the studies of inhibiting by pharmacologic approach. To test this concept and confirm the outcome obtained with pharmacologic inhibition, we knocked down the expression of DRP1 using specific siRNA and quantified viable *versus* dead cells in DRP1 siRNA transfected cardiomyocytes *versus* controls (Figure 5-1).

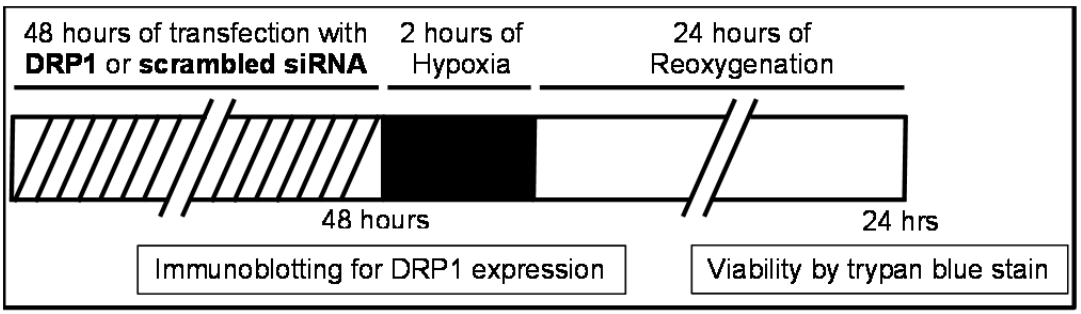

Figure 5-1. Scheme of experiments in Chapter 5.

2. Material

Cultured HL-1 cardiomyocytes, all chemicals, reagents and antibodies used in this Chapter are the same as those used in Chapter 3, if not annotated separately.

Mouse DRP1 siRNA designed to knockdown the expression of DRP1, the scrambled control siRNA, the DharmaFECT Transfection Reagent 1 and 5× siRNA buffers were all ordered from Thermo Fisher Scientific, Inc. (Pittsburg, PA).

3. Method

3.1 Knockdown the expression of DRP1 by specific siRNA

One previous study demonstrated that DRP1 siRNA can significantly reduce DRP1 mRNA expression in neonatal mouse cardiomyocytes (217). In our protocols, HL-1 cells were transfected with DRP1 siRNA for 48 hours per the manufacturer's protocol as detailed below:

i. HL-1 cardiomyocytes were grown on gelatin/fibronectin pre-coated 6-well plate to reach 30-40% confluence before transfection;

ii. DRP1 siRNA or scrambled siRNA were dissolved in 1× siRNA buffer to a stock concentration of 2 mM;

iii. the transfection construct was prepared as DRP1 siRNA or scrambled siRNA at 50 nM and DharmaFECT Transfection Reagent 1 at 1.25 µL/mL in antibiotic-free Claycomb medium;

iv. cells were rinsed once with antibiotic-free Claycomb medium and each well was treated with either DRP1 siRNA transfection construct (final volume of 2 mL), scrambled siRNA construct (final volume of 2 mL) or media alone (blank: final volume of 2 mL);

v. after 24 hours of incubation, the transfection construct (or media alone) was replaced by fully supplemented Claycomb medium; and

vi. after culturing the cells for another 24 hours (that is up to 48 hours post-transfection), cells were lysed with RIPA buffer supplemented with 1.5× protease

inhibitor and 1.5× phosphatase inhibitor. After obtaining the whole cell lysates, 10 µg of protein was loaded and immunoblotting (same methods described in Chapter 3, Section 3.4) was used to detect the expression of DRP1 in the three groups.

3.2 Cell viability assay after siRNA transfection

In separate experiments, HL-1 cardiomyocytes, grown on 60 mm culture dishes, were transfected with siRNA using the same method described above except that the final volume of transfection construct was 4.0 ml. At 48 hours post-transfection, cells were subjected to 2 hours of hypoxia (Refer to Chapter 3, Section 3.2). At 24 hours post-reoxygenation, viable versus dead cells were distinguished by trypan blue staining, counted, and % viability was calculated (refer to Chapter 4, Section 3.5).

3.3 Data and statistical analysis

Data are presented as means ± SEM and analyzed with GraphPad Prism software, GraphPad Software, Inc. (La Jolla, CA). One or two-way ANOVAs were performed as appropriate and pairwise *post-hoc* comparisons were made using the Newman–Keuls method if F-values reached significance. *P*- values < 0.05 were considered statistically significant.

4. Results

4.1 DRP1 siRNA reduced DRP1 expression by ~60%

As expected, there was no difference in DRP1 expression at 48 hours post-transfection in the scrambled siRNA group *versus* blank controls (Figure 5-2). In contrast, in cells transfected with DRP1 siRNA, the expression of DRP1 was decreased by ~ 60% when compared with either scrambled siRNA or media alone (blank): ***P*<0.01 in DRP1 siRNA *versus* blank control and scrambled siRNA groups,

respectively; Figure 5-2).

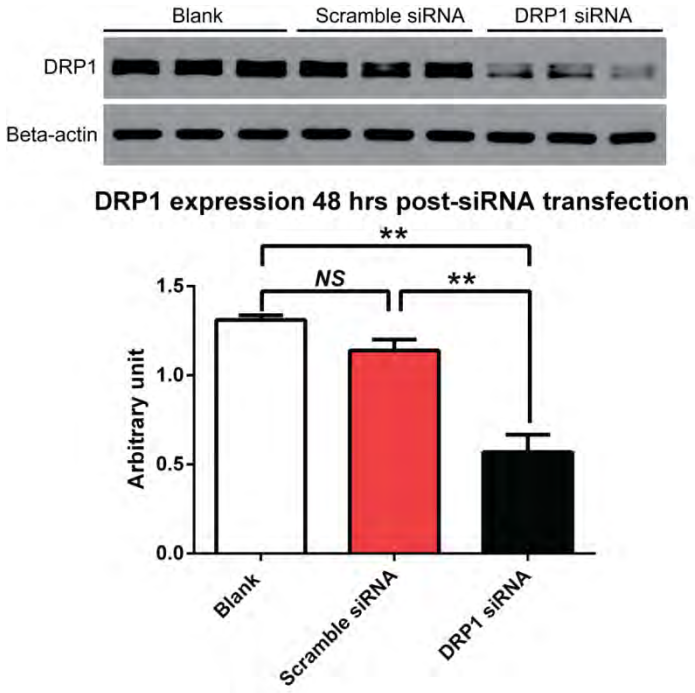

Figure 5-2. DRP1 siRNA significantly reduced DRP1 expression. Original immunoblots of DRP1 (top panels), and mean values of DRP1 expression (±SEM: bottom panels) in HL-1 cells transfected with either DRP1 siRNA or scrambled siRNA for 48 hours or incubated in media alone (blank). Data were obtained using whole cell lysates. N-values = 3 replicates per group. ***P*< 0.01 *versus* blank control and scrambled siRNA, respectively.

4.2 Downregulation of DRP1 expression increased HL-1 cardiomyocyte viability

In cells maintained under normoxic conditions, the concentration of transfection reagent used in our protocol had a small but significant toxic effect. HL-1 cell viability was reduced from approximately 96±2% in normoxic blank controls to 91±1% and 90±3% in normoxic cells that were treated with scrambled or DRP1 siRNA, respectively (Figure 5-3).

Figure 5-3. DRP1 silencing with siRNA increased HL-1 cardiomyocyte viability. Mean values of viability (% ± SEM) in HL-1 cells subjected to: i) normoxia and ii) 2 hours hypoxia followed by 24 hours reoxygenation. Data obtained in normoxic cells showed that incubation in transfection reagent had a small but significant toxic effect (** *P*<0.01 and ***P*<0.01). Nonetheless, knocking down DRP1 expression prior to hypoxia was protective: % cell viability was 76±1% *versus* 63±2% in blank and 60±1% in scramble controls, respectively (**: *P*< 0.01). N-values = 4 replicates per group; for each replicate, at least 250 cells were counted for every group.

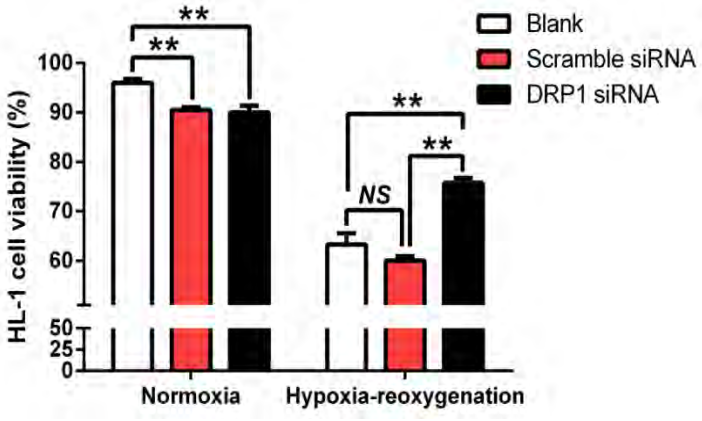

Two hours of hypoxia + 24 hours of reoxygenation reduced the proportion of viable cells in the blank control and scrambled siRNA groups to 63±2% and 60±1%, respectively (Figure 5-3). Knocking down DRP1 expression before hypoxia significantly increased HL-1 cardiomyocyte viability to 76±1% (**: $P < 0.01$ *versus* blank control and scrambled siRNA, respectively; Figure 5-3).

5. Summary

In summary, and consistent with our hypothesis, we found that knocking down DRP1 expression was protective. This is supported by our evidence that transfection with DRP1 siRNA: i) significantly reduced DRP1 expression; and ii) significantly increased cell viability (assessed by trypan blue staining) at 24 hours post-reoxygenation. The results of the genetic approach, that is to silence DRP1 expression before hypoxia, further confirms the data obtained by pharmacologic inhibition and corroborate the cause-effect relationship between DRP1 redistribution and cardiomyocyte injury in the context of HR.

CHAPTER 6

HYPOTHESIS IV: INHIBITION OF DRP1 AT REOXYGENATION–IS CARDIOPROTECTION MAINTAINED?

1. Rationale

To date, our studies summarized in Chapters 3-5 established that DRP1 translocation to mitochondria plays a cause-effect role in cardiomyocyte injury in the context of hypoxia-reoxygenation. This is supported by evidence that: i) HR triggered DRP1 redistribution to mitochondria, which was associated with cytochrome *c* release into cytosol, apoptotic activation and cardiomyocyte death, in addition to mitochondrial fragmentation; and ii) prehypoxic inhibition of DRP1, by either Mdivi-1 or downregulating its expression by siRNA, was cardioprotective (attenuated DRP1 accumulation to mitochondria; reduced cytochrome *c* leakage; decreased apoptotic activation indicated by decreased generation of cleaved caspase 3; increased cardiomyocyte viability and better preserved mitochondria morphology). However, in all our experiments, inhibition of DRP1 was implemented before the hypoxic insult; no protocols have been done to explore the cardioprotective effects in a more clinically relevant way; that is to apply the interventions at reoxygenation phase.

The purpose of Chapter 6 is to establish if inhibition of DRP1 at reoxygenation can still offer cardioprotection. Accordingly, we hypothesized that inhibition of DRP1 at reoxygenation will also be protective – but *possibly less robust than pretreatment*. To test this concept, Mdivi-1 (50 μM) was given at reoxygenation instead of before hypoxia. The major endpoint for the acute responses (up to 2 hours post-reoxygenation) was immunoblotting for the expression of cleaved caspase 3. The major endpoints for the late responses (at 24 hours post-R) included trypan blue staining for assessment of

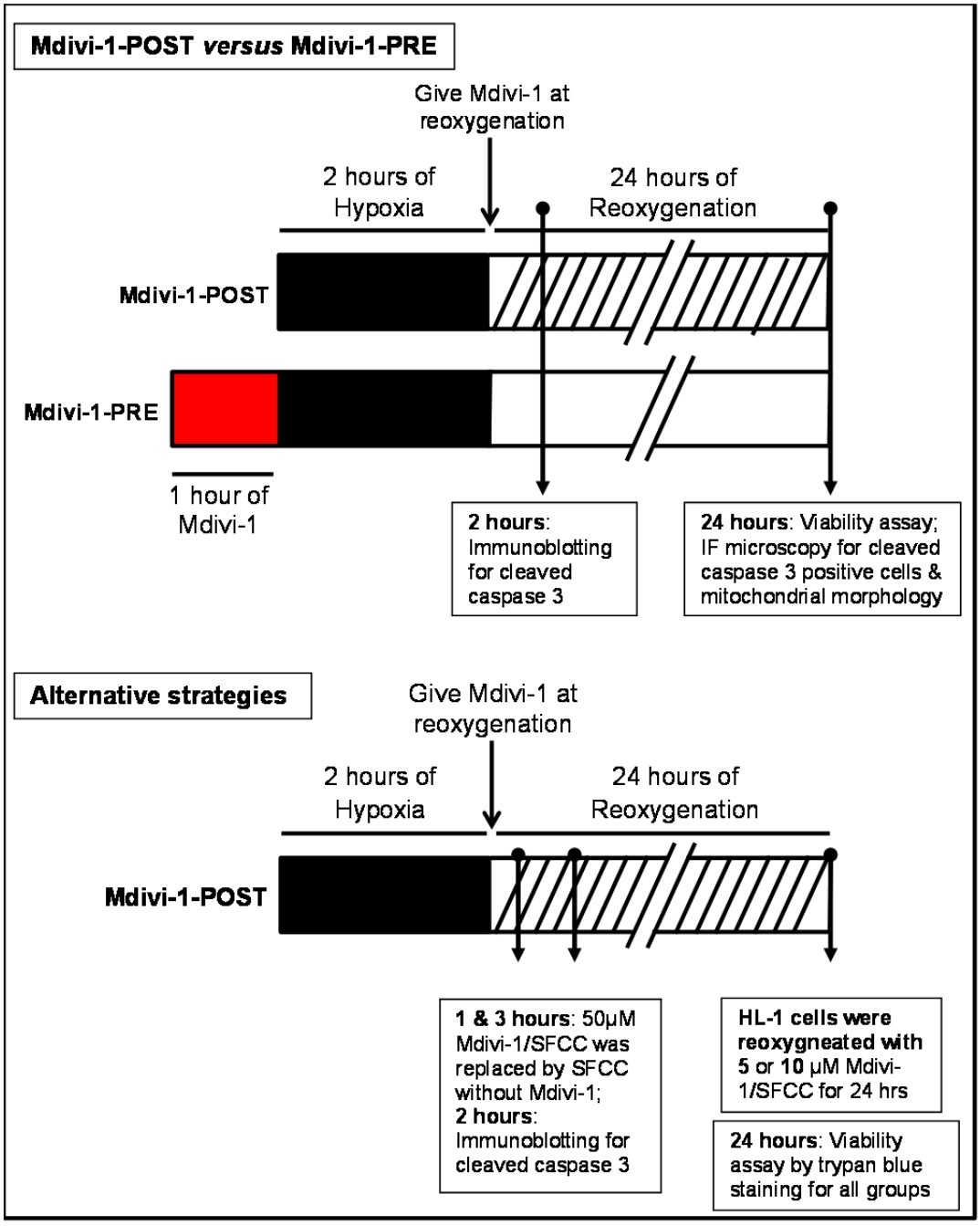

Figure 6-1. Experimental protocol for Chapter 6: acute and late responses in HR injury.

viability, and IF microscopy for detection of apoptotic cells and mitochondrial morphology. In addition, to exclude the possibility that cellular penetration of Mdivi-1 may be increased in posthypoxic cardiomyocytes because of increased membrane permeability, we did supplemental viability experiments using: i) lower doses of Mdivi-1 (5 and 10 μM), or ii) a shorter treatment duration (Mdivi-1 maintained in the media for 1

or 3 hours, rather than 24 hours, post-reoxygenation) (Figure 6-1). Finally, in an additional group of cells treated with Mdivi-1, 50 µM, for the first hour of reoxygenation, cleaved caspase 3 production was assessed by immunoblotting at 2 hours post-R and compared with Mdivi-1 pretreatment.

2. Materials

Cultured HL-1 cardiomyocytes, all chemicals and reagents and antibodies are the same as those used in previous Chapters if not annotated specifically.

3. Methods

3.1 HL-1 cardiomyocyte culture and hypoxia-reoxygenation

Refer to Chapter 3, Sections 3.1 and 3.2.

3.2 Cell lysis and fractionation

At 2 hours post-R, HL-1 cardiomyocytes were mechanically lysed and the lysates were further separated into cytosolic and HM-Mito fractions. For the detailed protocol used for cell lysis, refer to Chapter 3, Section 3.3.

3.3 Gel electrophoresis and immunoblotting

A total of 50-60 µg protein was loaded to each well and probed for expression of Cleaved caspase 3. For a detailed description of the immunoblotting protocol, refer to Chapter 3, Section 3.4 and Table 3-1.

3.4 Viability assay by trypan blue staining when HL-1 cardiomyocytes were reoxygenated with 50 µM Mdivi-1 for 24 hrs

HL-1 cardiomyocytes were reoxygenated with SFCC containing 50 µM Mdivi-1 and cell viability was assessed with trypan blue staining at 24 hours post-R. Two other groups were included: one received 1 hour of incubation of 50 µM Mdivi-1 prior to hypoxia, and the second served as controls (received DMSO vehicle only). For a

detailed description of the trypan blue staining protocol, refer to Chapter 4, Section 3.5.

3.5 IF microscopy

Refer to Chapter 4, Section 3.7. Briefly, at 24 hours post-R, cells were fixed and permeabilized, followed by incubation overnight at 4°C in primary antibodies against: i) ATPB + cleaved caspase 3 or ii) ATPB. Cells were imaged with a Leica TCS SP5 confocal system (Leica Microsystems, Heidelberg, Germany), using a 63× immersion oil objective and CCD camera. For identification of proteins or structures of interest, mitochondria were marked red by an antibody bound to Alexa Fluor 555, cleaved caspase 3 were labeled green by an antibody bound to Alexa Fluor 488, and nuclei were stained blue with DAPI.

3.5.1 Detection of apoptotic cells by IF microscopy

Refer to Chapter 4, Section 3.7.2. Briefly, for each image, we counted the number of cleaved caspase 3 positive cells (green), normalized to the total number of cells (marked by staining of DAPI (blue)-labeled nuclei). Results were obtained from four replicates of three independent experiments. For each replicate, 3-4 images were taken for vehicle and Mdivi-1 groups, respectively, and at least 100 cells were counted.

3.5.2 Mitochondrial morphology with or without posthypoxic Mdivi-1 treatment

Refer to Chapter 4, Section 3.7.1. Briefly, to resolve multi-focal profiles of mitochondrial morphology, the acquisition model was selected as XYZ and Z-Stack, with a step size of 0.4-0.5 µM. The sequential images were subsequently exported as TIFF files in either merged or separate channels, with each file representing an individual image of a Z-slice (every 0.4-0.5 µM in step size). The individual Z-slices were then reconstructed into a single Z-stack image composed of merged Z-slices using NIH ImageJ software Z-projection function (222). Confocal images were processed for

contrast and brightness adjustment and cropped to have uniform size for publication using Photoshop software (Adobe Systems Inc.). Representative images were obtained from four replicates of three independent experiments. For each replicate, at least 3-4 images were taken for vehicle and Mdivi-1 groups, respectively.

3.6 Viability assay when HL-1 cardiomyocytes were reoxygenated with 5 and 10 μM Mdivi-1 for 24 hours or with 50 μM Mdivi-1 for 1 and 3 hours

To address the possibility that the efficacy of Mdivi-1 treatment, given at reoxygenation *versus* pretreatment, may differ simply because of differences in membrane permeability and drug penetration, we used two different strategies. Firstly, we reoxygenated HL-1 cardiomyocytes with lower doses of Mdivi-1 (5 and 10 μM) for 24 hours. Secondly, we washed away the SFCC containing 50 μM Mdivi-1 at 1 and 3 hours post-R, and the cells were continuously be reoxygenated with SFCC without Mdivi-1 until to 24 hrs post-R. Viable *versus* dead cells for both alternative strategies were assayed and quantified by trypan blue staining.

3.7 Data and statistical analysis

Data are presented as means ± SEM and analyzed with GraphPad Prism software, (GraphPad Software Inc., La Jolla, CA). For comparison between two groups, unpaired student *t*-test was performed. For comparisons among three or more groups, one or two-way ANOVAs were performed as appropriate and pairwise *post-hoc* comparisons were made using the Newman–Keuls method if F-values reached significance. *P*- values < 0.05 were considered statistically significant.

4. Results

4.1 Mdivi-1 given at reoxygenation reduced the production of cleaved caspase 3

As expected from the outcome of Chapter 4, prehypoxic administration of 50 μM

Mdivi-1 (Mdivi-1-PRE), significantly attenuated caspase 3 cleavage (Figure 6-2). The same dose of Mdivi-1, when administered at reoxygenation (Mdivi-1-POST), had a comparable effect and significantly reduced the production of cleaved caspase 3: ***P*< 0.01 in both Mdivi-1-PRE and Mdivi-1-POST groups *versus* vehicle controls (Figure 6-2).

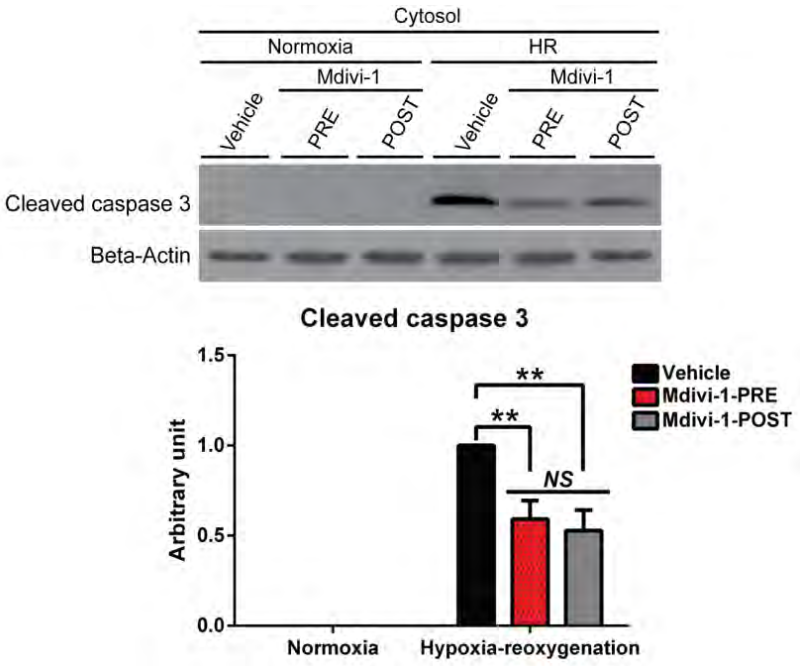

Figure 6-2. Mdivi-1 given at reoxygenation attenuated caspase 3 cleavage. Original immunoblots of cleaved caspase 3 (top panel), and mean values of cleaved caspase 3 (±SEM: bottom panel) in HL-1 cells subjected to i) normoxia, or ii) 2 hours hypoxia followed by 2 hours of reoxygenation. Mdivi-1-PRE = pretreatment with 50 µM Mdivi-1; Mdivi-1-POST = treatment with 50 µM Mdivi-1 at reoxygenation. Results obtained in the cytosolic fraction are shown. N-values = 4 replicates per group for the results of cleaved caspase 3 immunoblots. ***P*< 0.01 *versus* vehicle controls at 2 hours post-R.

4.2 Mdivi-1 given at reoxygenation exacerbated cardiomyocyte death

Two hours of hypoxia + 24 hours of reoxygenation reduced the proportion of viable cells (assessed by trypan blue staining) in the vehicle control group to 66±2% (Figure 6-3). As expected from our results in Chapter 4, administration of 50 µM Mdivi-1 before hypoxia significantly increased HL-1 cardiomyocyte viability to 78±3% (*****: *P*< 0.05 *versus* vehicle control; Figure 6-3). In contrast, the same dose of Mdivi-1 given at reoxygenation exacerbated cell death, with viability reduced to 35±6% (*****:*** *P*< 0.01 *versus* both vehicle control and Mdivi-1-PRE, respectively; Figure 6-3).

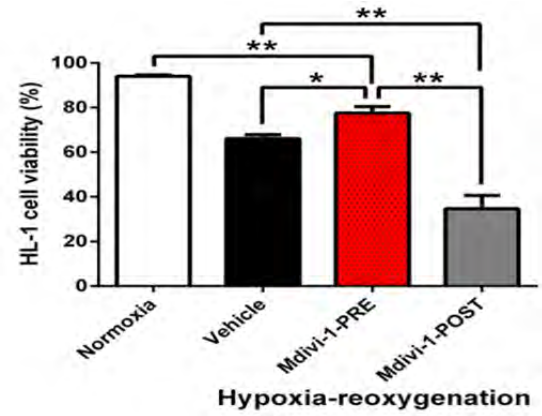

Figure 6-3. Mdivi-1 given at reoxygenation exacerbated cell death. Mean values of viability (%, ± SEM) in HL-1 cells subjected to 2 hours hypoxia followed by 24 hours reoxygenation or a time-matched normoxic period. Treatment with 50 µM Mdivi-1 before hypoxia was protective: % cell viability was 78±3% *versus* 66±2% in vehicle controls (*****: *P*< 0.05). Mdivi-1 (50 µM) given at reoxygenation for 24 hours exacerbated cell death and the viability decreased to 35±6% *(*****:** *P*< 0.01 *versus* vehicle control and Mdivi-1-PRE. N-values ≥ 6 replicates per group; for each replicate, at least 250 cells were counted for every group.

4.3 Mdivi-1 given at reoxygenation reduced the proportion of apoptotic cardiomyocytes as detected by IF

At 24 hours post-reoxygenation, the proportion of cleaved caspase 3-positive

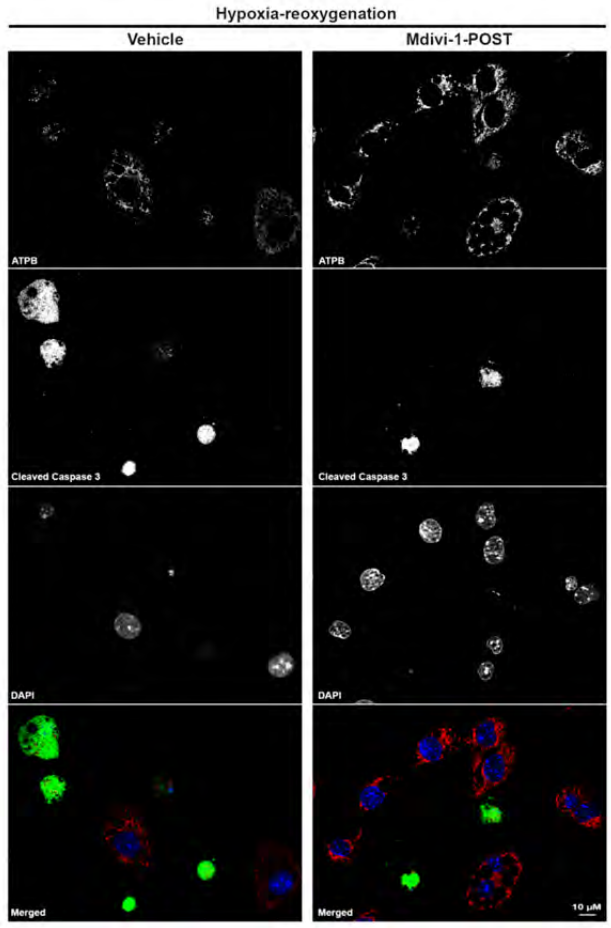

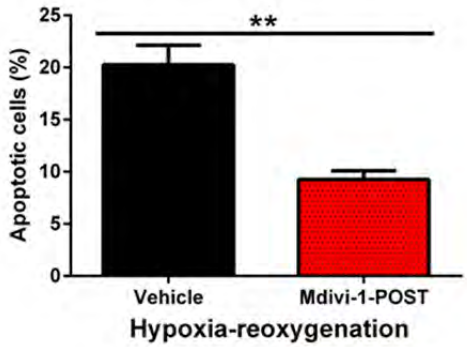

Figure 6-4. Mdivi-1 given at reoxygenation decreased the percentage of cleaved caspase 3-positive cells. Left panels: Original confocal IF images of HL-1 cells subjected to 2 hours hypoxia followed by 24 hours of reoxygenation. Cleaved caspase 3 was detected using a green fluorescence-labeled antibody, the mitochondrial network was labeled using an antibody targeting ATPB antibody (red) and nuclei were counter-stained with DAPI (blue). Representative images were taken from four replicates (N-values = 4 replicates per group). Right panel: quantitative analysis of cleaved caspase 3 positive HL-1 cells, expressed as a % of the total number of cells (marked by DAPI-labeled nuclei). Treatment with Mdivi-1 (50 µM) at reoxygenation did not increase apoptosis: % cleaved caspase 3 positive cells was significantly reduced from 20±2% in vehicle controls to 10±1% in Mdivi-1 treated cells (*******P*<0.01). N-values = 4 replicates per group; for each replicate, 3 – 4 images were taken for vehicle and Mdivi-1 groups, respectively; at least 100 cells were counted.

cells (as detected by green immunofluorescence) in vehicle-control cells was 20±2% (Figure 6-4). In contrast, in cells treated with 50 µM Mdivi-1 at reoxygenation, the % of apoptosis-positive cells was reduced to 10±1% (**: *P*< 0.01 *versus* vehicle-control; Figure 6-4).

4.4 Mdivi-1 given at reoxygenation did not preserve mitochondrial morphology

Qualitative inspection of cells stained with the mitochondrial marker ATPB showed that normoxic cells were, as expected, characterized by a fiber-like network of mitochondria (Figure 6-5: normoxia panel – left). Hypoxia-reoxygenation caused fragmentation (fission) of mitochondria, as indicated by the punctate pattern of ATPB staining that persisted at 24 hours post-R (Figure 6-5, hypoxia-reoxygenation panel – left). Mdivi-1 (50 µM) administered at reoxygenation did not attenuate fission and preserve the normal fiber-like mitochondrial phenotype but, rather, appeared to worsen mitochondrial disruption (Figure 6-5, hypoxia-reoxygenation panel – right).

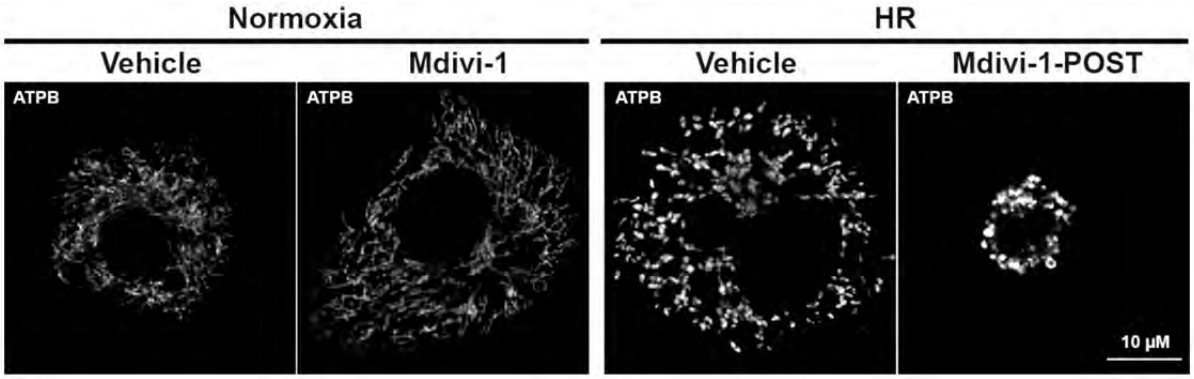

Figure 6-5. Mdivi-1 given at reoxygenation did not preserve mitochondrial structure. Original gray-scale confocal IF images of HL-1 cells subjected to 2 hours hypoxia followed by 24 hours reoxygenation using ATPB (mouse-derived) antibody to label the mitochondrial network. Representative images were taken from four replicates (N-values = 4 replicates per group). Hypoxia-reoxygenation caused mitochondrial fission; i.e., the mitochondrial phenotype was changed from the fiber-like network seen under normoxic conditions (left) into punctate dots (HR panel, – left). Mdivi-1 (50 µM) given at reoxygenation for 24 hours appeared to worsen mitochondrial phenotype (HR panel, – right).

4.5 Lower dose or shorter time of posthypoxic Mdivi-1 treatment did not offer cardioprotection

Two hours of hypoxia + 24 hours of reoxygenation reduced the proportion of

viable cells (assessed by trypan blue staining) in the vehicle control group to 63±2% (Figure 6-6). Lower doses of Mdivi-1 at reoxygenation, (5 and 10 µM), and shorter

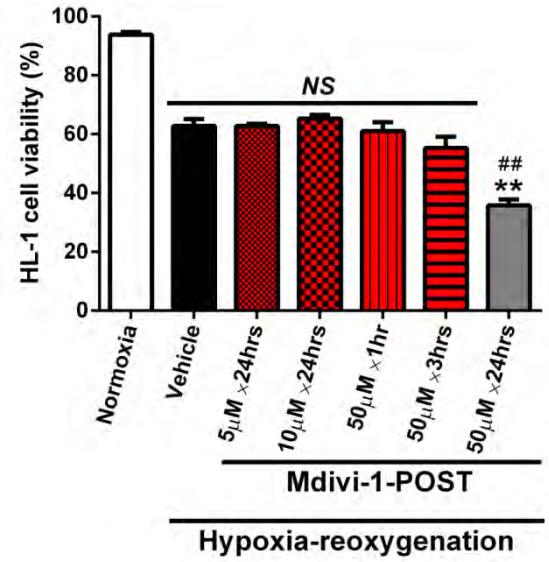

Figure 6-6. Lower dose or shorter time of posthypoxic Mdivi-1 treatment was not protective. Mean values of viability (%, ± SEM) in HL-1 cells subjected to 2 hours hypoxia followed by 24 hours reoxygenation or a time-matched normoxic period. Administration of Mdivi-1 at reoxygenation with lower doses (5 and 10 µM), or shorter (1 and 3 hour) incubation with 50 µM Mdivi-1, did not offer cardioprotection: ***NS***, not significantly different *versus* vehicle control. 50 µM Mdivi-1 given at reoxygenation for 24 hours exacerbated cell death and the viability decreased to 36±2% *(***: *P*< 0.01 *versus* all HR groups; ##: *P*< 0.01 *versus* normoxic controls). N-values ≥ 4 replicates per group; for each replicate, at least 250 cells were counted for every group.

incubation with 50 µM Mdivi-1 (1 and 3 hours) had no effect on viability: ***NS***, not significantly different *versus* vehicle control (Figure 6-6). However, we re-confirmed that 50 µM Mdivi-1 given at reoxygenation and maintained in the media for 24 hours worsened cell death and decreased viability to 36±2% *(***: *P*< 0.01 *versus* all other HR groups; Figure 6-6).

4.6 Shortened (1 hour) posthypoxic treatment with 50 µM Mdivi-1 attenuated caspase 3 cleavage

We reconfirmed that prehypoxic administration of 50 µM Mdivi-1 (Mdivi-1-PRE) significantly attenuated the generation of cleaved caspase 3 (Figure 6-7). The same dose of Mdivi-1, given at reoxygenation (Mdivi-1-POST) and maintained in the media for 1 hour, was protective, and indeed was significantly more effective in reducing caspase 3 cleavage than Mdivi-1-PRE: ***P*< 0.01 in both Mdivi-1-PRE and Mdivi-1-POST groups *versus* vehicle controls; **P*< 0.05 versus Mdivi-1-PRE (Figure 6-7).

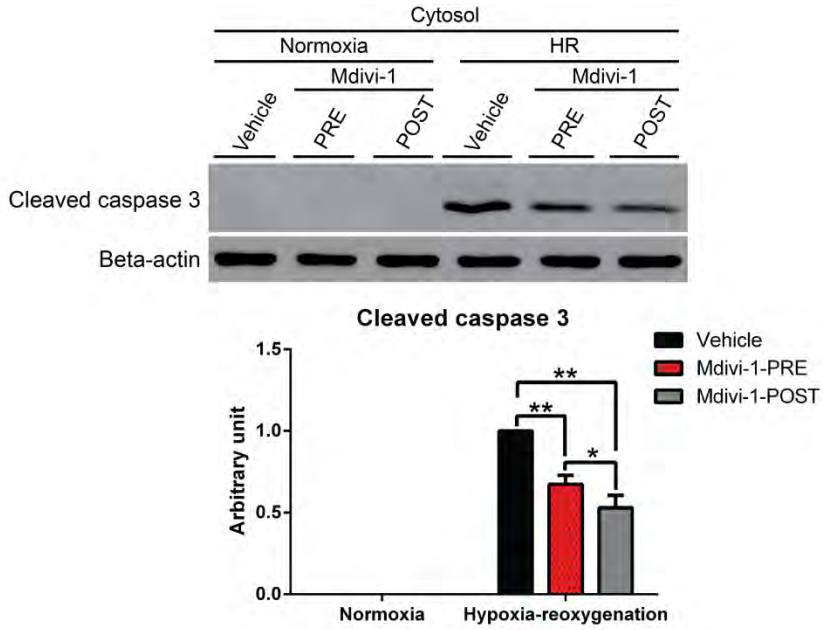

Figure 6-7. Shortened (1 hour) posthypoxic treatment with 50 µM Mdivi-1 attenuated caspase 3 cleavage. Original immunoblots of cleaved caspase 3 (top panel), and mean values of cleaved caspase 3 (±SEM: bottom panel) in HL-1 cells subjected to i) normoxia, or ii) 2 hours hypoxia followed by 2 hours of reoxygenation. Cells received 1 hour incubation of 50 µM Mdivi-1 before hypoxia or were reoxygenated with 50 µM Mdivi-1 for 1 hour, followed by incubation with SFCC for another hour. At 2 hours post-R, cells were lysed and lysates were separated into cytosolic and HM-Mito fractions. Results obtained in the cytosolic fraction are shown. N-values = 4 replicates per group. ***P*< 0.01 *versus* vehicle controls at 2 hours post-R. Mdivi-1-POST further decreased cleaved caspase 3 production: **P*< 0.05 *versus* Mdivi-1-PRE.

5. Summary

In this Chapter, we tested whether cardioprotection with Mdivi-1 was maintained when treatment was begun at reoxygenation. With 50 µM Mdivi-1 given at reoxygenation, the immunoblot data (up to 2 hours post-R) showed a significant decrease in caspase 3 cleavage, which was comparable to that seen with prehypoxic Mdivi-1 treatment. This finding (attenuation of apoptosis with 50 µM Mdivi-1 at reoxygenation) persisted at 24 hours post-R, as detected by IF staining. However, with 50 µM Mdivi-1 given at reoxygenation for 24 hours, HL-1 cell viability assessed by trypan blue staining was significantly decreased (rather than increased, as seen with prehypoxic Mdivi-1) *versus* controls.

The exacerbated cell death by trypan blue staining seen in this group may be a toxic effect of prolonged (24 hour) exposure to 50 µM of the inhibitor. This is supported by the finding that lower doses of Mdivi-1 maintained for 24 hours post-reoxygenation, or shorter, 1 or 3 hour exposures to Mdivi-1, did not increase cell death. Importantly,

however, none of the doses of Mdivi-1, given at reoxygenation, were protective. In addition, we consistently observed an apparent and unexplained dissociation between apoptotic cell death (by caspase 3 cleavage) *versus* total cell death (by trypan blue staining) for all groups treated with Mdivi-1 at reoxygenation.

CHAPTER 7

HYPOTHESIS V: EXACERBATION OF CELL DEATH WITH MDIVI-1 GIVEN AT REOXYGENATION – ROLE OF NECROPTOSIS?

1. Rationale

In Chapter 6, our studies found that posthypoxic treatment with 50 μM Mdivi-1 attenuated apoptosis as detected by immunoblotting and IF microscopy, but exacerbated total cell death as quantified by trypan blue staining. That is, there appears to be a dissociation between apoptotic cell death *versus* necrotic cell death. As discussed in Chapter 1, simultaneous inhibition of the apoptotic machinery and activation of the death receptor pathway can initiate the phenomenon of 'necroptosis', or programmed necrosis (Figure 1-3) (234, 235), and may provide a possible explanation for the paradox.

The key regulators of necroptosis are serine-threonine RIP kinases, including RIP1 and RIP3 (234, 235). There is a small molecule antagonist, Necrostain-1 (82, 236), that inhibits RIP1 kinase activity, its autophosphorylation and its interaction with RIP3, all of which are critical for programmed necroptosis (75). In non-cardiac system, Necrostatin-1 significantly increased *ex vivo* cell viability against necrotic (237) or necroptic stimuli (i.e., induction of death + pan-inhibitors of caspases (82), and attenuated *in vivo* infarct size in brain ischemic injury, retinal photoreceptor necrosis and renal ischemia-reperfusion injury (238-240). Recent studies suggest that necroptosis may also contribute to myocardial ischemia-reperfusion injury (83, 241-243). In cardiac models, addition of Necrostain-1 i) attenuated cardiomyocyte death caused by oxidative-stress (242, 244); ii) reduced infarct size in isolated perfused hearts subjected to ischemia-reperfusion (242, 245); and iii) limited infarct size in *in vivo* ischemia-

reperfusion studies (83, 242, 243).

Accordingly, we hypothesized that the increased total cell death, despite attenuation of apoptosis, seen with 50 µM Mdivi-1 given at reoxygenation, may be a consequence of necroptosis. If so, we propose that Necrostatin-1, co-administered with Mdivi-1 at reoxygenation, will reverse the exacerbation in cell death following Mdivi-1-POST treatment. To test our hypothesis (Figure 7-1), we used the same model – cultured HL-1 cardiomyocytes subjected to hypoxia-reoxygenation – described in Chapter 3. At the beginning of reoxygenation, cells were given either Mdivi-1 alone, Mdivi-1 + Necrostatin-1, or vehicle (DMSO). Viability was assessed by trypan blue staining at 24 hours post-R.

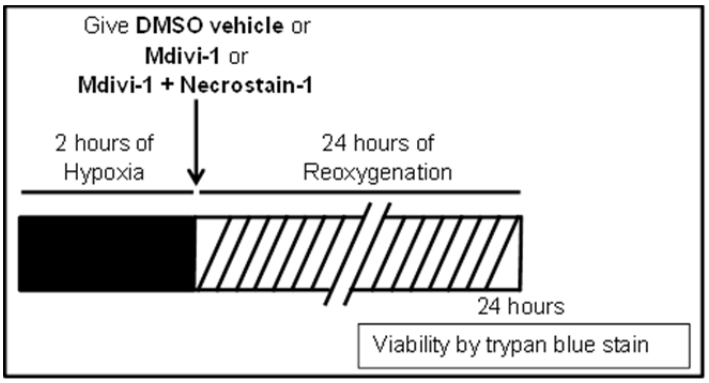

Figure 7-1. Scheme of experimental protocols in Chapter 7.

2. Materials

The model (cultured HL-1 cardiomyocytes) and all chemicals and reagents are the same as those used in Chapters 3 and 4 if not annotated specifically. Necrostatin-1 was ordered from Sigma-Aldrich, Inc. (St Louis, MO) and dissolved in DMSO in a stock concentration of 50 mM.

3. Methods

3.1 HL-1 cardiomyocyte culture

Refer to Chapter 3, Section 3.1.

3.2 Hypoxia-reoxygenation

Refer to Chapter 3, Section 3.2. There is published data, based on *in vitro* kinase activity assays, that Necrostatin-1 at concentrations of 30 – 100 µM effectively inhibits RIP1 kinase activity (82). Likewise, both 30 and 100 µM significantly attenuated C2C12 and H9C2 cell death by tert-Butyl hydroperoxide treatment (242). Therefore, based on these previous studies, we chose to use a dose of 50 µM Necrostatin-1. Following 2.0 hours of hypoxia, HL-1 cardiomyocytes were reoxygenated with SFCC containing DMSO vehicle, 50 µM Mdivi-1 or 50 µM Mdivi-1 + 50 µM Necrostatin-1.

3.3 Cell viability assay by trypan blue staining

Refer to Chapter 4, Section 3.5. Briefly, at 24 hours post-R, HL-1 cells were trypsinized and resuspended. Viable *versus* dead cells were assessed and quantified by trypan blue staining.

3.4 Data and statistical analysis

Data are presented as means ± SEM and analyzed with GraphPad Prism software, GraphPad Software Inc. (La Jolla, CA). Endpoints were compared among groups by one or two-way ANOVAs as appropriate and pairwise *post-hoc* comparisons were made using the Newman–Keuls method if F-values reached significance. *P*-values < 0.05 were considered statistically significant.

4. Results

4.1 Necrostatin-1 (50 µM), an inhibitor of RIP1, partially rescued the exacerbated necrosis induced by posthypoxic Mdivi-1 (50 µM) treatment

Two hours of hypoxia + 24 hours of reoxygenation reduced the proportion of viable cells in the vehicle control group to 67±2% (Figure 7-2). As expected from Chapter 6, administration of 50 µM Mdivi-1 at reoxygenation and maintained in the

media for 24 hours, significantly decreased cell viability to 37±5% (**: *P*< 0.01 *versus* vehicle control; Figure 7-2). Necrostatin-1 co-administered with Mdivi-1 at reoxygenation significantly increased viability to 50±3% (**: *P*< 0.01 *versus* Mdivi-1-POST; Figure 7-2); however, viability with Necrostatin-1 + Mdivi-1-POST remained significantly lower than vehicle control (**: *P*< 0.01; Figure 7-2).

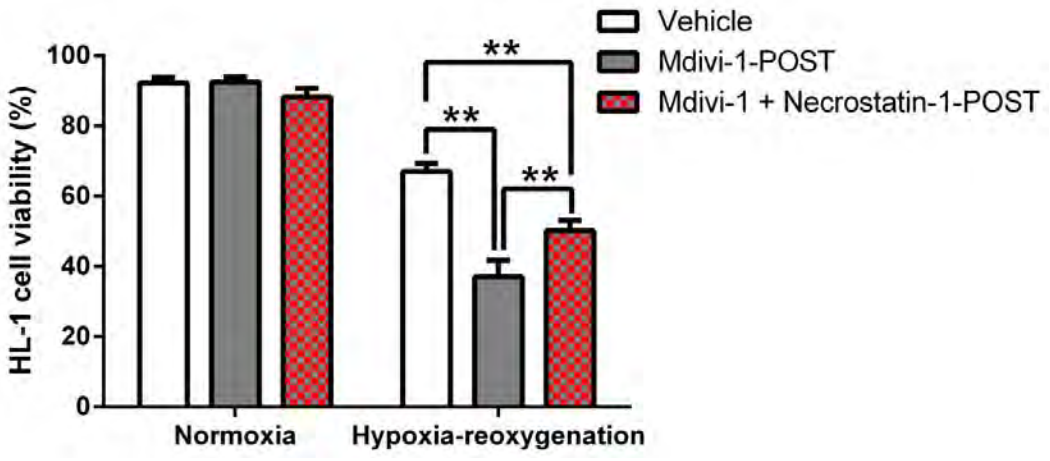

Figure 7-2. Necrostatin-1 (50 μM), an inhibitor of RIP1 partially rescued necrotic phenotype induced by posthypoxic Mdivi-1 (50 μM) treatment. Mean values of viability (%, ± SEM) in HL-1 cells subjected to 2 hours hypoxia followed by 24 hours of reoxygenation or a time-matched normoxic period. Treatment with Mdivi-1 at reoxygenation for 24 hours exacerbated cell death: % cell viability was 37±5% *versus* 67±2% in vehicle controls (**: *P*< 0.01). Necrostatin-1, co-administered with Mdivi-1 at reoxygenation significantly increased viability to 50±3% (**: *P*< 0.01 *versus* Mdivi-1-POST). However, this value remained significantly lower than vehicle control (**: *P*< 0.01). N-values ≥ 4 replicates per group in normoxic controls, and ≥ 5 replicates per group in HR groups; for each replicate, at least 250 cells were counted for every group.

4.2 Necrostain-1 (50 μM) alone had no effect on viability

In final, supplementary experiments, we assessed the effect of Necrostatin-1 alone, given under normoxic conditions or at reoxygenation, on total cell death assessed by trypan blue staining (Figure 7-3). The inhibitor had no effect on normoxic cells: viability was maintained at ≥90%, similar to values seen our normoxic cultures. Two hours of hypoxia + 24 hours of reoxygenation reduced the proportion of viable cells in the vehicle control group to 58±4% (Figure 7-3). Administration of Necrostatin-1 at reoxygenation had no effect on cell viability (***NS***, not significantly different from vehicle

controls, Figure 7-3).

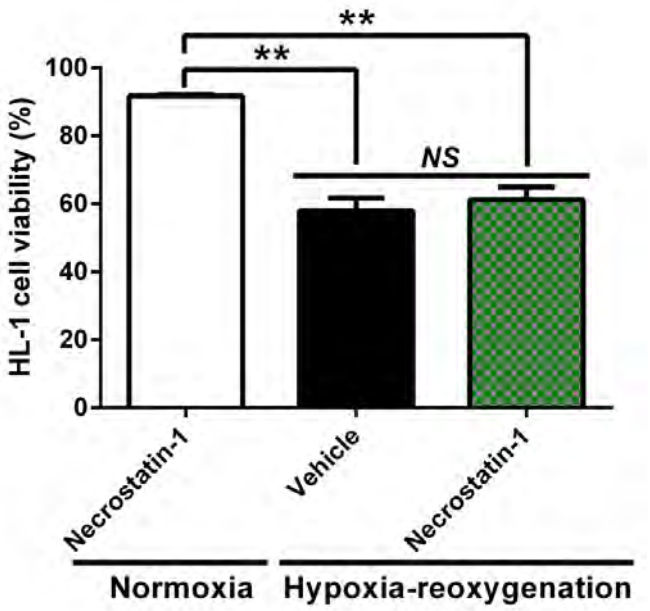

Figure 7-3. Necrostain-1 given at reoxygenation alone did not change viability. Mean values of viability (%, ± SEM) in HL-1 cells subjected to 2 hours hypoxia followed by 24 hours reoxygenation or a time-matched normoxic period. Hypoxia-reoxygenation reduced % cell viability 58±4%in vehicle controls. Necrostatin-1, administered alone at reoxygenation for 24 hours did not significantly change cell viability (61±4%; NS, not significantly differ from vehicle control). N-values ≥ 5 replicates per group; for each replicate, at least 250 cells were counted for every group.

5. Summary

Our studies this chapter show that Necrostatin-1, an inhibitor of RIP1, partially reversed the increase in HL-1 cardiomyocyte death seen with posthypoxic Mdivi-1 treatment (50 µM initiated at reoxygenation and maintained in the media for 24 hours). These data are consistent with the hypothesis that programmed necrosis may participate in the exacerbated cell death induced by Mdivi-1-POST. However, Necrostatin-1, when administered alone at reoxygenation, did not significantly change cell viability. This suggests that, in contrast to previous reports using other models, necroptosis may not be a significant cause of cell death in HL-1 cells subjected to hypoxia-reoxygenation.

CHAPTER 8

DISCUSSION

1. Summary of Results

In this project, I have tested three hypotheses and made three major observations. In the HL-1 cell model:

i. Hypoxia-reoxygenation triggers the subcellular redistribution of DRP1 (the master regulator of mitochondrial fission) from the cytosol to mitochondria and plays a mechanistic role in hypoxia-reoxygenation-induced cytochrome *c* release and cell apoptosis.

ii. Inhibition of DRP1 translocation prior to hypoxia is cytoprotective. This finding was demonstrated by both a pharmacologic approach (Mdivi-1) and genetic approach (siRNA).

iii. In contrast to our final hypothesis, inhibition of DRP1 in a time-frame that is relevant as a therapeutic strategy (i.e., begun at reoxygenation) is not protective. Rather, we observed a paradox. Mdivi-1, given at reoxygenation, attenuated apoptosis, but did not reduce total cell death and, in some cases (prolonged exposure at a dose of 50 μM) exacerbated cell death. This worsening of cell death was in part rescued by co-administration of Necrostatin-1, suggesting that necroptosis (programmed necrosis) may play a role.

2. Mitochondrial Fission and Cardiomyocyte Viability: Current Knowledge and New Contributions

Mitochondria are essential organelles of eukaryotic cells. Dysfunctional mitochondria not only disrupt bioenergetics but contribute to the pathogenesis of human diseases (191, 246). Mitochondrial fusion and fission, collectively named as

mitochondrial dynamics, are one of the core mechanisms responsible for maintaining mitochondrial health and functional integrity (191, 246).

The currently available knowledge of mitochondrial dynamics and its significance in physiology and pathophysiology is mainly derived from research from lower eukaryotic systems such as yeast (191, 246), and from non-cardiac models(191, 206, 246-248) including neurodegenerative disorders, e.g., hereditary Parkinson's disease (206, 247, 248). There is general agreement that mitochondrial fusion favors cell survival by allowing lipid membrane and context exchange between damaged and healthy mitochondria, while fission has been associated with cell death, mitochondrial damage, and initiation of apoptosis (206, 247, 248).

As discussed Chapter 1, mitochondria are recognized as the epicenter in mediating myocardial ischemia-reperfusion injury; as a result, mitochondria have emerged as a cellular target in efforts to mitigate IR injury (184-186). In the past decade, the major emphasis has been on the mPTP and modulation of its opening (249-252). However, emerging evidence suggests that other aspects related to the preservation of the function and structure of mitochondria (186, 187) (in addition to, in combination with, or instead of the status of the mPTP) may play a role in cardioprotection. Recent specific attention has focused on mitochondrial dynamics, particularly, mitochondrial fission, as a mediator of cell fate in the setting of IR injury (188). However, the role of mitochondrial fission in the pathogenesis of myocardial ischemia-reperfusion injury remains largely unexplored. In fact, only three previous publications have specifically and directly focused on the role of mitochondrial fission in IR (or HR) injury in myocyte or heart models (185, 216, 217).

2.1 Fission and cardioprotection

In 2010, Ong and colleagues were the first to reveal that inhibition of mitochondrial fission, either by genetic modification of key proteins (transfection with mitofusins or a dominant-negative mutant of DRP1) or by pharmacologic inhibition of DRP1 with Mdivi-1, attenuated mitochondrial fragmentation (detected by electron microscopy) and reduced death caused by hypoxia-reoxygenation (assessed by trypan blue staining) in HL-1 cells and isolated adult rat cardiomyocytes. In addition, pretreatment with Mdivi-1 was shown to reduce myocardial infarct size in the *in vivo* mouse model coronary artery occlusion-reperfusion (185). However, Ong *et al*. provided no direct, biochemical evidence of DRP1 translocation to mitochondria in response to HR or IR, and no direct evidence that DRP1 translocation was inhibited by Mdivi-1 (or by protein transfection).

In the current study, using cell fractionation and immunoblotting, we demonstrated the mechanistic link between DRP1 translocation, cytochrome *c* release into cytosol and apoptosis (reflected by increase in expression of cleaved caspase 3). Most importantly, we established a cause-effect relationship between DRP1 translocation to mitochondria and cardiomyocyte injury in the setting of HR injury, and provided support for this finding using two different strategies (pharmacologic inhibition of DRP1 translocation with Mdivi-1 and genetic downregulation of DRP1 expression with siRNA; Chapters 4 and 5).

Our results are consistent with related studies, in which DRP1 dephosphorylation and translocation to mitochondria were inhibited as a result of genetic manipulation of other targets. For example, in 2011, Wang *et al*., found that overexpression of microRNA 499: i) down-regulated the expression of calcineurins, the key phosphatases

responsible for DRP1 dephosphorylaton and activation (198, 253), which had the effect of ii) attenuating mitochondrial translocation of DRP1, and iii) was associated with increased cardiomyocyte viability and reduced infarct size (196). A second example is provided by Din *et al.* (254), who manipulated Pim-1 (proviral integration site for Moloney murine leukemia virus), a proto-oncogene that encodes a serine/threonine-protein kinase that plays multiple roles in cell survival, proliferation and differentiation. Using transgenic mice over-expressing wild-type or dominant-negative Pim-1, Din and colleague found that manipulation of wild-type Pim-1 decreased the expression of DRP1 and increased phosphorylation of DRP1, while over-expression of dominant-negative Pim-1 increased total DRP1, decreased DRP1 phosphorylation and augmented the translocation of DRP1 to mitochondria (254). These effects of dominant-negative Pim-1 were rescued by over-expressing a dominant-negative form of PUMA (p53 upregulated modulator of apoptosis); dominant-negative PUMA attenuated DRP1 translocation to mitochondria, blunted mitochondrial fission and rescued cardiomyocyte death caused by glucose deprivation + cyanide treatment (254).

In contrast, complex results from Kim and colleagues are more difficult to interpret (195). In non-cardiac cell lines (e.g., NIH3T3, mouse embryonic fibroblast and HEK293 cells), Siah1a/2 (seven in absentia homolog 1a/2; an E3 ubiquitin-protein ligase) was shown to degrade the mitochondrial scaffolding protein AKAP121 (A-kinase anchor protein 121) in the setting of hypoxia. AKAP121 reportedly increases the phosphorylation (and thus inhibits) DRP1 in mitochondrial fractions and prevents its interaction with FIS1, thus attenuating mitochondrial fission. Changing the focus to heart, Kim *et al*. found that deletion of Siah2 in transgenic mice attenuated infarct size at 24 hours following permanent coronary artery occlusion. In addition, knockdown of

Siah2 and DRP1 in H9C2 cells mitigated mitochondrial fragmentation and increased cell viability following simulated IR, while knockdown of AKAP121 exacerbated mitochondrial fission and cell injury (195). However, in non-cardiac cell lines, overexpression of AKAP121 increased the expression of non-phosphorylated DRP1 in the heavy-membrane mitochondrial fraction, an effect that, surprisingly, was not accompanied by an increase in the fragmented mitochondrial phenotype (195).

2.2 Timing of Mdivi-1 treatment

All studies discussed to this point have implemented pharmacologic treatment/genetic approaches to inhibit DRP1 translocation as a pre-treatment. With the exception of two very recently published studies (216, 217), the effect of inhibition of DRP1 translocation and mitochondrial fission, initiated in a therapeutically relevant manner (at reoxygenation) has not been explored. Therefore, we tested the hypothesis that inhibition of DRP1 at reoxygenation will also be protective, although possibly less robust than pretreatment, by giving Mdivi-1 at relief of hypoxia.

Our results do not support this hypothesis. We first found that 50 μM of Mdivi-1 (same dose that was protective when given as a pretreatment), administered at reoxygenation and maintained in the media for 24 hours post-R, attenuated caspase 3 cleavage and apoptosis but, paradoxically, increased (rather than decreased) total cell death. This unexpected observation was made in Chapter 6, and, in separate experiments, confirmed in Chapter 7. As a possible explanation, we speculated that this exacerbated cell death may be a toxic effect explained by either prolonged exposure (24 hours *versus* 1 hour in the pretreatment experiments), or an increase in permeability of HL-1 cells following hypoxia-reoxygenation and thus a greater than expected dose delivered to the cells. As alternative strategies, we shortened the

exposure to 50 µM Mdivi-1 to only the first 1 hour of reoxygenation, or treated with lower concentrations of Mdivi-1 (5 and 10 µM) throughout the 24 hours of reoxygenation. The alternative doses had no effect of total cell viability by trypan blue staining when compared with vehicle; the doses were neither toxic nor protective. However, as seen with 24 hour exposure to 50 µM Mdivi-1, 1 hour of incubation with 50 µM Mdivi-1 had significantly reduced the production of cleaved caspase 3.

In contrast, in two recent studies both inhibition of DRP1 before hypoxia, and DRP1 inhibition initiated at reperfusion, were reported to be cardioprotective (216, 217). In one study, Mdivi-1 (25 µM) was used as the inhibitor (217) while, in the second, P110 (a short peptide inhibitor of mitochondrial fission that acts by mimicking the homologous sequence between DRP1 and FIS1 and blocks their interaction (255)), conjugated to TAT-carrier to enhance cell penetration, was administered (216). When examining these studies and focusing on the protocols in which treatment was begun at reoxygenation, we found three major differences from our experiments that may contribute to the different results: i) both studies used *in vivo* or *ex vivo* perfused heart ischemia-reperfusion models; ii) the ischemic time was relative short, 30 mins, compared with our 2 hours of hypoxia; and iii) the major endpoints used to evaluate the beneficial effects were recovery of ventricular function and improved bioenergetics, rather than cell viability or infarct size (216, 217). However, the specific reason for the difference in outcomes is not known.

2.3 Mdivi-1, necroptosis and hypoxia-reoxygenation injury

Finally, to investigate if necroptosis (refer to Chapter 1, Section 2.2.3), may participate in the exacerbated cell death seen when 50 µM Mdivi-1 was given at reoxygenation, HL-1 cells were treated with either Mdivi-1 alone or Mdivi-1 +

Necrostatin-1, an inhibitor of RIP1. Our results showed that co-administration of Necrostatin-1 partially rescued HL-1 cardiomyocyte death associated with prolonged posthypoxic Mdivi-1 incubation, supporting a possible role of programmed necrosis. Our studies also indicated that Necrostatin-1 alone, given at reoxygenation did not change viability. This appears to disagree with previous studies, in which application of Necrostatin-1 provided cytoprotection against oxidative and ischemic insults (243-245). For example, Necrostain-1, administered 5 min before (243) or at the end of a 30 min period of coronary artery occlusion (83, 242) significantly reduced infarct size in murine hearts, with the proposed mechanism of cardioprotection attributed to inhibited phosphorylation and interaction of RIP1 and RIP3 (243). In other reports showing protection with Necrostatin-1: i) cardiomyocytes were stressed with peroxide instead of hypoxia or ischemia (244); ii) Necrostatin-1 was administered before ischemia (245); and iii) studies were conducted in non-cardiac tissues (237-240), e.g., kidney and neuronal studies. Given these differences among protocols, additional investigation will be required to identify the reasons for the discrepancy.

3. Technical Limitations

The most obvious potential limitation of this work is that all experiments in the current study were conducted using HL-1 cells, an immortal murine cardiac muscle cell line. The merits of using this model are evident, e.g., i) ample amounts of tissue are available for technical troubleshooting and refining the study design (i.e., optimizing immunoblotting protocols for the key proteins involved in fission); ii) the study does not rely on the use of animals; and iii) unlike studies conducted in intact hearts, it provides a ‘pure’ system for mechanistic studies that is not influenced or contaminated by the presence of other cell types. However, our hypotheses will require future testing and

confirmation in primary cardiomyocyte cultures and *in vivo*. A second potential concern is the limitations involved in the use of pharmacologic inhibitors (Mdivi-1, Necrostatin-1) and the possibility of non-specific effects. For Mdivi-1, this concern was addressed by our second, genetic approach with siRNA, and is diminished by the fact that consistent results were obtained with both strategies. Third, as shown in the Appendix, we acknowledge that our subcellular fractionation protocol collected only ~1/3 of all mitochondria. While this is a standard yield that is considered acceptable, it is possible that the other 2/3 of the mitochondria that were not collected by our fractionation protocol may represent a specific population that may differ from those evaluated by our protocols. Finally, while we investigated Mdivi-1 given only before hypoxia, and given only at reoxygenation, we did not assess the effects of Mdivi-1 (and possible importance of fission) during hypoxia. This omission was due to a technical constraint: Mdivi-1 is not soluble in the ischemic buffer.

4. Conclusion and Future Directions

The major conclusion of this dissertation work is that DRP1 translocation to mitochondria may play a mechanistic role in mediating cardiomyocyte injury in the context of hypoxia-reoxygenation injury. It is important to acknowledge that the focus of the work was on DRP1 inhibition, mitochondrial fission and cardiomyocyte death, without exploring the relationship between mitochondrial fragmentation and other important and established mediators of cardiomyocyte IR injury, e.g., mPTP opening, ROS production and calcium overload (Refer to Chapter 1, Section 2). In this regard, Ong *et al.* reported that inhibition of mitochondrial fission significantly delayed the time taken to induce mPTP opening in both HL-1 cells and primary adult rat cardiomyocytes (185). The possibility for relationships among mechanisms probably extends beyond

fission and the mPTP, and may provide a basis for future, productive investigations. Finally, we focused entirely on mitochondrial fission; the other side of the complex phenomenon of mitochondrial dynamics, that is mitochondrial fusion, was not considered. The effect of our protocols on expression of proteins that regulate mitochondrial fusion (e.g., MFN1/2 and OPA1) and the role of fusion in ischemia-reperfusion injury, both warrant future study.

APPENDIX

TECHNICAL CONSIDERATIONS

1. Cell Fractionation, Mitochondrial Isolation and its Quality Control

1.1 Rationale

Owing to the pioneering work from George Palade (256) and later modification, functional, pure, high quality mitochondria can be isolated from tissues and cultured cell lines with high yield efficiency. The three key factors that contribute to the quantity and quality of mitochondrial harvest are: i) appropriate mechanical disruption of the cells without causing damage to mitochondria; ii) the use of differential centrifugation to pellet mitochondria and avoid contamination from other cellular components with different sedimentation coefficients; and iii) use of a sucrose-based buffer to maintain functional and morphological integrity of harvested mitochondria for hours after isolation (220). In the current research project, one of the major technical components is to isolate mitochondria in HL-1 cardiomyocyte and perform biochemical assessment of the key regulators of mitochondrial fission and apoptosis in total cell lysates and cytosolic and mitochondria-enriched heavy membrane (HM-Mito) fractions. Therefore, it is of critical importance to ensure that our mitochondrial isolation protocol does not introduce artifacts.

A second issue that may affect our measurements is that mitochondria are highly dynamic organelles. Mitochondrial phenotype and size are determined by the balance between fission-promoting *versus* fusion-promoting factors, including, in our experiments, the administration of Mdivi-1, an antagonist of DRP1 inhibits mitochondrial fission. Therefore, it is important to establish whether mitochondrial yield by our isolation protocol is affected by alterations in mitochondrial morphology.

Finally, we use immunoblotting to identify the differential expression of target proteins among different sample groups (257). The validity of the immunoblot method, and the quantitative measurement of protein expression, depends on accurate, equal

protein loading from each sample. Therefore, multiple methods have been developed to ensure that there is equal protein loaded (258). One method is to employ a high-abundance housekeeping protein as loading control, e.g., GAPDH or beta actin. For each sample, the intensity of the protein of interest is normalized to the intensity of its respective loading control; analysis and comparisons are performed using the final, normalized results. Another approach is to use a total protein stain, e.g., amido black, to document equal protein loading, a technique that has been proposed to be more accurate for comparison of low-abundance proteins of interest (258).

The purpose of this section of the Appendix is to describe the outcome of supplementary experiments performed to address these technical issues and establish that: i) our isolation protocol achieves an acceptable mitochondrial yield ; ii) the isolated mitochondria are pure with low cross-contamination from other cellular components; and iii) our sucrose-based separation protocol is not affected by hypoxia-reoxygenation and the accompanying changes in mitochondrial morphology and size.

1.2 Materials

HL-1 cardiomyocyte cultures, all chemicals, reagents and antibodies used in this chapter are the same as those used in Chapters 3 and 4, if not annotated separately.

1.3 Methods

1.3.1 Evaluation of mitochondrial isolation efficiency and cross-contamination between fractions

1.3.1.1 Evaluation of mitochondrial isolation efficiency with Mdivi-1 treatment and cross-contamination between fractions in normoxia

HL-1 cardiomyocytes, grown to 90-95% confluence, were incubated with Mdivi-1 (50 µM), DMSO vehicle or media alone as blank control. The total incubation time was five hours to match the time course of the Mdivi-1 treatment experiment focusing on acute responses (Chapter 4, Section 3.2). Cells were subsequently mechanically lysed with isolation buffer and the lysate was further separated into cytosolic and HM-Mito fractions by using the same protocol previously described (refer to Chapter 3, Section

3.3).

Typically, when separating the lysate into the two subcellular fractions, the pellet obtained from the first low-speed centrifugation (500g × 5 min), considered to contain debris, is discarded. To investigate whether mitochondria were present in this pellet, and yield was decreased by discarding the pellet, we dissolved the first pellet with isolation buffer containing 1% Triton X-100 and included this in the analysis. Immunoblotting was used to resolve the relative intensity of VDAC (a mitochondrial-specific protein) and beta-actin (cytosolic protein) in cytosolic, HM-Mito and first-pellet fractions. Additionally, anti-DRP1 antibody was used to detect the relative concentration of DRP1 in three fractions. By comparing the intensity of VDAC, beta-actin and DRP1 in all fractions in Mdivi-1, vehicle and blank control groups, we are able to identify i) the percentage of mitochondria isolated by the protocol; ii) if the isolation is affected by the morphological change of mitochondria with Mdivi-1 treatment; and iii) the purity of the cytosolic and mitochondrial fractions.

1.3.1.2 Cross-contamination between fractions with Mdivi-1 treatment in the context of hypoxia-reoxygenation

HL-1 cardiomyocytes, grown to 90-95% confluence were subjected to 2 hours of hypoxia followed by reoxygenation. Prior to hypoxia, cells received 1 hour of incubation with Mdivi-1 (50 µM) or DMSO vehicle. At 5 and 120 min post-R, cells were lysed and the lysate was separated to cytosolic and HM-Mito fractions. To investigate the purity of each fraction, immunoblotting was used to resolve the relative intensity of VDAC and beta-actin.

1.3.2 Loading control: housekeep genes versus total protein stain

To test the concept that our use of VDAC and beta-actin to monitor equal protein loading was appropriate, and that the significant difference in DRP1 expression in different experimental groups was not an artifact of unequal loading, we performed additional experiments using the total protein stain, amido black. HL-1 cells were transfected with DRP1 siRNA for 48 hrs per the manufacturer's protocol (refer to

Chapter 5, Section 3.1). Cells were lysed with RIPA buffer supplemented with 1.5× protease inhibitor and 1.5× phosphatase inhibitor. Protein (10 µg) was loaded and immunoblotting was used to detect DRP1 expression in DRP1 siRNA, scrambled siRNA and blank control groups. After transfer, one membrane blot was stained with amido black, and the stain was scanned. The blot was then washed in TBST and blocked with 5% milk-TBST. A second blot was directly blocked with 5% milk-TBST without staining with amido black. Antibodies against beta-actin and DRP1 were employed to detect the expression of these two proteins in both blots. Finally, the relative concentration of DRP1 was compared based on normalization to beta-actin or amido black staining as the index of total protein loaded.

In another set of experiments, HL-1 cardiomyocytes, grown to 90-95% confluence were subjected to 2 hours of hypoxia + reoxygenation; normoxic cells were maintained in SFCC. Cells were subsequently lysed and lysate was separated to cytosolic and HM-Mito fractions. Protein (35 µg) from the HM-Mito fraction was loaded in each well. Prior blocking with 5% milk-TBST, the membrane blot was first stained with amido black and the intensity of staining was recorded. Subsequently, immunoblotting is used to resolve the relative expression of VDAC and DRP1 in the HM-Mito fraction.

1.4 Results

1.4.1 Our isolation protocol produces high yield of mitochondrial with minimal cross-contamination between fractions

1.4.1.1 Yield is not affected by Mdivi-1 incubation and ~1/3 of the mitochondria are collected by our protocol in normoxia

Our Immunoblot results (Figure AP-1, bottom lane) showed that VDAC, the marker of mitochondria, was only present in the first pellet and HM-Mito fractions, with no signal in cytosolic fraction. In addition, there was an ~equal intensity of VDAC in the first pellet and HM-Mito fractions from all samples (Mdivi-1-treated, vehicle-treated and blank control groups). These data provide evidence that cytosolic fraction is not

contaminated by mitochondrial proteins, and Mdivi-1 administration does not affect the mitochondrial harvest. Further, the immunoblots of beta-actin showed minimal contamination of the HM-Mito fraction by cytosolic protein (Figure AP-1, top lane).

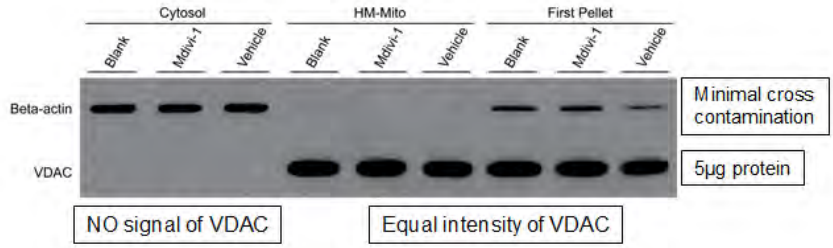

Figure AP-1. Mitochondrial isolation is not affected by Mdivi-1 treatment. Original immunoblots of beta-actin (top panel) and VDAC (bottom panel) in HL-1 cells incubated for five hours under normoxic condition with 50 μM Mdivi-1, vehicle or media alone. Results obtained in the cytosolic, HM-Mito and first pellet fractions are shown in the three panels, respectively. VDAC only appears in HM-Mito and first pellet fractions, and there is equal intensity of VDAC expression across the three treatments. Moreover, only a weak beta-actin signal (indicative of contamination with cytosol) was detected in HM-Mito fraction.

Finally, using the protein concentration and volume of each sample (Table AP-1), we calculated that we collected ~1/3 of the mitochondria with our protocol.

Table AP-1. Calculation of yield:

Fractions	[Protein, μg/μL]	Volume (μL)	VDAC intensity	Ratio of each fraction
Cytosol	2.15±0.07	400	N/A	N/A
HM-Mito	1.27±0.14	100	**Equal**	**0.43**
First Pellet	0.73±0.06	400		**1.00**

(~1/3 of mitochondria were isolated with our protocol.)

1.4.1.2 DRP1 is not lost during fractionation

The immunoblot result of DRP1 showed that, under normoxic conditions, the DRP1 signal was located almost entirely in the cytosolic fraction, although we collected ~1/3 of mitochondria in the HM-Mito fraction (Figure AP-2).

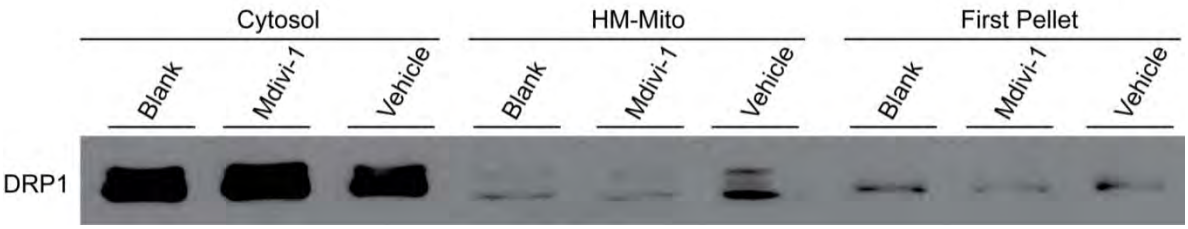

Figure AP-2. Under normoxic conditions: DRP1 was not 'lost' in the first pellet. Although we collected ~1/3 of the mitochondria in the HM fraction, the majority of DRP1 was expressed in the cytosolic fraction. Original immunoblots of DRP1 in HL-1 cells incubated for five hours under normoxic conditions with 50 µM Mdivi-1, vehicle or media alone. Results obtained in the cytosolic, HM-Mito and first pellet fractions are shown in the three panels, respectively. Although we collected ~1/3 of the mitochondria in the HM fraction, the majority of DRP1 was expressed in the cytosolic fraction.

1.4.1.3 Minimal cross-contamination is maintained with Mdivi-1 treatment in the setting of hypoxia-reoxygenation

In sections 1.4.1.1 and 1.4.1.2, we demonstrated that, under normoxia: i) we harvested ~1/3 of the mitochondria with our isolation protocol and had minimal cross-contamination between fractions; and ii) the yield and purity of each fraction was not affected by Mdivi-1 administration. It is also important to establish that, under conditions of hypoxia-reoxygenation, Mdivi-1 does not decrease the purity of each fraction. Immunoblot results in Figure AP-3 show minimal contamination of the HM-Mito fraction by cytosol (indicated by the weak beta-actin signal in HM-Mito fraction). i.e., Purity of the fractions is maintained following hypoxia-reoxygenation, and is not affected by Mdivi-1 administration (Figure AP-3).

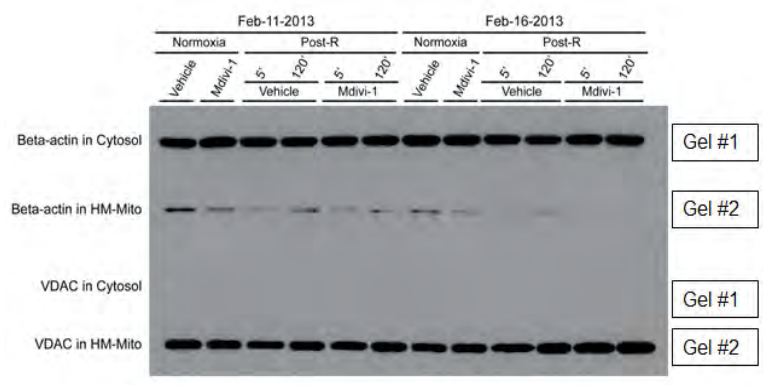

Figure AP-3. Minimal cross-contamination is maintained with Mdivi-1 treatment in the setting of hypoxia-reoxygenation. Original immunoblots of beta-actin (top panels), and VDAC (bottom panels) in HL-1 cells subjected to i) normoxia; or ii) 2 hours hypoxia followed by 5 min or 2 hours reoxygenation. Results obtained in the cytosolic (Gel #1) and HM-Mito (Gel #2) fractions are shown, respectively.

1.4.2 Housekeeping genes and total protein stains as loading control

1.4.2.1 Beta-actin and total protein staining showed equal protein loading for whole-cell lysate

As expected, DRP1 expression at 48 hours post-transfection was significantly reduced in the DRP1 siRNA group when compared with either blank control or scrambled siRNA (top lanes of the left panel, Figure AP-4). The beta-actin signal showed that an equal amount of protein was in each lane, and the obvious difference in DRP1 signal is not due to poor protein loading. In the bottom lanes of the left panel, incubation with antibody was performed following amido black staining. Both the beta-actin signal (bottom lanes of left panel, Figure AP-4) and total protein staining (right panel, Figure AP-4) showed that protein was equally loaded in each well, with no apparent superiority of the amido black method. Most importantly, the difference in DRP1 expression was not explained by unequal loading.

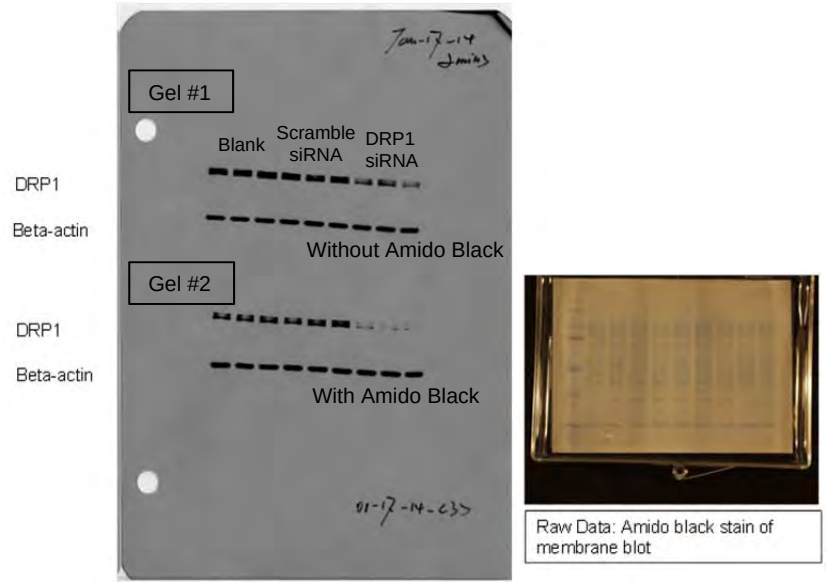

Figure AP-4. Beta-actin and total protein staining both confirmed equal protein loading with whole-cell lysate. Left panel: original immunoblots of DRP1 and beta-actin (top and bottom rows of each pair, respectively) in HL-1 cells transfected and maintained under normoxic conditions with DRP1 siRNA, scrambled siRNA and media alone (blank). Results were obtained from whole cell lysates at 48 hours post-transfection. Right panel: amido black stain of membrane blot transferred from Gel #2. Both beta-actin and total protein stain showed equal protein loading.

1.4.2.2 VDAC and total protein staining showed equal protein loading in the HM-Mito fraction

As shown in Figure AP-5 (left) and as expected, hypoxia-reoxygenation triggered DRP1 translocation to mitochondria. Both the VDAC signal and total protein staining (Figure AP-5, right) showed equal protein loading, and confirm that the difference in

DRP1 signal between normoxic controls and the HR groups is not due to unequal protein loading.

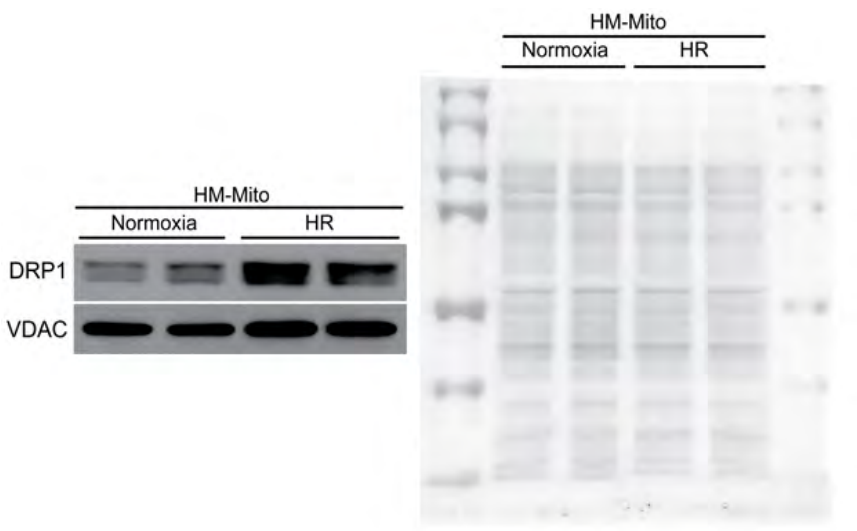

Figure AP-5. VDAC and total protein staining both confirmed equal protein loading from the HM-Mito fraction. Left panel: original immunoblots of DRP1 and VDAC (top and bottom rows, respectively) in HL-1 cells subjected hypoxia-reoxygenation. Results were obtained in the HM-Mito fractions. Right panel: amido black stain of membrane blot transferred from the same gel shown in the left panel. Both VDAC and total protein staining showed equal protein loading.

2. Hue Analysis

2.1 Rationale

One of the goals of the experiments reported in Chapter4 was to quantify the association of DRP1 with mitochondria at 24 hours following reoxygenation (late responses), with and without Mdivi-1 treatment. We used three separate methods to address this issue; immunoblotting for DRP1, as well as co-localization (using ImageJ) and hue analysis (using SigmaScan) of red and green signals in cells stained with fluorescent antibodies and viewed by confocal microscopy (refer to Chapter 4, Section 3.7.3). Both immunoblotting and co-localization analysis are standard and well-established techniques. Additional description of the principles of the lesser-described method, hue analysis, is provided below, in order to assist in understanding the results of Chapter 4, Section 4.3.4

2.2 Principle of hue analysis

Hue analysis is based on the optical principle that color images are composed of 256 hues (Figure AP-6). Using merged confocal images in which both mitochondria (red) and DRP1 (green) were visualized, the numbers of red, green and yellow pixels

(as objectively defined in Figure AP-6) were quantified using SigmaScan 5.0 (Systat Software Inc., San Jose, CA). Red + yellow pixels represent the total mitochondrial

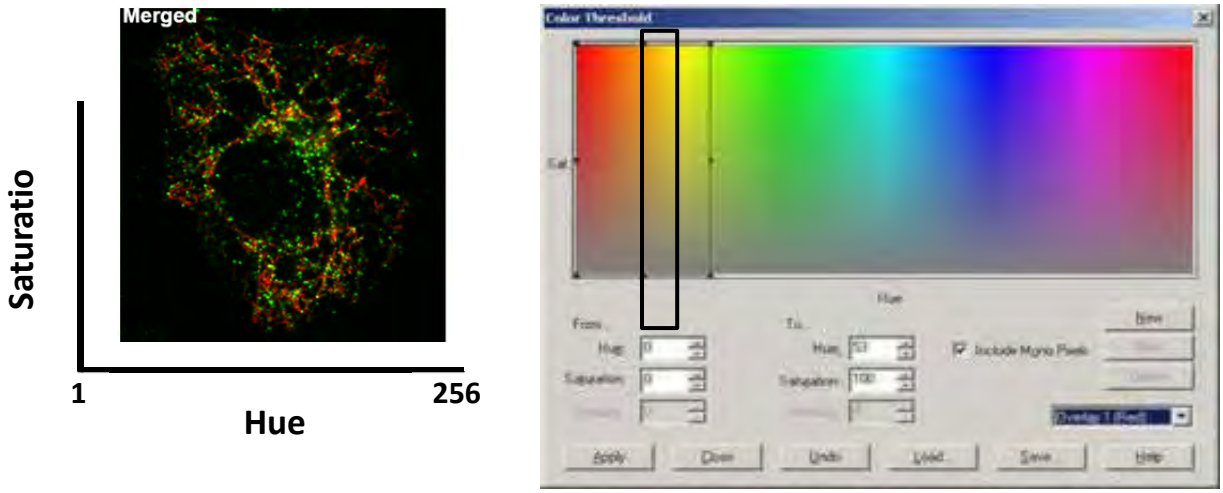

Figure AP-6. Principle of hue analysis
Optical principle: color image composed of 256 hues (red, green, blue)
Merged IF images: red (mitochondria) + green (DRP1)
Goal: quantify the number yellow pixels (overlap of green and red fluorescent signals)
red + yellow = total mitochondrial signal = hue 2 to 45
yellow + green = total DRP1 signal = hue 37 to 85
yellow = hue 37 to 45

SigmaScan: obtain hue histogram
Tabulate # of pixels for each of the 256 hues
For merged IF images (no blue), hue 2 to 85
Quantify:
number of red + yellow pixels: sum of hue 2 to 45
number of yellow + green pixels: sum of hue 37 to 85
number of yellow pixels: sum of hue 37 to 45
Calculate:
(yellow pixels) / (red + yellow pixels) * 100%
(yellow pixels) / (yellow + green pixels) * 100%

signal, green + yellow pixels represent the total DRP1 signal, while yellow pixels (overlap of red and green) reflect the proportion of the DRP1 signal spatially associated with the mitochondrial signal. Accordingly, to quantify the spatial association of DRP1 with mitochondria, we calculated the percentage of yellow pixels occupied by both red and green pixels normalized to either: i) red + yellow pixels (total mitochondrial signal); or ii) green + yellow pixels (total DRP1 signals) (Figure AP-6). As discussed in Chapter 4, the outcome of the hue analysis was consistent with both the immunoblot data and standard co-localization analysis.

REFERENCES

1. Go AS, Mozaffarian D, Roger VL, Benjamin EJ, Berry JD, Borden WB, et al. Heart disease and stroke statistics--2013 update: a report from the American Heart Association. Circulation. 2013;127(1):e6-e245.
2. Geltman EM. Infarct size as a determinant of acute and long-term prognosis. Cardiol Clin. 1984;2(1):95-103.
3. Maroko PR, Libby P, Ginks WR, Bloor CM, Shell WE, Sobel BE, et al. Coronary artery reperfusion. I. Early effects on local myocardial function and the extent of myocardial necrosis. J Clin Invest. 1972;51(10):2710-6.
4. Ellis SG, Henschke CI, Sandor T, Wynne J, Braunwald E, Kloner RA. Time course of functional and biochemical recovery of myocardium salvaged by reperfusion. J Am Coll Cardiol. 1983;1(4):1047-55.
5. Braunwald E, Kloner RA. Myocardial reperfusion: a double-edged sword? J Clin Invest. 1985;76(5):1713-9.
6. Karki P, Coccaro E, Fliegel L. Sustained intracellular acidosis activates the myocardial Na^+/H^+ exchanger independent of amino acid Ser(703) and p90(rsk). Biochim Biophys Acta. 2010;1798(8):1565-76.
7. Poole-Wilson PA. Regulation of intracellular pH in the myocardium; relevance to pathology. Mol Cell Biochem. 1989;89(2):151-5.
8. Garlick PB, Radda GK, Seeley PJ. Studies of acidosis in the ischaemic heart by phosphorus nuclear magnetic resonance. Biochem J. 1979;184(3):547-54.
9. Khuri SF, Flaherty JT, O'Riordan JB, Pitt B, Brawley RK, Donahoo JS, et al. Changes in intramyocardial ST segment voltage and gas tensions with regional myocardial ischemia in the dog. Circ Res. 1975;37(4):455-63.

10. Garcia-Dorado D, Ruiz-Meana M, Inserte J, Rodriguez-Sinovas A, Piper HM. Calcium-mediated cell death during myocardial reperfusion. Cardiovasc Res. 2012;94(2):168-80.

11. Kleinbongard P, Baars T, Heusch G. Calcium antagonists in myocardial ischemia/reperfusion--update 2012. Wien Med Wochenschr. 2012;162(13-14):302-10.

12. Talukder MA, Kalyanasundaram A, Zuo L, Velayutham M, Nishijima Y, Periasamy M, et al. Is reduced SERCA2a expression detrimental or beneficial to postischemic cardiac function and injury? Evidence from heterozygous SERCA2a knockout mice. Am J Physiol Heart Circ Physiol. 2008;294(3):H1426-34.

13. Saotome M, Katoh H, Satoh H, Nagasaka S, Yoshihara S, Terada H, et al. Mitochondrial membrane potential modulates regulation of mitochondrial Ca2+ in rat ventricular myocytes. Am J Physiol Heart Circ Physiol. 2005;288(4):H1820-8.

14. Webster KA. Mitochondrial membrane permeabilization and cell death during myocardial infarction: roles of calcium and reactive oxygen species. Future Cardiol. 2012;8(6):863-84.

15. Inserte J, Barba I, Hernando V, Abellan A, Ruiz-Meana M, Rodriguez-Sinovas A, et al. Effect of acidic reperfusion on prolongation of intracellular acidosis and myocardial salvage. Cardiovasc Res. 2008;77(4):782-90.

16. Philipson KD, Bersohn MM, Nishimoto AY. Effects of pH on Na^{+}-Ca^{2+} exchange in canine cardiac sarcolemmal vesicles. Circ Res. 1982;50(2):287-93.

17. Balnave CD, Vaughan-Jones RD. Effect of intracellular pH on spontaneous Ca^{2+} sparks in rat ventricular myocytes. J Physiol. 2000;528 Pt 1:25-37.

18. Mandel F, Kranias EG, Grassi de Gende A, Sumida M, Schwartz A. The effect of pH on the transient-state kinetics of Ca^{2+}-Mg^{2+}-ATPase of cardiac sarcoplasmic reticulum. A comparison with skeletal sarcoplasmic reticulum. Circ Res. 1982;50(2):310-7.

19. Javadov S, Hunter JC, Barreto-Torres G, Parodi-Rullan R. Targeting the mitochondrial permeability transition: cardiac ischemia-reperfusion versus carcinogenesis. Cell Physiol Biochem. 2011;27(3-4):179-90.

20. Mozaffari MS, Liu JY, Abebe W, Baban B. Mechanisms of load dependency of myocardial ischemia reperfusion injury. Am J Cardiovasc Dis. 2013;3(4):180-96.

21. Groenendyk J, Agellon LB, Michalak M. Coping with endoplasmic reticulum stress in the cardiovascular system. Annu Rev Physiol. 2013;75:49-67.

22. Michalak M, Opas M. Endoplasmic and sarcoplasmic reticulum in the heart. Trends Cell Biol. 2009;19(6):253-9.

23. Glembotski CC. Endoplasmic reticulum stress in the heart. Circ Res. 2007;101(10):975-84.

24. Groenendyk J, Sreenivasaiah PK, Kim do H, Agellon LB, Michalak M. Biology of endoplasmic reticulum stress in the heart. Circ Res. 2010;107(10):1185-97.

25. Hetz C, Chevet E, Harding HP. Targeting the unfolded protein response in disease. Nat Rev Drug Discov. 2013;12(9):703-19.

26. Toth A, Nickson P, Mandl A, Bannister ML, Toth K, Erhardt P. Endoplasmic reticulum stress as a novel therapeutic target in heart diseases. Cardiovasc Hematol Disord Drug Targets. 2007;7(3):205-18.

27. Thuerauf DJ, Marcinko M, Gude N, Rubio M, Sussman MA, Glembotski CC. Activation of the unfolded protein response in infarcted mouse heart and hypoxic

cultured cardiac myocytes. Circ Res. 2006;99(3):275-82.

28. Elahi MM, Kong YX, Matata BM. Oxidative stress as a mediator of cardiovascular disease. Oxid Med Cell Longev. 2009;2(5):259-69.

29. Pagliaro P, Moro F, Tullio F, Perrelli MG, Penna C. Cardioprotective pathways during reperfusion: focus on redox signaling and other modalities of cell signaling. Antioxid Redox Signal. 2011;14(5):833-50.

30. Griendling KK, FitzGerald GA. Oxidative stress and cardiovascular injury: Part I: basic mechanisms and *in vivo* monitoring of ROS. Circulation. 2003;108(16):1912-6.

31. Raedschelders K, Ansley DM, Chen DD. The cellular and molecular origin of reactive oxygen species generation during myocardial ischemia and reperfusion. Pharmacol Ther. 2012;133(2):230-55.

32. Drose S. Differential effects of complex II on mitochondrial ROS production and their relation to cardioprotective pre- and postconditioning. Biochim Biophys Acta. 2013;1827(5):578-87.

33. Becker LB. New concepts in reactive oxygen species and cardiovascular reperfusion physiology. Cardiovasc Res. 2004;61(3):461-70.

34. Braunersreuther V, Jaquet V. Reactive oxygen species in myocardial reperfusion injury: from physiopathology to therapeutic approaches. Curr Pharm Biotechnol. 2012;13(1):97-114.

35. Konstantinidis K, Whelan RS, Kitsis RN. Mechanisms of cell death in heart disease. Arterioscler Thromb Vasc Biol. 2012;32(7):1552-62.

36. Zorov DB, Filburn CR, Klotz LO, Zweier JL, Sollott SJ. Reactive oxygen species (ROS)-induced ROS release: a new phenomenon accompanying induction of the

mitochondrial permeability transition in cardiac myocytes. J Exp Med. 2000;192(7):1001-14.

37. Chen YR, Zweier JL. Cardiac mitochondria and reactive oxygen species generation. Circ Res. 2014;114(3):524-37.

38. Rodrigo R, Libuy M, Feliu F, Hasson D. Molecular basis of cardioprotective effect of antioxidant vitamins in myocardial infarction. Biomed Res Int. 2013;2013:437613.

39. Carreira RS, Lee P, Gottlieb RA. Mitochondrial therapeutics for cardioprotection. Curr Pharm Des. 2011;17(20):2017-35.

40. Penna C, Perrelli MG, Pagliaro P. Mitochondrial pathways, permeability transition pore, and redox signaling in cardioprotection: therapeutic implications. Antioxid Redox Signal. 2013;18(5):556-99.

41. Folino A, Losano G, Rastaldo R. Balance of nitric oxide and reactive oxygen species in myocardial reperfusion injury and protection. J Cardiovasc Pharmacol. 2013;62(6):567-75.

42. Walters AM, Porter GA, Jr., Brookes PS. Mitochondria as a drug target in ischemic heart disease and cardiomyopathy. Circ Res. 2012;111(9):1222-36.

43. Zamzami N, Kroemer G. The mitochondrion in apoptosis: how Pandora's box opens. Nat Rev Mol Cell Biol. 2001;2(1):67-71.

44. Baines CP, Kaiser RA, Sheiko T, Craigen WJ, Molkentin JD. Voltage-dependent anion channels are dispensable for mitochondrial-dependent cell death. Nat Cell Biol. 2007;9(5):550-5.

45. Giorgio V, von Stockum S, Antoniel M, Fabbro A, Fogolari F, Forte M, et al. Dimers of mitochondrial ATP synthase form the permeability transition pore. Proc

Natl Acad Sci U S A. 2013;110(15):5887-92.

46. Rasola A, Sciacovelli M, Pantic B, Bernardi P. Signal transduction to the permeability transition pore. FEBS Lett. 2010;584(10):1989-96.

47. Baines CP, Kaiser RA, Purcell NH, Blair NS, Osinska H, Hambleton MA, et al. Loss of cyclophilin D reveals a critical role for mitochondrial permeability transition in cell death. Nature. 2005;434(7033):658-62.

48. Tsujimoto Y, Shimizu S. Role of the mitochondrial membrane permeability transition in cell death. Apoptosis. 2007;12(5):835-40.

49. Taylor RC, Cullen SP, Martin SJ. Apoptosis: controlled demolition at the cellular level. Nat Rev Mol Cell Biol. 2008;9(3):231-41.

50. Adrain C, Brumatti G, Martin SJ. Apoptosomes: protease activation platforms to die from. Trends Biochem Sci. 2006;31(5):243-7.

51. Brocheriou V, Hagege AA, Oubenaissa A, Lambert M, Mallet VO, Duriez M, et al. Cardiac functional improvement by a human Bcl-2 transgene in a mouse model of ischemia/reperfusion injury. J Gene Med. 2000;2(5):326-33.

52. Chen Z, Chua CC, Ho YS, Hamdy RC, Chua BH. Overexpression of Bcl-2 attenuates apoptosis and protects against myocardial I/R injury in transgenic mice. Am J Physiol Heart Circ Physiol. 2001;280(5):H2313-20.

53. Hochhauser E, Kivity S, Offen D, Maulik N, Otani H, Barhum Y, et al. Bax ablation protects against myocardial ischemia-reperfusion injury in transgenic mice. Am J Physiol Heart Circ Physiol. 2003;284(6):H2351-9.

54. Whelan RS, Kaplinskiy V, Kitsis RN. Cell death in the pathogenesis of heart disease: mechanisms and significance. Annu Rev Physiol. 2010;72:19-44.

55. Kung G, Konstantinidis K, Kitsis RN. Programmed necrosis, not apoptosis, in the

heart. Circ Res. 2011;108(8):1017-36.

56. Riedl SJ, Shi Y. Molecular mechanisms of caspase regulation during apoptosis. Nat Rev Mol Cell Biol. 2004;5(11):897-907.

57. Chiong M, Wang ZV, Pedrozo Z, Cao DJ, Troncoso R, Ibacache M, et al. Cardiomyocyte death: mechanisms and translational implications. Cell Death Dis. 2011;2:e244.

58. Hernando V, Inserte J, Sartorio CL, Parra VM, Poncelas-Nozal M, Garcia-Dorado D. Calpain translocation and activation as pharmacological targets during myocardial ischemia/reperfusion. J Mol Cell Cardiol. 2010;49(2):271-9.

59. Yoshida K, Yamasaki Y, Kawashima S. Calpain activity alters in rat myocardial subfractions after ischemia or reperfusion. Biochim Biophys Acta. 1993;1182(2):215-20.

60. Chen M, He H, Zhan S, Krajewski S, Reed JC, Gottlieb RA. Bid is cleaved by calpain to an active fragment *in vitro* and during myocardial ischemia/reperfusion. J Biol Chem. 2001;276(33):30724-8.

61. Chae SU, Ha KC, Piao CS, Chae SW, Chae HJ. Estrogen attenuates cardiac ischemia-reperfusion injury via inhibition of calpain-mediated bid cleavage. Arch Pharm Res. 2007;30(10):1225-35.

62. Hotta Y, Nishimaki H, Takeo T, Itoh G, Yajima M, Otsuka-Murakami H, et al. Differences in the effects of Na^{+}-H^{+} exchange inhibitors on cardiac function and apoptosis in guinea-pig ischemia-reperfused hearts. Eur J Pharmacol. 2004;503(1-3):109-22.

63. Eigel BN, Gursahani H, Hadley RW. Na+/Ca2+ exchanger plays a key role in inducing apoptosis after hypoxia in cultured guinea pig ventricular myocytes. Am

J Physiol Heart Circ Physiol. 2004;287(4):H1466-75.

64. Jeremias I, Kupatt C, Martin-Villalba A, Habazettl H, Schenkel J, Boekstegers P, et al. Involvement of CD95/Apo1/Fas in cell death after myocardial ischemia. Circulation. 2000;102(8):915-20.

65. Lee P, Sata M, Lefer DJ, Factor SM, Walsh K, Kitsis RN. Fas pathway is a critical mediator of cardiac myocyte death and MI during ischemia-reperfusion *in vivo*. Am J Physiol Heart Circ Physiol. 2003;284(2):H456-63.

66. Levine B, Kroemer G. Autophagy in the pathogenesis of disease. Cell. 2008;132(1):27-42.

67. Klionsky DJ, Emr SD. Autophagy as a regulated pathway of cellular degradation. Science. 2000;290(5497):1717-21.

68. Gustafsson AB, Gottlieb RA. Autophagy in ischemic heart disease. Circ Res. 2009;104(2):150-8.

69. Gottlieb RA, Finley KD, Mentzer RM, Jr. Cardioprotection requires taking out the trash. Basic Res Cardiol. 2009;104(2):169-80.

70. Dong Y, Undyala VV, Gottlieb RA, Mentzer RM, Jr., Przyklenk K. Autophagy: definition, molecular machinery, and potential role in myocardial ischemia-reperfusion injury. Journal of cardiovascular pharmacology and therapeutics. 2010;15(3):220-30.

71. Sala-Mercado JA, Wider J, Undyala VV, Jahania S, Yoo W, Mentzer RM, Jr., et al. Profound cardioprotection with chloramphenicol succinate in the swine model of myocardial ischemia-reperfusion injury. Circulation. 2010;122(11 Suppl):S179-84.

72. Inserte J, Garcia-Dorado D, Hernando V, Soler-Soler J. Calpain-mediated

impairment of Na^+/K^+-ATPase activity during early reperfusion contributes to cell death after myocardial ischemia. Circ Res. 2005;97(5):465-73.

73. Inserte J, Garcia-Dorado D, Hernando V, Barba I, Soler-Soler J. Ischemic preconditioning prevents calpain-mediated impairment of Na^+/K^+-ATPase activity during early reperfusion. Cardiovasc Res. 2006;70(2):364-73.

74. Inserte J, Garcia-Dorado D, Ruiz-Meana M, Agullo L, Pina P, Soler-Soler J. Ischemic preconditioning attenuates calpain-mediated degradation of structural proteins through a protein kinase A-dependent mechanism. Cardiovasc Res. 2004;64(1):105-14.

75. Ofengeim D, Yuan J. Regulation of RIP1 kinase signalling at the crossroads of inflammation and cell death. Nat Rev Mol Cell Biol. 2013;14(11):727-36.

76. Christofferson DE, Li Y, Yuan J. Control of life-or-death decisions by RIP1 kinase. Annu Rev Physiol. 2014;76:129-50.

77. Baud V, Karin M. Signal transduction by tumor necrosis factor and its relatives. Trends Cell Biol. 2001;11(9):372-7.

78. Li J, Yin Q, Wu H. Structural basis of signal transduction in the TNF receptor superfamily. Adv Immunol. 2013;119:135-53.

79. Walczak H. Death receptor-ligand systems in cancer, cell death, and inflammation. Cold Spring Harb Perspect Biol. 2013;5(5):a008698.

80. Christofferson DE, Yuan J. Necroptosis as an alternative form of programmed cell death. Curr Opin Cell Biol. 2010;22(2):263-8.

81. Zhang DW, Shao J, Lin J, Zhang N, Lu BJ, Lin SC, et al. RIP3, an energy metabolism regulator that switches TNF-induced cell death from apoptosis to necrosis. Science. 2009;325(5938):332-6.

82. Degterev A, Hitomi J, Germscheid M, Ch'en IL, Korkina O, Teng X, et al. Identification of RIP1 kinase as a specific cellular target of necrostatins. Nat Chem Biol. 2008;4(5):313-21.

83. Lim SY, Davidson SM, Mocanu MM, Yellon DM, Smith CC. The cardioprotective effect of necrostatin requires the cyclophilin-D component of the mitochondrial permeability transition pore. Cardiovasc Drugs Ther. 2007;21(6):467-9.

84. Koshinuma S, Miyamae M, Kaneda K, Kotani J, Figueredo VM. Combination of necroptosis and apoptosis inhibition enhances cardioprotection against myocardial ischemia-reperfusion injury. J Anesth. 2013.

85. Bond JM, Herman B, Lemasters JJ. Protection by acidotic pH against anoxia/reoxygenation injury to rat neonatal cardiac myocytes. Biochem Biophys Res Commun. 1991;179(2):798-803.

86. Panagiotopoulos S, Daly MJ, Nayler WG. Effect of acidosis and alkalosis on postischemic Ca gain in isolated rat heart. Am J Physiol. 1990;258(3 Pt 2):H821-8.

87. Kitakaze M, Weisfeldt ML, Marban E. Acidosis during early reperfusion prevents myocardial stunning in perfused ferret hearts. J Clin Invest. 1988;82(3):920-7.

88. Shen AC, Jennings RB. Myocardial calcium and magnesium in acute ischemic injury. Am J Pathol. 1972;67(3):417-40.

89. Reimer KA, Lowe JE, Jennings RB. Effect of the calcium antagonist verapamil on necrosis following temporary coronary artery occlusion in dogs. Circulation. 1977;55(4):581-7.

90. Ashraf M, White F, Bloor CM. Ultrastructural influence of reperfusing dog myocardium with calcium-free blood after coronary artery occlusion. Am J Pathol.

1978;90(2):423-34.

91. Murphy E, Perlman M, London RE, Steenbergen C. Amiloride delays the ischemia-induced rise in cytosolic free calcium. Circ Res. 1991;68(5):1250-8.

92. Takahashi K, Takahashi T, Suzuki T, Onishi M, Tanaka Y, Hamano-Takahashi A, et al. Protective effects of SEA0400, a novel and selective inhibitor of the Na^+/Ca^{2+} exchanger, on myocardial ischemia-reperfusion injuries. Eur J Pharmacol. 2003;458(1-2):155-62.

93. Imahashi K, Pott C, Goldhaber JI, Steenbergen C, Philipson KD, Murphy E. Cardiac-specific ablation of the Na^+-Ca^{2+} exchanger confers protection against ischemia/reperfusion injury. Circ Res. 2005;97(9):916-21.

94. Martindale JJ, Fernandez R, Thuerauf D, Whittaker R, Gude N, Sussman MA, et al. Endoplasmic reticulum stress gene induction and protection from ischemia/reperfusion injury in the hearts of transgenic mice with a tamoxifen-regulated form of ATF6. Circ Res. 2006;98(9):1186-93.

95. Tao J, Zhu W, Li Y, Xin P, Li J, Liu M, et al. Apelin-13 protects the heart against ischemia-reperfusion injury through inhibition of ER-dependent apoptotic pathways in a time-dependent fashion. Am J Physiol Heart Circ Physiol. 2011;301(4):H1471-86.

96. Lam CK, Zhao W, Cai W, Vafiadaki E, Florea SM, Ren X, et al. Novel role of HAX-1 in ischemic injury protection involvement of heat shock protein 90. Circ Res. 2013;112(1):79-89.

97. Guo J, Bian Y, Bai R, Li H, Fu M, Xiao C. Globular adiponectin attenuates myocardial ischemia/reperfusion injury by upregulating endoplasmic reticulum Ca^{2+}-ATPase activity and inhibiting endoplasmic reticulum stress. J Cardiovasc

Pharmacol. 2013;62(2):143-53.

98. Jolly SR, Kane WJ, Bailie MB, Abrams GD, Lucchesi BR. Canine myocardial reperfusion injury. Its reduction by the combined administration of superoxide dismutase and catalase. Circ Res. 1984;54(3):277-85.

99. Otani H, Tanaka H, Inoue T, Umemoto M, Omoto K, Tanaka K, et al. *In vitro* study on contribution of oxidative metabolism of isolated rabbit heart mitochondria to myocardial reperfusion injury. Circ Res. 1984;55(2):168-75.

100. Wang P, Chen H, Qin H, Sankarapandi S, Becher MW, Wong PC, et al. Overexpression of human copper, zinc-superoxide dismutase (SOD1) prevents postischemic injury. Proc Natl Acad Sci U S A. 1998;95(8):4556-60.

101. Obal D, Dai S, Keith R, Dimova N, Kingery J, Zheng YT, et al. Cardiomyocyte-restricted overexpression of extracellular superoxide dismutase increases nitric oxide bioavailability and reduces infarct size after ischemia/reperfusion. Basic Res Cardiol. 2012;107(6):305.

102. Zeymer U, Suryapranata H, Monassier JP, Opolski G, Davies J, Rasmanis G, et al. The Na^+/H^+ exchange inhibitor eniporide as an adjunct to early reperfusion therapy for acute myocardial infarction. Results of the evaluation of the safety and cardioprotective effects of eniporide in acute myocardial infarction (ESCAMI) trial. J Am Coll Cardiol. 2001;38(6):1644-50.

103. Mentzer RM, Jr., Bartels C, Bolli R, Boyce S, Buckberg GD, Chaitman B, et al. Sodium-hydrogen exchange inhibition by cariporide to reduce the risk of ischemic cardiac events in patients undergoing coronary artery bypass grafting: results of the EXPEDITION study. Ann Thorac Surg. 2008;85(4):1261-70.

104. Roberts BN, Christini DJ. NHE inhibition does not improve Na^+ or Ca^{2+} overload

during reperfusion: using modeling to illuminate the mechanisms underlying a therapeutic failure. PLoS Comput Biol. 2011;7(10):e1002241.

105. Andersen AD, Bentzen BH, Salling H, Klingberg H, Kanneworff M, Grunnet M, et al. The cardioprotective effect of brief acidic reperfusion after ischemia in perfused rat hearts is not mimicked by inhibition of the Na^+/H^+ exchanger NHE1. Cell Physiol Biochem. 2011;28(1):13-24.

106. The EMIP-FR Group. Effect of 48-h intravenous trimetazidine on short- and long-term outcomes of patients with acute myocardial infarction, with and without thrombolytic therapy; A double-blind, placebo-controlled, randomized trial. European Myocardial Infarction Project--Free Radicals. Eur Heart J. 2000;21(18):1537-46.

107. El-Hamamsy I, Stevens LM, Carrier M, Pellerin M, Bouchard D, Demers P, et al. Effect of intravenous N-acetylcysteine on outcomes after coronary artery bypass surgery: a randomized, double-blind, placebo-controlled clinical trial. J Thorac Cardiovasc Surg. 2007;133(1):7-12.

108. Murry CE, Jennings RB, Reimer KA. Preconditioning with ischemia: a delay of lethal cell injury in ischemic myocardium. Circulation. 1986;74(5):1124-36.

109. Conti CR. Stunning, hibernating, now preconditioning. Clin Cardiol. 1992;15(8):554-5.

110. Yellon DM, Baxter GF, Garcia-Dorado D, Heusch G, Sumeray MS. Ischaemic preconditioning: present position and future directions. Cardiovasc Res. 1998;37(1):21-33.

111. Schulz R, Cohen MV, Behrends M, Downey JM, Heusch G. Signal transduction of ischemic preconditioning. Cardiovasc Res. 2001;52(2):181-98.

112. Kloner RA, Jennings RB. Consequences of brief ischemia: stunning, preconditioning, and their clinical implications: part 2. Circulation. 2001;104(25):3158-67.

113. Jenkins DP, Pugsley WB, Alkhulaifi AM, Kemp M, Hooper J, Yellon DM. Ischaemic preconditioning reduces troponin T release in patients undergoing coronary artery bypass surgery. Heart. 1997;77(4):314-8.

114. Heusch G. Cardioprotection: chances and challenges of its translation to the clinic. Lancet. 2013;381(9861):166-75.

115. Zhao ZQ, Corvera JS, Halkos ME, Kerendi F, Wang NP, Guyton RA, et al. Inhibition of myocardial injury by ischemic postconditioning during reperfusion: comparison with ischemic preconditioning. Am J Physiol Heart Circ Physiol. 2003;285(2):H579-88.

116. Ovize M, Thibault H, Przyklenk K. Myocardial conditioning: opportunities for clinical translation. Circ Res. 2013;113(4):439-50.

117. Przyklenk K, Bauer B, Ovize M, Kloner RA, Whittaker P. Regional ischemic 'preconditioning' protects remote virgin myocardium from subsequent sustained coronary occlusion. Circulation. 1993;87(3):893-9.

118. Kharbanda RK, Mortensen UM, White PA, Kristiansen SB, Schmidt MR, Hoschtitzky JA, et al. Transient limb ischemia induces remote ischemic preconditioning *in vivo*. Circulation. 2002;106(23):2881-3.

119. Schmidt MR, Smerup M, Konstantinov IE, Shimizu M, Li J, Cheung M, et al. Intermittent peripheral tissue ischemia during coronary ischemia reduces myocardial infarction through a KATP-dependent mechanism: first demonstration of remote ischemic perconditioning. Am J Physiol Heart Circ Physiol.

2007;292(4):H1883-90.

120. Jimenez-Navarro MF, Carrasco-Chinchilla F, Munoz-Garcia AJ, Dominguez-Franco A, Caballero-Borrego J, Alonso-Briales JH, et al. Remote ischemic postconditioning: does it protect against ischemic damage in percutaneous coronary revascularization? justification and design of a randomized placebo-controlled clinical trial. Cardiology. 2011;119(3):164-9.

121. Hausenloy DJ. Cardioprotection techniques: preconditioning, postconditioning and remote conditioning (basic science). Curr Pharm Des. 2013;19(25):4544-63.

122. Goto M, Liu Y, Yang XM, Ardell JL, Cohen MV, Downey JM. Role of bradykinin in protection of ischemic preconditioning in rabbit hearts. Circ Res. 1995;77(3):611-21.

123. Xi L, Das A, Zhao ZQ, Merino VF, Bader M, Kukreja RC. Loss of myocardial ischemic postconditioning in adenosine A_1 and bradykinin B_2 receptors gene knockout mice. Circulation. 2008;118(14 Suppl):S32-7.

124. Liu GS, Thornton J, Van Winkle DM, Stanley AW, Olsson RA, Downey JM. Protection against infarction afforded by preconditioning is mediated by A1 adenosine receptors in rabbit heart. Circulation. 1991;84(1):350-6.

125. Kitakaze M, Hori M, Takashima S, Sato H, Inoue M, Kamada T. Ischemic preconditioning increases adenosine release and 5'-nucleotidase activity during myocardial ischemia and reperfusion in dogs. Implications for myocardial salvage. Circulation. 1993;87(1):208-15.

126. Methner C, Schmidt K, Cohen MV, Downey JM, Krieg T. Both A_{2a} and A_{2b} adenosine receptors at reperfusion are necessary to reduce infarct size in mouse hearts. Am J Physiol Heart Circ Physiol. 2010;299(4):H1262-4.

127. Schultz JE, Rose E, Yao Z, Gross GJ. Evidence for involvement of opioid receptors in ischemic preconditioning in rat hearts. Am J Physiol. 1995;268(5 Pt 2):H2157-61.

128. Schultz JE, Hsu AK, Gross GJ. Morphine mimics the cardioprotective effect of ischemic preconditioning via a glibenclamide-sensitive mechanism in the rat heart. Circ Res. 1996;78(6):1100-4.

129. Zatta AJ, Kin H, Yoshishige D, Jiang R, Wang N, Reeves JG, et al. Evidence that cardioprotection by postconditioning involves preservation of myocardial opioid content and selective opioid receptor activation. Am J Physiol Heart Circ Physiol. 2008;294(3):H1444-51.

130. Engelman JA, Luo J, Cantley LC. The evolution of phosphatidylinositol 3-kinases as regulators of growth and metabolism. Nat Rev Genet. 2006;7(8):606-19.

131. Hausenloy DJ, Yellon DM. New directions for protecting the heart against ischaemia-reperfusion injury: targeting the Reperfusion Injury Salvage Kinase (RISK)-pathway. Cardiovasc Res. 2004;61(3):448-60.

132. Van Winkle DM, Chien GL, Wolff RA, Soifer BE, Kuzume K, Davis RF. Cardioprotection provided by adenosine receptor activation is abolished by blockade of the KATP channel. Am J Physiol. 1994;266(2 Pt 2):H829-39.

133. Kitakaze M, Hori M, Morioka T, Minamino T, Takashima S, Sato H, et al. Alpha 1-adrenoceptor activation mediates the infarct size-limiting effect of ischemic preconditioning through augmentation of 5'-nucleotidase activity. J Clin Invest. 1994;93(5):2197-205.

134. Yang XM, Philipp S, Downey JM, Cohen MV. Postconditioning's protection is not dependent on circulating blood factors or cells but involves adenosine receptors

and requires PI3-kinase and guanylyl cyclase activation. Basic Res Cardiol. 2005;100(1):57-63.

135. Tong H, Rockman HA, Koch WJ, Steenbergen C, Murphy E. G protein-coupled receptor internalization signaling is required for cardioprotection in ischemic preconditioning. Circ Res. 2004;94(8):1133-41.

136. Brooks MJ, Andrews DT. Molecular mechanisms of ischemic conditioning: translation into patient outcomes. Future Cardiol. 2013;9(4):549-68.

137. Buchholz B, V DA, Giani JF, Siachoque N, Dominici FP, Turyn D, et al. Ischemic preconditioning reduces infarct size through the alpha-1 adrenergic receptor pathway. J Cardiovasc Pharmacol. Jun;63(6):504-11, 2014.

138. Tsang A, Hausenloy DJ, Mocanu MM, Yellon DM. Postconditioning: a form of "modified reperfusion" protects the myocardium by activating the phosphatidylinositol 3-kinase-Akt pathway. Circ Res. 2004;95(3):230-2.

139. Yang XM, Proctor JB, Cui L, Krieg T, Downey JM, Cohen MV. Multiple, brief coronary occlusions during early reperfusion protect rabbit hearts by targeting cell signaling pathways. J Am Coll Cardiol. 2004;44(5):1103-10.

140. Xuan YT, Guo Y, Zhu Y, Han H, Langenbach R, Dawn B, et al. Mechanism of cyclooxygenase-2 upregulation in late preconditioning. J Mol Cell Cardiol. 2003;35(5):525-37.

141. Dawn B, Xuan YT, Guo Y, Rezazadeh A, Stein AB, Hunt G, et al. IL-6 plays an obligatory role in late preconditioning via JAK-STAT signaling and upregulation of iNOS and COX-2. Cardiovasc Res. 2004;64(1):61-71.

142. Xuan YT, Guo Y, Zhu Y, Wang OL, Rokosh G, Messing RO, et al. Role of the protein kinase C-epsilon-Raf-1-MEK-1/2-p44/42 MAPK signaling cascade in the

activation of signal transducers and activators of transcription 1 and 3 and induction of cyclooxygenase-2 after ischemic preconditioning. Circulation. 2005;112(13):1971-8.

143. Heusch G, Musiolik J, Gedik N, Skyschally A. Mitochondrial STAT3 activation and cardioprotection by ischemic postconditioning in pigs with regional myocardial ischemia/reperfusion. Circ Res. 2011;109(11):1302-8.

144. Xuan YT, Guo Y, Han H, Zhu Y, Bolli R. An essential role of the JAK-STAT pathway in ischemic preconditioning. Proc Natl Acad Sci USA. 2001;98(16):9050-5.

145. Yellon DM, Hausenloy DJ. Myocardial reperfusion injury. N Engl J Med. 2007;357(11):1121-35.

146. Hausenloy DJ, Tsang A, Yellon DM. The reperfusion injury salvage kinase pathway: a common target for both ischemic preconditioning and postconditioning. Trends Cardiovasc Med. 2005;15(2):69-75.

147. Somers SJ, Frias M, Lacerda L, Opie LH, Lecour S. Interplay between SAFE and RISK pathways in sphingosine-1-phosphate-induced cardioprotection. Cardiovasc Drugs Ther. 2012;26(3):227-37.

148. Lacerda L, Somers S, Opie LH, Lecour S. Ischaemic postconditioning protects against reperfusion injury via the SAFE pathway. Cardiovasc Res. 2009;84(2):201-8.

149. Lecour S. Activation of the protective Survivor Activating Factor Enhancement (SAFE) pathway against reperfusion injury: Does it go beyond the RISK pathway? J Mol Cell Cardiol. 2009;47(1):32-40.

150. Hausenloy DJ, Tsang A, Mocanu MM, Yellon DM. Ischemic preconditioning

protects by activating prosurvival kinases at reperfusion. Am J Physiol Heart Circ Physiol. 2005;288(2):H971-6.

151. Strohm C, Barancik T, Bruhl ML, Kilian SA, Schaper W. Inhibition of the ER-kinase cascade by PD98059 and UO126 counteracts ischemic preconditioning in pig myocardium. J Cardiovasc Pharmacol. 2000;36(2):218-29.

152. Tong H, Imahashi K, Steenbergen C, Murphy E. Phosphorylation of glycogen synthase kinase-3beta during preconditioning through a phosphatidylinositol-3-kinase--dependent pathway is cardioprotective. Circ Res. 2002;90(4):377-9.

153. Tamareille S, Mateus V, Ghaboura N, Jeanneteau J, Croue A, Henrion D, et al. RISK and SAFE signaling pathway interactions in remote limb ischemic perconditioning in combination with local ischemic postconditioning. Basic Res Cardiol. 2011;106(6):1329-39.

154. Kis A, Yellon DM, Baxter GF. Second window of protection following myocardial preconditioning: an essential role for PI3 kinase and p70S6 kinase. J Mol Cell Cardiol. 2003;35(9):1063-71.

155. Quinlan CL, Costa AD, Costa CL, Pierre SV, Dos Santos P, Garlid KD. Conditioning the heart induces formation of signalosomes that interact with mitochondria to open mitoKATP channels. Am J Physiol Heart Circ Physiol. 2008;295(3):H953-H61.

156. Hausenloy DJ, Yellon DM. Reperfusion injury salvage kinase signalling: taking a RISK for cardioprotection. Heart Fail Rev. 2007;12(3-4):217-34.

157. Sanada S, Kitakaze M, Asanuma H, Harada K, Ogita H, Node K, et al. Role of mitochondrial and sarcolemmal K(ATP) channels in ischemic preconditioning of the canine heart. Am J Physiol Heart Circ Physiol. 2001;280(1):H256-63.

158. Nakai Y, Horimoto H, Mieno S, Sasaki S. Mitochondrial ATP-sensitive potassium channel plays a dominant role in ischemic preconditioning of rabbit heart. Eur Surg Res. 2001;33(2):57-63.

159. Andersen A, Povlsen JA, Botker HE, Nielsen-Kudsk JE. Ischemic preconditioning reduces right ventricular infarct size through opening of mitochondrial potassium channels. Cardiology. 2012;123(3):177-80.

160. Rajesh KG, Sasaguri S, Zhitian Z, Suzuki R, Asakai R, Maeda H. Second window of ischemic preconditioning regulates mitochondrial permeability transition pore by enhancing Bcl-2 expression. Cardiovasc Res. 2003;59(2):297-307.

161. Hausenloy DJ, Maddock HL, Baxter GF, Yellon DM. Inhibiting mitochondrial permeability transition pore opening: a new paradigm for myocardial preconditioning? Cardiovasc Res. 2002;55(3):534-43.

162. Lim SY, Davidson SM, Hausenloy DJ, Yellon DM. Preconditioning and postconditioning: the essential role of the mitochondrial permeability transition pore. Cardiovasc Res. 2007;75(3):530-5.

163. Ardehali H. Cytoprotective channels in mitochondria. J Bioenerg Biomembr. 2005;37(3):171-7.

164. Kowaltowski AJ, Seetharaman S, Paucek P, Garlid KD. Bioenergetic consequences of opening the ATP-sensitive K^+ channel of heart mitochondria. Am J Physiol Heart Circ Physiol. 2001;280(2):H649-57.

165. Dos Santos P, Kowaltowski AJ, Laclau MN, Seetharaman S, Paucek P, Boudina S, et al. Mechanisms by which opening the mitochondrial ATP- sensitive K^+ channel protects the ischemic heart. Am J Physiol Heart Circ Physiol. 2002;283(1):H284-95.

166. Garlid KD, Dos Santos P, Xie ZJ, Costa AD, Paucek P. Mitochondrial potassium transport: the role of the mitochondrial ATP-sensitive K^+ channel in cardiac function and cardioprotection. Biochim Biophys Acta. 2003;1606(1-3):1-21.

167. Belisle E, Kowaltowski AJ. Opening of mitochondrial K^+ channels increases ischemic ATP levels by preventing hydrolysis. J Bioenerg Biomembr. 2002;34(4):285-98.

168. Wang L, Cherednichenko G, Hernandez L, Halow J, Camacho SA, Figueredo V, et al. Preconditioning limits mitochondrial Ca^{2+} during ischemia in rat hearts: role of K(ATP) channels. Am J Physiol Heart Circ Physiol. 2001;280(5):H2321-8.

169. Korge P, Honda HM, Weiss JN. Protection of cardiac mitochondria by diazoxide and protein kinase C: implications for ischemic preconditioning. Proc Natl Acad Sci U S A. 2002;99(5):3312-7.

170. Carroll R, Gant VA, Yellon DM. Mitochondrial K(ATP) channel opening protects a human atrial-derived cell line by a mechanism involving free radical generation. Cardiovasc Res. 2001;51(4):691-700.

171. Ozcan C, Bienengraeber M, Dzeja PP, Terzic A. Potassium channel openers protect cardiac mitochondria by attenuating oxidant stress at reoxygenation. Am J Physiol Heart Circ Physiol. 2002;282(2):H531-9.

172. Narayan P, Mentzer RM, Jr., Lasley RD. Adenosine A_1 receptor activation reduces reactive oxygen species and attenuates stunning in ventricular myocytes. J Mol Cell Cardiol. 2001;33(1):121-9.

173. Vanden Hoek T, Becker LB, Shao ZH, Li CQ, Schumacker PT. Preconditioning in cardiomyocytes protects by attenuating oxidant stress at reperfusion. Circ Res. 2000;86(5):541-8.

174. Hashimoto K, Minatoguchi S, Hashimoto Y, Wang N, Qiu X, Yamashita K, et al. Role of protein kinase C, K(ATP) channels and DNA fragmentation in the infarct size-reducing effects of the free radical scavenger T-0970. Clin Exp Pharmacol Physiol. 2001;28(3):193-9.

175. Lee TM, Su SF, Chou TF, Lee YT, Tsai CH. Loss of preconditioning by attenuated activation of myocardial ATP-sensitive potassium channels in elderly patients undergoing coronary angioplasty. Circulation. 2002;105(3):334-40.

176. Tritapepe L, De Santis V, Vitale D, Guarracino F, Pellegrini F, Pietropaoli P, et al. Levosimendan pre-treatment improves outcomes in patients undergoing coronary artery bypass graft surgery. Br J Anaesth. 2009;102(2):198-204.

177. Di Lisa F, Menabo R, Canton M, Barile M, Bernardi P. Opening of the mitochondrial permeability transition pore causes depletion of mitochondrial and cytosolic NAD+ and is a causative event in the death of myocytes in postischemic reperfusion of the heart. J Biol Chem. 2001;276(4):2571-5.

178. Ganote CE, Armstrong SC. Effects of CCCP-induced mitochondrial uncoupling and cyclosporin A on cell volume, cell injury and preconditioning protection of isolated rabbit cardiomyocytes. J Mol Cell Cardiol. 2003;35(7):749-59.

179. Baines CP, Song CX, Zheng YT, Wang GW, Zhang J, Wang OL, et al. Protein kinase Cepsilon interacts with and inhibits the permeability transition pore in cardiac mitochondria. Circ Res. 2003;92(8):873-80.

180. De Paulis D, Chiari P, Teixeira G, Couture-Lepetit E, Abrial M, Argaud L, et al. Cyclosporine A at reperfusion fails to reduce infarct size in the *in vivo* rat heart. Basic Res Cardiol. 2013;108(5):379.

181. Ghaffari S, Kazemi B, Toluey M, Sepehrvand N. The effect of prethrombolytic

cyclosporine-A injection on clinical outcome of acute anterior ST-elevation myocardial infarction. Cardiovasc Ther. 2013;31(4):e34-9.

182. Piot C, Croisille P, Staat P, Thibault H, Rioufol G, Mewton N, et al. Effect of cyclosporine on reperfusion injury in acute myocardial infarction. N Engl J Med. 2008;359(5):473-81.

183. Abou-Sleiman PM, Muqit MM, Wood NW. Expanding insights of mitochondrial dysfunction in Parkinson's disease. Nat Rev Neurosci. 2006;7(3):207-19.

184. Nakagawa T, Shimizu S, Watanabe T, Yamaguchi O, Otsu K, Yamagata H, et al. Cyclophilin D-dependent mitochondrial permeability transition regulates some necrotic but not apoptotic cell death. Nature. 2005;434(7033):652-8.

185. Ong SB, Subrayan S, Lim SY, Yellon DM, Davidson SM, Hausenloy DJ. Inhibiting mitochondrial fission protects the heart against ischemia/reperfusion injury. Circulation. 2010;121(18):2012-22.

186. Sheng ZH, Cai Q. Mitochondrial transport in neurons: impact on synaptic homeostasis and neurodegeneration. Nat Rev Neurosci. 2012;13(2):77-93.

187. Winklhofer KF. Parkin and mitochondrial quality control: toward assembling the puzzle. Trends Cell Biol. 2014, Jun;24(6):332-341.

188. Ong SB, Hausenloy DJ. Mitochondrial morphology and cardiovascular disease. Cardiovasc Res. 2010;88(1):16-29.

189. Chan DC. Mitochondrial dynamics in disease. N Engl J Med. 2007;356(17):1707-9.

190. Shutt TE, McBride HM. Staying cool in difficult times: mitochondrial dynamics, quality control and the stress response. Biochim Biophys Acta. 2013;1833(2):417-24.

191. Liesa M, Palacin M, Zorzano A. Mitochondrial dynamics in mammalian health and disease. Physiol Rev. 2009;89(3):799-845.

192. Dimmer KS, Scorrano L. (De)constructing mitochondria: what for? Physiology (Bethesda). 2006;21:233-41.

193. Rugarli EI, Langer T. Mitochondrial quality control: a matter of life and death for neurons. EMBO J. 2012;31(6):1336-49.

194. Martinou JC, Youle RJ. Which came first, the cytochrome c release or the mitochondrial fission? Cell Death Differ. 2006;13(8):1291-5.

195. Kim H, Scimia MC, Wilkinson D, Trelles RD, Wood MR, Bowtell D, et al. Fine-tuning of Drp1/Fis1 availability by AKAP121/Siah2 regulates mitochondrial adaptation to hypoxia. Mol Cell. 2011;44(4):532-44.

196. Wang JX, Jiao JQ, Li Q, Long B, Wang K, Liu JP, et al. miR-499 regulates mitochondrial dynamics by targeting calcineurin and dynamin-related protein-1. Nat Med. 2011;17(1):71-8.

197. Guo C, Hildick KL, Luo J, Dearden L, Wilkinson KA, Henley JM. SENP3-mediated deSUMOylation of dynamin-related protein 1 promotes cell death following ischaemia. EMBO J. 2013;32(11):1514-28.

198. Cribbs JT, Strack S. Reversible phosphorylation of Drp1 by cyclic AMP-dependent protein kinase and calcineurin regulates mitochondrial fission and cell death. EMBO Rep. 2007;8(10):939-44.

199. Jahani-Asl A, Slack RS. The phosphorylation state of Drp1 determines cell fate. EMBO Rep. 2007;8(10):912-3.

200. Chang CR, Blackstone C. Cyclic AMP-dependent protein kinase phosphorylation of Drp1 regulates its GTPase activity and mitochondrial morphology. J Biol Chem.

2007;282(30):21583-7.

201. Wang Z, Jiang H, Chen S, Du F, Wang X. The mitochondrial phosphatase PGAM5 functions at the convergence point of multiple necrotic death pathways. Cell. 2012;148(1-2):228-43.

202. Dhingra R, Kirshenbaum LA. Regulation of mitochondrial dynamics and cell fate. Circ J. 2014;78(4):803-10.

203. Gandre-Babbe S, van der Bliek AM. The novel tail-anchored membrane protein Mff controls mitochondrial and peroxisomal fission in mammalian cells. Mol Biol Cell. 2008;19(6):2402-12.

204. Otera H, Wang C, Cleland MM, Setoguchi K, Yokota S, Youle RJ, et al. Mff is an essential factor for mitochondrial recruitment of Drp1 during mitochondrial fission in mammalian cells. J Cell Biol. 2010;191(6):1141-58.

205. Palmer CS, Elgass KD, Parton RG, Osellame LD, Stojanovski D, Ryan MT. Adaptor proteins MiD49 and MiD51 can act independently of Mff and Fis1 in Drp1 recruitment and are specific for mitochondrial fission. J Biol Chem. 2013;288(38):27584-93.

206. Detmer SA, Chan DC. Functions and dysfunctions of mitochondrial dynamics. Nat Rev Mol Cell Biol. 2007;8(11):870-9.

207. Frank S, Gaume B, Bergmann-Leitner ES, Leitner WW, Robert EG, Catez F, et al. The role of dynamin-related protein 1, a mediator of mitochondrial fission, in apoptosis. Dev Cell. 2001;1(4):515-25.

208. Olichon A, Elachouri G, Baricault L, Delettre C, Belenguer P, Lenaers G. OPA1 alternate splicing uncouples an evolutionary conserved function in mitochondrial fusion from a vertebrate restricted function in apoptosis. Cell Death Differ.

2007;14(4):682-92.

209. Estaquier J, Arnoult D. Inhibiting Drp1-mediated mitochondrial fission selectively prevents the release of cytochrome c during apoptosis. Cell Death Differ. 2007;14(6):1086-94.

210. Tanaka A, Youle RJ. A chemical inhibitor of DRP1 uncouples mitochondrial fission and apoptosis. Mol Cell. 2008;29(4):409-10.

211. Germain M, Mathai JP, McBride HM, Shore GC. Endoplasmic reticulum BIK initiates DRP1-regulated remodelling of mitochondrial cristae during apoptosis. EMBO J. 2005;24(8):1546-56.

212. Neuspiel M, Zunino R, Gangaraju S, Rippstein P, McBride H. Activated mitofusin 2 signals mitochondrial fusion, interferes with Bax activation, and reduces susceptibility to radical induced depolarization. J Biol Chem. 2005;280(26):25060-70.

213. Kong D, Xu L, Yu Y, Zhu W, Andrews DW, Yoon Y, et al. Regulation of Ca^{2+}-induced permeability transition by Bcl-2 is antagonized by Drpl and hFis1. Mol Cell Biochem. 2005;272(1-2):187-99.

214. Sobrado M, Ramirez BG, Neria F, Lizasoain I, Arbones ML, Minami T, et al. Regulator of calcineurin 1 (Rcan1) has a protective role in brain ischemia/reperfusion injury. J Neuroinflammation. 2012;9:48.

215. Aurora AB, Mahmoud AI, Luo X, Johnson BA, van Rooij E, Matsuzaki S, et al. MicroRNA-214 protects the mouse heart from ischemic injury by controlling Ca^{2+} overload and cell death. J Clin Invest. 2012;122(4):1222-32.

216. Disatnik MH, Ferreira JC, Campos JC, Gomes KS, Dourado PM, Qi X, et al. Acute inhibition of excessive mitochondrial fission after myocardial infarction

prevents long-term cardiac dysfunction. J Am Heart Assoc. 2013;2(5):e000461.

217. Sharp WW, Fang YH, Han M, Zhang HJ, Hong Z, Banathy A, et al. Dynamin-related protein 1 (Drp1)-mediated diastolic dysfunction in myocardial ischemia-reperfusion injury: therapeutic benefits of Drp1 inhibition to reduce mitochondrial fission. FASEB J. 2014;28(1):316-26.

218. Claycomb WC, Lanson NA, Jr., Stallworth BS, Egeland DB, Delcarpio JB, Bahinski A, et al. HL-1 cells: a cardiac muscle cell line that contracts and retains phenotypic characteristics of the adult cardiomyocyte. Proc Natl Acad Sci USA. 1998;95(6):2979-84.

219. Hamacher-Brady A, Brady NR, Gottlieb RA. Enhancing macroautophagy protects against ischemia/reperfusion injury in cardiac myocytes. J Biol Chem. 2006;281(40):29776-87.

220. Frezza C, Cipolat S, Scorrano L. Organelle isolation: functional mitochondria from mouse liver, muscle and cultured fibroblasts. Nat Protoc. 2007;2(2):287-95.

221. Cassidy-Stone A, Chipuk JE, Ingerman E, Song C, Yoo C, Kuwana T, et al. Chemical inhibition of the mitochondrial division dynamin reveals its role in Bax/Bak-dependent mitochondrial outer membrane permeabilization. Dev Cell. 2008;14(2):193-204.

222. Schneider CA, Rasband WS, Eliceiri KW. NIH Image to ImageJ: 25 years of image analysis. Nat Methods. 2012;9(7):671-5.

223. Nicholson DW, Ali A, Thornberry NA, Vaillancourt JP, Ding CK, Gallant M, et al. Identification and inhibition of the ICE/CED-3 protease necessary for mammalian apoptosis. Nature. 1995;376(6535):37-43.

224. Kumar S. The apoptotic cysteine protease CPP32. Int J Biochem Cell Biol.

1997;29(3):393-6.

225. Fernandes-Alnemri T, Litwack G, Alnemri ES. CPP32, a novel human apoptotic protein with homology to Caenorhabditis elegans cell death protein Ced-3 and mammalian interleukin-1 beta-converting enzyme. J Biol Chem. 1994;269(49):30761-4.

226. Yoshioka K, Yoshida K, Cui H, Wakayama T, Takuwa N, Okamoto Y, et al. Endothelial PI3K-C2alpha, a class II PI3K, has an essential role in angiogenesis and vascular barrier function. Nat Med. 2012;18(10):1560-9.

227. Yilmaz M, Maass D, Tiwari N, Waldmeier L, Schmidt P, Lehembre F, et al. Transcription factor Dlx2 protects from TGFbeta-induced cell-cycle arrest and apoptosis. EMBO J. 2011;30(21):4489-99.

228. Zinchuk V, Zinchuk O, Okada T. Quantitative colocalization analysis of multicolor confocal immunofluorescence microscopy images: pushing pixels to explore biological phenomena. Acta Histochem Cytochem. 2007;40(4):101-11.

229. Adler J, Parmryd I. Colocalization analysis in fluorescence microscopy. Methods Mol Biol. 2013;931:97-109.

230. Bolte S, Cordelieres FP. A guided tour into subcellular colocalization analysis in light microscopy. J Microsc. 2006;224(Pt 3):213-32.

231. Ino-Oka E, Chiba S, Urae J, Sekino M, Satoh M, Takeuchi K, et al. Attempt of quantitative analysis of visual evaluation for (123)I-BMIPP myocardial scintigraphy images. Clin Exp Hypertens. 2011;33(4):264-9.

232. Yabusaki K, Faits T, McMullen E, Figueiredo JL, Aikawa M, Aikawa E. A novel quantitative approach for eliminating sample-to-sample variation using a hue saturation value analysis program. PLoS One. 2014;9(3):e89627.

233. MacKenna DA, Omens JH, McCulloch AD, Covell JW. Contribution of collagen matrix to passive left ventricular mechanics in isolated rat hearts. Am J Physiol. 1994;266(3 Pt 2):H1007-18.

234. Vanden Berghe T, Linkermann A, Jouan-Lanhouet S, Walczak H, Vandenabeele P. Regulated necrosis: the expanding network of non-apoptotic cell death pathways. Nat Rev Mol Cell Biol. 2014;15(2):135-47.

235. Linkermann A, Green DR. Necroptosis. N Engl J Med. 2014;370(5):455-65.

236. Linkermann A, Hackl MJ, Kunzendorf U, Walczak H, Krautwald S, Jevnikar AM. Necroptosis in immunity and ischemia-reperfusion injury. Am J Transplant. 2013;13(11):2797-804.

237. Davis CW, Hawkins BJ, Ramasamy S, Irrinki KM, Cameron BA, Islam K, et al. Nitration of the mitochondrial complex I subunit NDUFB8 elicits RIP1- and RIP3-mediated necrosis. Free Radic Biol Med. 2010;48(2):306-17.

238. Northington FJ, Chavez-Valdez R, Graham EM, Razdan S, Gauda EB, Martin LJ. Necrostatin decreases oxidative damage, inflammation, and injury after neonatal HI. J Cereb Blood Flow Metab. 2011;31(1):178-89.

239. Trichonas G, Murakami Y, Thanos A, Morizane Y, Kayama M, Debouck CM, et al. Receptor interacting protein kinases mediate retinal detachment-induced photoreceptor necrosis and compensate for inhibition of apoptosis. Proc Natl Acad Sci U S A. 2010;107(50):21695-700.

240. Linkermann A, Brasen JH, Himmerkus N, Liu S, Huber TB, Kunzendorf U, et al. Rip1 (receptor-interacting protein kinase 1) mediates necroptosis and contributes to renal ischemia/reperfusion injury. Kidney Int. 2012;81(8):751-61.

241. Szobi A, Rajtik T, Carnicka S, Ravingerova T, Adameova A. Mitigation of

postischemic cardiac contractile dysfunction by CaMKII inhibition: effects on programmed necrotic and apoptotic cell death. Mol Cell Biochem. 2014;388(1-2):269-76.

242. Smith CC, Davidson SM, Lim SY, Simpkin JC, Hothersall JS, Yellon DM. Necrostatin: a potentially novel cardioprotective agent? Cardiovasc Drugs Ther. 2007;21(4):227-33.

243. Oerlemans MI, Liu J, Arslan F, den Ouden K, van Middelaar BJ, Doevendans PA, et al. Inhibition of RIP1-dependent necrosis prevents adverse cardiac remodeling after myocardial ischemia-reperfusion *in vivo*. Basic Res Cardiol. 2012;107(4):270.

244. Liu J, van Mil A, Vrijsen K, Zhao J, Gao L, Metz CH, et al. MicroRNA-155 prevents necrotic cell death in human cardiomyocyte progenitor cells via targeting RIP1. J Cell Mol Med. 2011;15(7):1474-82.

245. Dmitriev YV, Minasian SM, Demchenko EA, Galagudza MM. Study of cardioprotective effects of necroptosis inhibitors on isolated rat heart subjected to global ischemia-reperfusion. Bull Exp Biol Med. 2013;155(2):245-8.

246. Westermann B. Mitochondrial fusion and fission in cell life and death. Nat Rev Mol Cell Biol. 2010;11(12):872-84.

247. Youle RJ, van der Bliek AM. Mitochondrial fission, fusion, and stress. Science. 2012;337(6098):1062-5.

248. Knott AB, Perkins G, Schwarzenbacher R, Bossy-Wetzel E. Mitochondrial fragmentation in neurodegeneration. Nat Rev Neurosci. 2008;9(7):505-18.

249. Gong D, Zhang H, Hu S. Mitochondrial aldehyde dehydrogenase 2 activation and cardioprotection. J Mol Cell Cardiol. 2013;55:58-63.

250. Hausenloy DJ, Boston-Griffiths EA, Yellon DM. Cyclosporin A and cardioprotection: from investigative tool to therapeutic agent. Br J Pharmacol. 2012;165(5):1235-45.

251. Perrelli MG, Pagliaro P, Penna C. Ischemia/reperfusion injury and cardioprotective mechanisms: Role of mitochondria and reactive oxygen species. World J Cardiol. 2011;3(6):186-200.

252. Rao VK, Carlson EA, Yan SS. Mitochondrial permeability transition pore is a potential drug target for neurodegeneration. Biochim Biophys Acta. 2013, Sep 18.

253. Cereghetti GM, Stangherlin A, Martins de Brito O, Chang CR, Blackstone C, Bernardi P, et al. Dephosphorylation by calcineurin regulates translocation of Drp1 to mitochondria. Proc Natl Acad Sci USA. 2008;105(41):15803-8.

254. Din S, Mason M, Volkers M, Johnson B, Cottage CT, Wang Z, et al. Pim-1 preserves mitochondrial morphology by inhibiting dynamin-related protein 1 translocation. Proc Natl Acad Sci USA. 2013;110(15):5969-74.

255. Qi X, Qvit N, Su YC, Mochly-Rosen D. A novel Drp1 inhibitor diminishes aberrant mitochondrial fission and neurotoxicity. J Cell Sci. 2013;126(Pt 3):789-802.

256. Hogeboom GH, Schneider WC, Pallade GE. Cytochemical studies of mammalian tissues; isolation of intact mitochondria from rat liver; some biochemical properties of mitochondria and submicroscopic particulate material. J Biol Chem. 1948;172(2):619-35.

257. Magi B, Liberatori S. Immunoblotting techniques. Methods Mol Biol. 2005;295:227-54.

258. Aldridge GM, Podrebarac DM, Greenough WT, Weiler IJ. The use of total protein stains as loading controls: an alternative to high-abundance single-protein

controls in semi-quantitative immunoblotting. J Neurosci Methods. 2008;172(2):250-4.

ABSTRACT

MITOCHONDRIAL DYNAMICS: EXPLORING A NOVEL TARGET AGAINST MYOCARDIAL ISCHEMIA-REPERFUSION INJURY

by

YI DONG

August 2014

Advisor: Karin Przyklenk, Ph.D.

Major: Physiology

Degree: Doctor of Philosophy

Mitochondrial fusion and fission, collectively termed mitochondrial dynamics, are among the core mechanisms responsible for maintaining mitochondrial health and functional integrity. Dynamin-related protein 1 (DRP1) is a key regulator of mitochondrial fission. Recent studies suggest that i) mitochondrial dynamics, particularly, mitochondrial fission, serves as a mediator of cell fate in the setting of ischemia-reperfusion (IR) injury, and, ii) inhibition of DRP1 and mitochondrial fission provides cardioprotection against IR injury. However, the precise role of DRP1 translocation to mitochondria in the pathogenesis of myocardial ischemia-reperfusion injury has not been established.

Using an established model of hypoxia-reoxygenation (HR) in cultured HL-1 cardiomyocytes, we tested three hypotheses:

i. subcellular redistribution of DRP1 is i) triggered by HR, and ii) plays a mechanistic role in HR-induced cytochrome c release and cell apoptosis;
ii. inhibition of DRP1 translocation prior to hypoxia is cardioprotective;
iii. inhibition of DRP1 in a time-frame that is relevant as a therapeutic strategy (i.e., begun at reoxygenation) will also attenuate cardiomyocyte death, although

possibly less robust than pretreatment.

In support of Hypothesis I, our results demonstrated that HR was associated with DRP1 translocation to mitochondria, cytochrome *c* release into cytosol, and caspase 3 cleavage (harbinger of apoptosis). Subsequently, and consistent with Hypothesis II, we established a cause-effect relationship between DRP1 translocation and cardiomyocyte injury in the setting of HR injury. Both pretreatment with Mdivi-1 (a specific inhibitor of DRP1; 50 µM) and knockdown of DRP1 expression by transfection with DRP1 siRNA significantly reduced DRP1 translocation to mitochondria, attenuated cytochrome *c* release, blunted caspase 3 cleavage and apoptotic cell death, better-preserved mitochondrial morphology and improved cell viability. However, in contrast to Hypothesis III, Mdivi-1 given at reoxygenation, was not cardioprotective. Rather, we observed a paradoxical result: Mdivi-1, given at reoxygenation, attenuated apoptosis, but did not reduce total cell death and, in some cases (prolonged exposure at a dose of 50 µM) exacerbated cell death. This exacerbated cell death with delayed Mdivi-1 treatment was in part rescued by co-administration of Necrostatin-1, suggesting that necroptosis (programmed necrosis) may play a role in this phenomenon. In conclusion, our results show that DRP1 translocation to mitochondria plays a mechanistic role in mediating cardiomyocyte injury in the context of hypoxia-reoxygenation injury, and reveal a complex temporal relationship between inhibition of mitochondrial fission and cardioprotection.

AUTOBIOGRAPHICAL STATEMENT

YI DONG

Education

Jun 2014	**Ph.D. in Physiology** Wayne State University, Detroit MI (Expected Graduation in June 2014)
Jul 2008	**Master of Medicine in Surgery** Huazhong University of Science and Technology, Wuhan Hubei, China
Jul 2005	**Bachelor of Medicine** Medical College of Nanchang University, Nanchang, Jiangxi, China

Clinic Training

Sep 2005 – Jul 2008	**Graduate Surgery Residency,** Union Hospital, Wuhan Hubei, China
Mar 2004	**Internship in Psychiatry,** Jiangxi Mental Health Ctr, Nanchang Jiangxi, China
Jun 2004 – Jun 2005	**Internship and Medical Student Resident,** Fourth Affiliated Hospital of Nanchang University, Nanchang Jiangxi, China

Abstract presentation

1. Dong Y, Undyala VV, Przyklenk K. Inhibition of Mitochondrial Fission as a Novel Molecular Target to Attenuate Myocardial Ischemia-Reperfusion Injury: Critical Importance of the Timing of Treatment. Presented at *American Heart Association National Scientific Sessions 2013*, Dallas, TX: Nov 2013.
2. Dong Y, Undyala VV, Kumar R, Przyklenk K. Mitochondrial translocation of dynamin-related protein 1 promotes lethal ischemia-reperfusion injury. *Circulation* 2012; 126: A13470. Presented at *American Heart Association National Scientific Sessions 2012*, Los Angeles, CA: Nov 2012.
3. Dong Y, Undyala VV, Kumar R, Przyklenk K. DRP1 Mitochondrial Translocation: A Possible Mechanism for Cytochrome C Release, Activation of Apoptosis and Cell Death in Myocardial Ischemia-Reperfusion Injury? Presented at the *American Society for Biochemistry and Molecular Biology Special Symposium* – Mitochondria: Energy, Signals and Homeostasis, East Lansing, MI: Jun 2012.

Publications

1. Dong Y, Undyala VV, Przyklenk K. Inhibition of Mitochondrial Fission as a Novel Molecular Target to Attenuate Myocardial Ischemia-Reperfusion Injury: Critical Importance of the Timing of Treatment. **(Manuscript in preparation)**
2. Calo L, Dong Y, Kumar R, Przyklenk K, Sanderson TH. Mitochondrial dynamics: an emerging paradigm in ischemia-reperfusion injury. Current pharmaceutical design. Apr 10 2013;19(39):6848-6857.
3. Przyklenk K, Dong Y, Undyala VV, Whittaker P. Autophagy as a therapeutic target for ischaemia /reperfusion injury? Concepts, controversies, and challenges. Cardiovasc Res. May 1 2012;94(2):197-205.
4. Vinten-Johansen J, Granfeldt A, Mykytenko J, Undyala VV, Dong Y, Przyklenk K. The multidimensional physiological responses to postconditioning. Antioxid Redox Signal. Mar 1 2011;14(5):791-810.
5. Dong Y, Undyala VV, Gottlieb RA, Mentzer RM, Jr., Przyklenk K. Autophagy: definition, molecular machinery, and potential role in myocardial ischemia-reperfusion injury. J Cardiovasc Pharmacol Ther. Sep 2010;15(3):220-230.
6. Dong Y, Dong NG, Shi JW, Hong H, Xie T, Hu C, Chen S, Deng C. Cyclic RGDfK Peptide Modulates the Integrin αVβ3 Expression in Myofibroblasts. *Chinese J Clinic Thoracic Cardiovasc Surgery*. Oct 2008; 15(5):360-364.

Awards and Honors

Oct 2013	American Heart Association's Council on Basic Cardiovascular Sciences (BCVS) Abstract Travel Grant
Jun 2012	Best Poster Presentation Award, International Summer School of Mitochondria & the American Society for Biochemistry and Molecular Biology Special Symposium – Mitochondria: Energy, Signals and Homeostasis, East Lansing, MI
Jun 2010	Honors at the Competence Exam for Ph.D. students, Dept. of Physiology, Wayne State University School of Medicine, Detroit, MI
7/2008–8/2012	IBS fellowship, Wayne State University School of Medicine, Detroit, MI